Journal of Palaeogeography
2015, 4(2): 109−166
DOI: 10.3724/SP.J.1261.2015.00071

Review

The landslide problem

G. Shanmugam*

Department of Earth and Environmental Sciences, The University of Texas at Arlington, Arlington, TX 76019, USA

Abstract The synonymous use of the general term “landslide”, with a built-in reference to a sliding motion, for all varieties of mass-transport deposits (MTD), which include slides, slumps, debrites, topples, creeps, debris avalanches *etc.* in subaerial, sublacustrine, submarine, and extraterrestrial environments has created a multitude of conceptual and nomenclatural problems. In addition, concepts of triggers and long-runout mechanisms of mass movements are loosely applied without rigor. These problems have enormous implications for studies in process sedimentology, sequence stratigraphy, palaeogeography, petroleum geology, and engineering geology. Therefore, the objective of this critical review is to identify key problems and to provide conceptual clarity and possible solutions. Specific issues are the following: (1) According to “limit equilibrium analyses” in soil mechanics, sediment failure with a sliding motion is initiated over a shear surface when the factor of safety for slope stability (*F*) is less than 1. However, the term landslide is not meaningful for debris flows with a flowing motion. (2) Sliding motion can be measured in oriented core and outcrop, but such measurement is not practical on seismic profiles or radar images. (3) Although 79 MTD types exist in the geological and engineering literature, only slides, slumps, and debrites are viable depositional facies for interpreting ancient stratigraphic records. (4) The use of the term landslide for high-velocity debris avalanches is inappropriate because velocities of mass-transport processes cannot be determined in the rock record. (5) Of the 21 potential triggering mechanisms of sediment failures, frequent short-term events that last for only a few minutes to several hours or days (*e.g.*, earthquakes, meteorite impacts, tsunamis, tropical cyclones, *etc.*) are more relevant in controlling deposition of deep-water sands than sporadic long-term events that last for thousands to millions of years (*e.g.*, sea-level lowstands). (6) The comparison of *H*/*L* (fall height/runout distance) ratios of MTD in subaerial environments with *H*/*L* ratios of MTD in submarine and extraterrestrial environments is incongruous because of differences in data sources (*e.g.*, outcrop vs. seismic or radar images). (7) Slides represent the pre-transport disposition of strata and their reservoir quality (*i.e.*, porosity and permeability) of the provenance region, whereas debrites reflect post-transport depositional texture and reservoir quality. However, both sandy slides and sandy debrites could generate blocky wireline (gamma-ray) log motifs. Therefore, reservoir characterization of deep-water strata must be based on direct examination of the rocks and related process-specific facies interpretations, not on wireline logs or on seismic profiles and related process-vague facies interpretations. A solution to these problems is to apply the term “landslide” solely to cases in which a sliding motion can be empirically determined. Otherwise, a general term MTD is appropriate. This decree is not just a quibble over semantics; it is a matter of portraying the physics of mass movements accurately. A precise interpretation of a depositional facies (*e.g.*, sandy slide vs. sandy debrite) is vital not

* Correspondence author. E-mail: shanshanmugam@aol.com.
Received: 2014−10−24 Accepted: 2014−12−29

only for maintaining conceptual clarity but also for characterizing petroleum reservoirs.

Key words debris flows, landslides, mass-transport deposits (MTD), slides, slumps, soil strength, triggering mechanisms, reservoir characterization

1 Introduction

The general term "landslide" is very popular. A cursory Google search of the term landslide has yielded 6,100,000 results. The reason is that the topic of landslides is of interest to researchers in a wide range of scientific disciplines, which include sedimentology, oceanography, geomorphology, volcanology, seismology, glaciology, areology (*i.e.*, geology of Mars), deep-sea structural engineering, highway engineering, soil mechanics, climate change, eustasy, natural hazards, and petroleum exploration and production. Not surprisingly, each scientific community has arrived at its own nomenclatural scheme (Hansen, 1984). However, there is no conceptual link between different schemes on landslides. Consequently, the term landslide means different things to different populace. This conceptual disconnect and its consequences are the primary focus of this paper.

Since the early recognition of subaerial "landslides" in 186 BC in China (Li, 1989), their common occurrences in subaerial and submarine environments have been well documented worldwide (Figure 1). In subaerial settings, for example, fault-induced alluvial fans are dominated by mass-transport deposits (McPherson *et al.*, 1987). Aspects of subaerial, sublacustrine, and submarine landslides have been reviewed adequately during the past 140 years (Baltzer, 1875; Howe, 1909; Reynolds, 1932; Ladd, 1935; Sharpe, 1938; Ward, 1945; Popov, 1946; Eckel, 1958; Yatsu, 1967; Hutchinson, 1968; Zaruba and Mencl, 1969; Blong, 1973; Crozier, 1973; Coates, 1977; Woodcock, 1979; Hansen, 1984; Varnes, 1984; Brabb and Harrod, 1989; Schwab *et al.*, 1993; Hampton *et al.*, 1996; Elverhøi *et al.*, 1997; Locat and Lee, 2000, 2002; Hungr *et al.*, 2001; Dykstra, 2005; Glade *et al.*, 2005; Solheim *et al.*, 2005a; Masson *et al.*, 2006; Shanmugam, 2009, 2012a, 2013a; Moernaut and De Batist, 2011; Shipp *et al.*, 2011; Clague and Stead, 2012; Krastel *et al.*, 2014, among others). On Earth, landslides have been recognized on bathymetric images (Figure 2) (Greene *et al.*, 2006), on seismic profiles (Figure 3) (Solheim *et al.*, 2005b) (Gee *et al.*, 2006), in outcrops (Heim, 1882; Macdonald *et al.*, 1993), and in conventional cores (Shanmugam, 2006a, 2012a). On Mars, landslides have been interpreted using shaded-relief map of the Thaumasia Plateau (Thermal Emission Imaging System infrared [THEMIS IR]) by Montgomery *et al.* (2009, their Figure 9).

1.1 Importance of mass-transport deposits (MTD)

Mass-transport deposits (MTD) are important not only because of their volumetric significance in the sedimentary record (Gamboa *et al.*, 2010), but also because of their frequent impacts on human lives both socially and economically (USGS, 2010; Petley, 2012). Since the birth of modern deep-sea exploration by the voyage of H.M.S. Challenger (December 21, 1872−May 24, 1876), organized by the Royal Society of London and the Royal Navy (Murray and Renard, 1891), oceanographers have made considerable progress in understanding the world′s oceans. Nevertheless, the physical processes that are responsible for transporting sediment downslope into the deep sea are still poorly understood. This is simply because the physics and hydrodynamics of these processes are difficult to observe and measure directly in deep-marine and extraterrestrial environments. This observational impediment has created an enormous challenge for understanding and communicating the mechanics of gravity-driven downslope processes with clarity. Furthermore, deep-marine environments are known for their complexity of processes and their deposits, composed not only of mass-transport deposits but also of bottom-current reworked deposits (Shanmugam, 2006a, 2012a). Thus a plethora of confusing concepts and classifications exists.

MTD constitute major geohazards on subaerial environments (Geertsema *et al.*, 2009; Glade *et al.*, 2005; Jakob and Hungr, 2005; Kirschbaum *et al.*, 2010). They are ubiquitous on submarine slopes (Figure 1) and are destructive (Hampton, *et al.*, 1996). Submarine mass movements may bear a tsunamigenic potential and are capable of methane gas release into the seawater and atmosphere (Urgeles *et al.*, 2007). The U.S. Geological Survey (USGS, 2010) has compiled data on worldwide damages caused by large subaerial and submarine MTD in the 20th and 21st centuries (Table 1). Annual losses associated with MTD have been estimated to be about 1−2 billion dollars in the U.S. alone (Schuster and Highland, 2001). Recently, the Oso landslide, which occurred on March 22, 2014 near Seattle

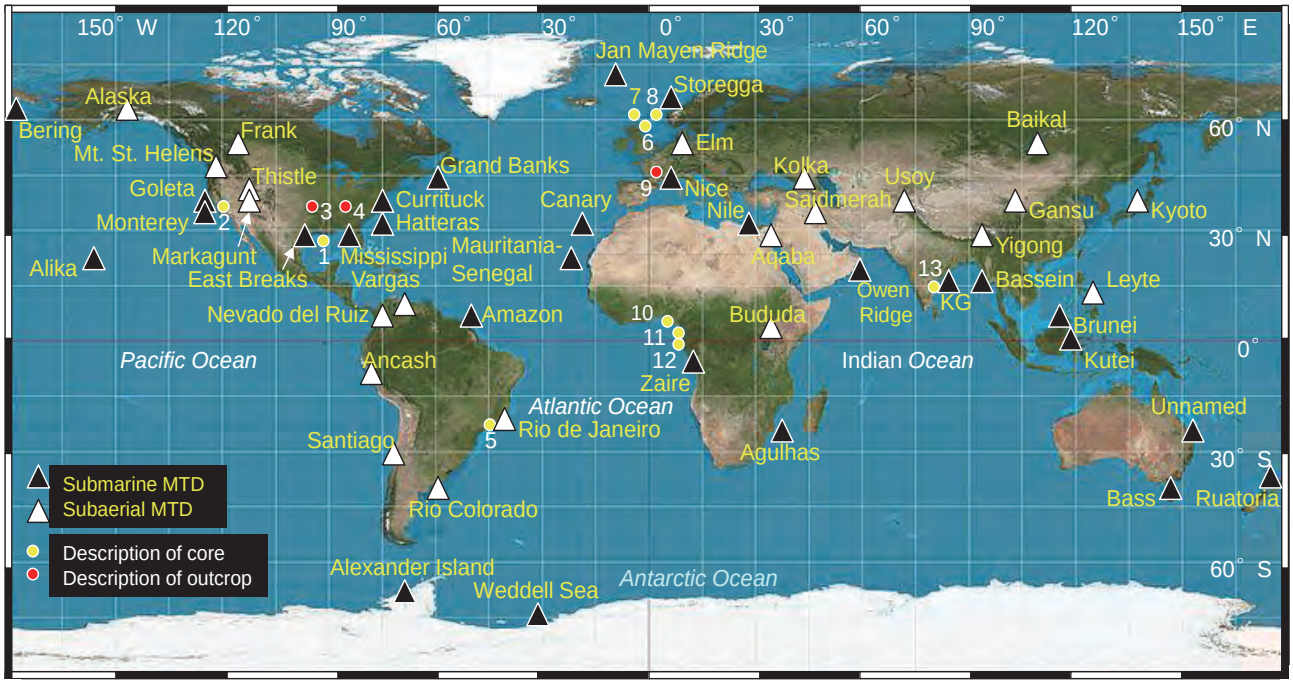

Figure 1 Map showing 50 examples (locations) of submarine (black triangle) and subaerial (white triangle) mass-transport deposits (MTD) that are often erroneously called "landslides" (see Tables 1, 2, and 5). Submarine and subaerial classification of each MTD denotes its depositional setting. Note locations of core studies (numbered yellow circles) and outcrop studies (numbered red circles) of deep-water successions carried out by the present author worldwide on MTD and SMTD (see Table 3 for details). 28 Submarine MTD: Bering, Bering Sea (Karl *et al.*, 1996; Nelson *et al.*, 2011); Goleta, U.S. Pacific Margin (Greene *et al.*, 2006); Monterey, U.S. Pacific Margin (Paull *et al.*, 2005); Alika, Hawaii, Pacific (Normark *et al.*, 1993); East Breaks, U.S. Gulf of Mexico (McGregor *et al.*, 1993); Mississippi, U.S. Gulf of Mexico (Weimer, 1989, 1990; McAdoo *et al.*, 2000; Nelson *et al.*, 2011); Grand Banks, North Atlantic, Canada (Heezen and Ewing, 1952; Piper and Aksu, 1987; Bornhold *et al.*, 2003); Currituck, U.S. Atlantic Margin (Locat *et al.*, 2009); Hatteras, U.S. Atlantic Margin (Embley, 1980); Amazon, Equatorial Atlantic (Damuth *et al.*, 1988; Piper *et al.*, 1997); Alexander Island, Antarctica (Macdonald *et al.*, 1993); Weddell Sea, Antarctica (Gales *et al.*, 2014); Jan Mayen Ridge, Norwegian−Greenland Sea (Laberg *et al.*, 2014); Storegga, Norwegian Sea (Bugge *et al.*, 1987; Haflidason *et al.*, 2005); Nice, Mediterranean Sea (Dan *et al.*, 2007); Nile, Mediterranean Sea (Newton *et al.*, 2004); Canary, SW off Morocco, North Atlantic (Masson *et al.*, 1997); Mauritania-Senegal, W Africa, North Atlantic (Jacobi, 1976); Zaire (formerly known as Congo), W Africa, S Atlantic (Shepard and Emery, 1973); Owen Ridge, Oman coast, Indian Ocean (Rodriguez *et al.*, 2013); Agulhas, SE Africa, Indian Ocean (Dingle, 1977); KG (Krishna-Godavari Basin), Bay of Bengal, NE Indian Ocean (Shanmugam *et al.*, 2009); Bassein, NE Indian Ocean (Moore *et al.*, 1976); Brunei, NW Borneo Margin (Gee *et al.*, 2007); Kutei, Makassar Strait, Indonesia (Jackson, 2004); Unnamed, offshore New South Wales/Queensland, Australia (Clarke *et al.*, 2012); Bass, SE Australia (Mitchell *et al.*, 2007); Ruatoria, Hikurangi Margin, New Zealand (Collot *et al.*, 2001). 22 Subaerial MTD: Alaska, State of Alaska, U.S. (USGS, 2010); Frank, Canada (Cruden and Hungr, 1986); Mt. St. Helens, State of Washington, U.S. (Schuster, 1983; Tilling *et al.*, 1990); Markagunt, State of Utah, U.S. (Hacker *et al.*, 2014); Thistle, State of Utah, U.S. (USGS, 2010); Vargas, Venezuela (USGS, 2010); Nevado del Ruiz, Colombia (Pierson, 1990); Ancash, Peru (USGS, 2010); Santiago, Chile (Sepúlveda *et al.*, 2006); Rio de Janeiro, Brazil (USGS, 2010); Rio Colorado, Argentina (USGS, 2010); Elm, Swiss Alps (Heim, 1882); Aqaba, Gulf of Aqaba (Klinger *et al.*, 1999); Bududa, Uganda (USGS, 2010); Kolka, Russia (North Ossetia) (USGS, 2010); Saidmerah, Iran (Harrison and Falcon, 1938); Usoy, Tajikistan (Bolt *et al.*, 1975; USGS, 2010); Baikal, Olkhon Island (Lake Baikal, Siberia) (Tyszkowski *et al.* 2014); Gansu, China (USGS, 2010); Yigong, Tibet (USGS, 2010); Kyoto, Japan (USGS, 2010); Leyte, Philippines (USGS, 2010); Blank world map credit: http://upload.wikimedia.org/wikipedia/commons/8/83/Equirectangular_projection_SW.jpg (accessed December 27, 2014).

(US), killed 43 people (PBS, 2014; Wikipedia, 2014). During a 7-year global survey (2004−2010), a total of 2,620 MTD had caused a loss of 32,322 human lives (Petley, 2012).

MTD vary in size greatly. The world's largest submarine MTD is the Agulhas Slump in SE Africa (Dingle, 1977), which is 20,331 km^3 in size (Figure 1, Table 2). This submarine MTD is 10 times volumetrically larger than the world's largest subaerial MTD (Markagunt gravity slide, southwest Utah, Figure 1), which is 2,000 km^3

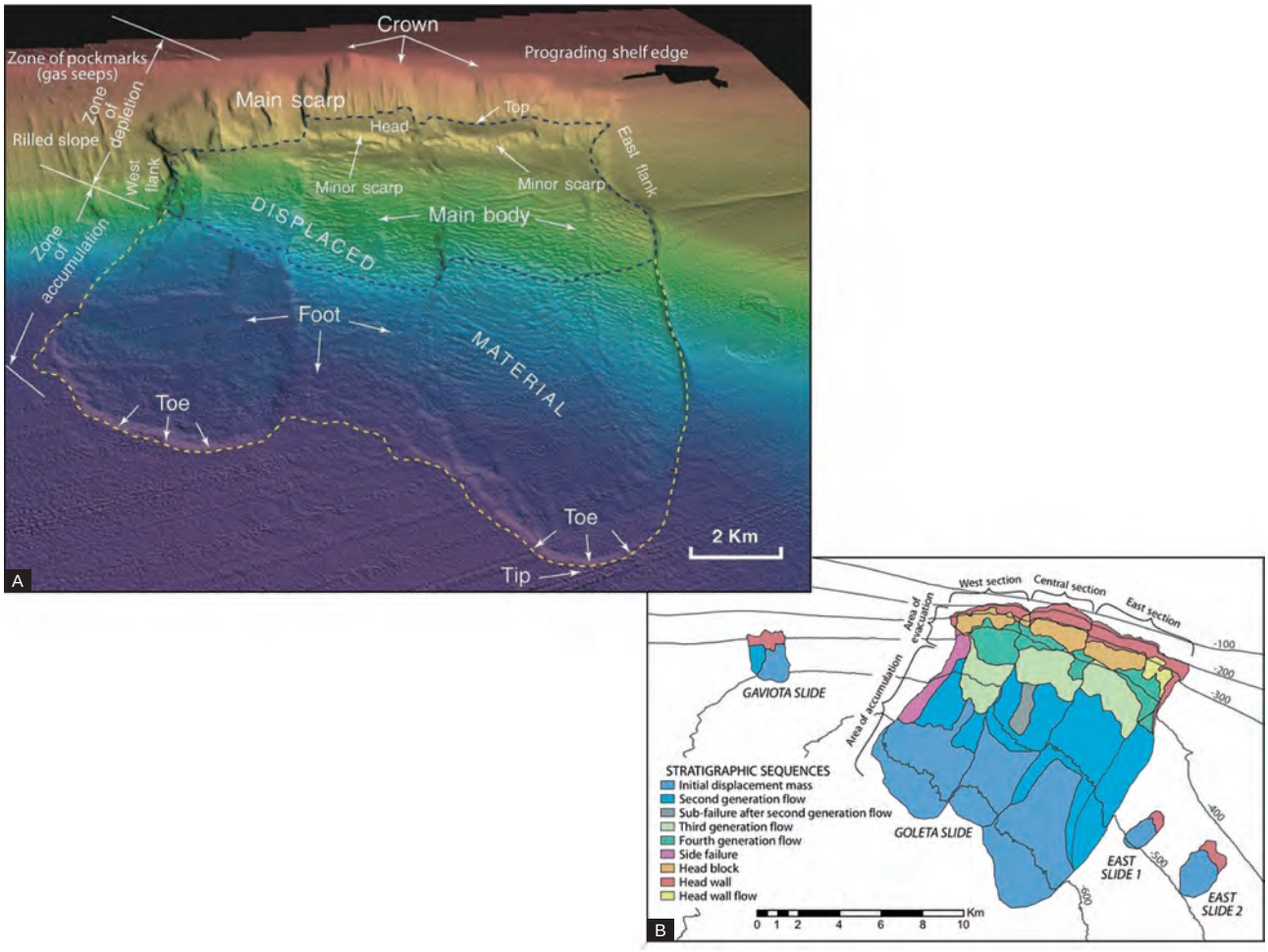

Figure 2 A−Multibeam bathymetric image of the Goleta slide complex in the Santa Barbara Channel, southern California. Note lobe-like (dashed line) distribution of displaced material that was apparently detached from the main scarp near the shelf edge. This mass transport complex is composed of multiple segments of failed material; B−Sketch of the Goleta mass transport complex in the Santa Barbara Channel, southern California showing three distinct segments (*i.e.*, west, central, and east). Contour intervals (−100, −200, −300, −400, −500, and −600) are in meters. From Greene *et al.* (2006). Images courtesy of H. G. Greene. Credit: European Geosciences Union.

in size (Table 2). On Mars, MTD of immense dimensions (*e.g.*, 3,000 km wide) have been studied (Montgomery *et al.*, 2009, their Figure 9). Large submarine MTD have important implications for developing deep-water petroleum reservoirs. In fact, many petroleum reservoirs currently produce oil and gas from sandy mass-transport deposits (SMTD) worldwide (Shanmugam, 2006a, 2012a). Petroleum-related examples are: (1) the occurrence of submarine landslides in all continental margins that are areas of active petroleum exploration (Mienert *et al.*, 2002, their Figure 1); (2) potential petroleum reservoirs associated with a submarine landslide located off Baltimore Canyon on the U.S. Atlantic margin (Malahoff *et al.*, 1978); (3) the location of the Ormen Lange gas field inside the Storegga Slide scar, offshore Norway (Solheim *et al.*, 2005a; Bryn *et al.*, 2005); (4) petroleum-producing reservoirs composed of SMTD and associated sand injections in the North Sea, including the Gryphon Field (Shanmugam *et al.*, 1995; Purvis *et al.*, 2002; Duranti and Hurst, 2004), Norwegian Sea (Shanmugam *et al.*, 1994), Gulf of Mexico (Shanmugam, 2006a, 2012a), Mexico (Grajales-Nishimura *et al.*, 2000), Brazil (Shanmugam, 2006a), Nigeria (Shanmugam, 1997), Australia (Meckel, 2010), China (Zou *et al.*, 2012), and the Bay of Bengal, India (Shanmugam *et al.*, 2009); (5) the use of 3-D seismic data in predicting reservoir properties of submarine landslides in the Saguenay Fjord, Canada (Hart *et al.*, 2001); (6) reservoir characterization of SMTD (Meckel, 2011); and (7) hydrocarbon traps associated with MTD (Beaubouef and Abreu, 2010; Alves and Cartwright, 2010). Furthermore, MTD form a significant component of deep-water stratigraphy in the Espírito Santo Basin, SE Brazil, where MTD constitute more than 50% of Eocene-

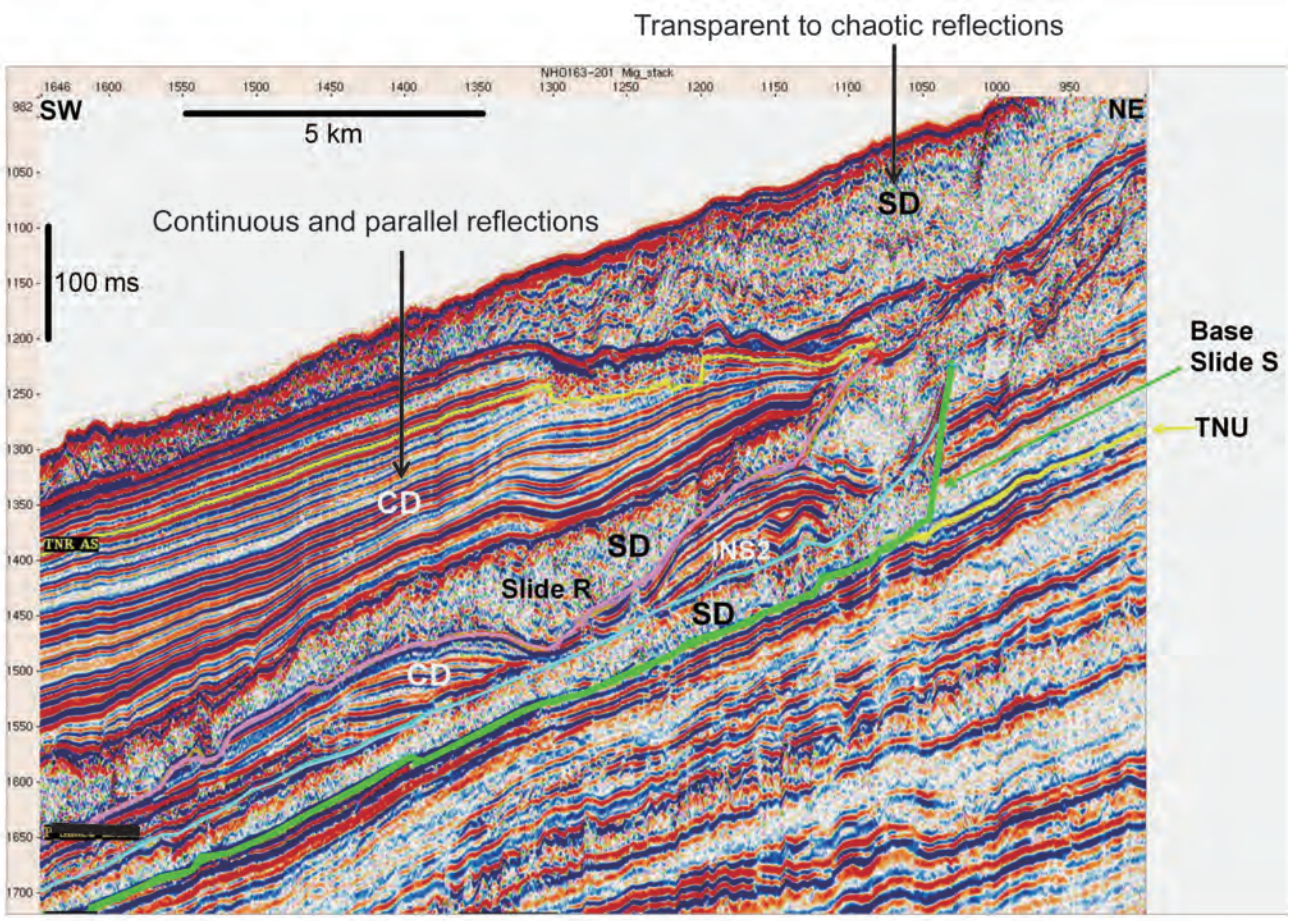

Figure 3 Seismic profile showing transparent (homogeneous) to chaotic internal reflections of slide deposits (SD). Note continuous and parallel internal reflections of contourite deposits (CD). The Storegga Slide on the mid-Norwegian continental margin. TNU=Local slip plane. Profile courtesy of A. Solheim. Modified after Solheim *et al.* (2005b). With permission from Elsevier Copyright Clearance Center's RightsLink: Licensee: G. Shanmugam. License Number: 3570801423159. License Date: February 16, 2015.

Table 1 Worldwide large subaerial and submarine mass-transport deposits (MTD), their sizes (volume), triggering mechanisms, and damages in the 20th and 21st Centuries. The term "landslide" was originally used to describe these examples. Modified after USGS (2010).

Year	Location	Name and type	Triggering mechanism	Size, damage, and loss of human life
1911	Tajikistan	Usoy MTD	Usoy earthquake, magnitude 7.4	2,000,000,000 m^3 54 deaths
1914	Argentina	Rio Barrancas and Rio Colorado debris flow	Failure of ancient MTD dam	2,000,000 m^3 Length of flow: 300 km
1919	Indonesia (Java)	Kelut MTD	Eruption of Kelut Volcano	185 km (length) Lahars caused 5,110 deaths, and destroyed or damaged 104 villages
1920	China (Gansu), Haiyuan	Loess flows, MTD	Haiyuan earthquake, magnitude 8.5	50,000 km^2 (area) 100,000+ deaths
1920	Mexico	Rio Huitzilapan debris flows	Earthquake, magnitude 6.5−7.0	>40 km (length) 600−870 deaths
1921	Kazakh Republic	Alma-Ata debris flow	Snow melt, subsequent rainfall	500 deaths
1933	China (Sichuan)	Deixi MTD	Deixi earthquake, magnitude 7.5	>150,000,000 m^3 2,500 deaths

Table 1, continued

Year	Location	Name and type	Triggering mechanism	Size, damage, and loss of human life
1938	Japan (Hyogo)	Mount Rokko MTD	Rainfall	505 deaths or missing, 130,000 homes were destroyed or badly damaged.
1941	Peru	Huaraz debris flow	Failure of moraine dam	10,000,000 m^3 4,000−6,000 deaths
1945	Peru	Cerro Condor-Sencca MTD	Erosional under-cutting	5,500,000 m^3 13 bridges were destroyed.
1949	Tajikistan (Tien Shan Mtns.)	Khait MTD	Khait earthquake, magnitude 7.4	245,000,000 m^3 7,200 deaths
1953	Japan (Wakayama)	Arida River MTD	Rainfall Major typhoon (cyclone)	1,046 deaths
1953	Japan (City of Kyoto)	Arida River MTD	Rainfall	336 deaths 5,122 homes were destroyed.
1958	Japan (Shizuoka)	Kanogawa MTD	Rainfall	1,094 deaths 19,754 homes were destroyed.
1960	Chile	Rupanco region MTD	Valdivia earthquake, magnitude 7.5, preceded by heavy rain	40,000,000 m^3 210 deaths
1962	Peru (Ancash)	Nevados Huascaran MTD	Not known	13,000,000 m^3 4,000−5,000 deaths
1963	Italy (Friuli−Venezia Griulia)	Vaoint Reservoir MTD	Not known	250,000,000 m^3 2,000 deaths
1964	United States (Alaska)	Alaska earthquake MTD (also known as “Prince William Sound earthquake”)	Alaska earthquake, magnitude 9.0	211,000,000 m^3 submarine lMTD at Seward; Turnagain Heights MTD, 9,600,000 m^3 Loss: $280,000,000 (1964 dollars); 122 deaths
1965	China (Yunnan)	MTD	Not known	450,000,000 m^3 444 deaths.
1966	Brazil (Rio de Janeiro)	MTD	Rainfall	1,000 deaths
1970	Peru (Ancash)	Nevados Huascaran MTD	Earthquake, magnitude 7.7	30,000,000−50,000,000 m^3 18,000 deaths
1974	Peru	Mayunmarca MTD	Rainfall	1,600,000,000 m^3 450 deaths
1976	Guatemala	Guatemala earthquake MTD	Guatemala earthquake, magnitude 7.5	10,000 MTDs over an area of 16,000 km^2 200 deaths
1980	China (Yichang, Hubei)	Yanchihe MTD	Mining activity-occurred on man-made layered slopes	150,000,000 m^3 284 deaths
1980	United States (Washington)	Mount St. Helens MTD	Eruption of Mount St. Helens volcano	This is the world′s largest historical MTD. 3,700,000,000 m^3 250 homes, 47 bridges, 24 km of rail, and 298 km of highway were destroyed; 57 deaths.
1983	United States (Utah)	Thistle MTD	Snow melt and subsequent rainfall	21,000,000 m^3; This is the most expensive disaster to fix in U.S. history with a loss of $600,000,000 (1983 dollars).

Table 1, continued

Year	Location	Name and type	Triggering mechanism	Size, damage, and loss of human life
1983	China (Gansu)	Saleshan MTD	Rainfall	35,000,000 m^3 237 deaths
1983	Ecuador	Chunchi MTD	Rain and/or snow (wettest year of century)	1,000,000 m^3 150 deaths
1985	Colombia (Tolima)	Nevado del Ruiz debris flows	Eruption of Nevado del Ruiz volcano	23,000 deaths
1985	Puerto Rico (Mameyes)	MTD	Rainfall from tropical storm	129 deaths
1986	Papua, New Guinea (East New Britain)	Bairaman MTD	Bairaman earthquake, magnitude 7.1	200,000,000 m^3
1987	Ecuador (Napo)	Reventador MTD	Reventador earthquakes, magnitude 6.1 and 6.9 and rainfall	75,000,000−110,000,000 m^3 1,000 deaths
1987	Venezuela	Rio Limon, debris flow	Rainfall	2,000,000 m^3 210 deaths
1987	Colombia	Villa Tina MTD	Pond leakage	20,000,000 m^3 217 deaths
1988	Brazil	Rio de Janeiro and Petropolis MTD	Rainfall	Approximately 300 deaths
1989	China (Huaying, Sichuan)	Xikou MTD	Rainfall	221 deaths
1991	China (Zhaotong, Yunan)	Touzhai MTD	Rainfall	18,000,000 m^3 216 deaths
1991	Chile	Antofagasta debris flows	Rainfall	500,000,000−700,000,000 m^3 “Hundreds” of deaths were reported.
1993	Ecuador	La Josefina MTD	Mine excavation and heavy rainfall	20,000,000−25,000,000 m^3 13 bridges destroyed
1994	Colombia (Cauca)	Paez MTD	Paez earthquake, magnitude 6.0	250 km^2 (area) 272 deaths
1998	Northern India (Malpa Himalaya Region)	Large MTD	Rainfall	221 deaths
1998	Italy (Campania)	MTD	Rainfall	More than 100 individual slope failures
1998	Honduras, Guatemala, Nicaragua, El Salvador	MTD	Rainfall	Hurricane Mitch caused torrential rainfall. Approximately 10,000 deaths
1999	Venezuela (Vargas, northern coastal area)	MTD	Rainfall	Nearly 1m of heavy rain fall in a 3-day period. There were as many as 30,000 deaths. Loss: $1,900,000,000 in 2001 U.S. dollars
1999	Taiwan	MTD	Chi−Chi earthquake, magnitude 7.3	11,000 km^2 (area) 158 deaths
2000	Tibet	Yigong MTD	Meltwater from snow and glacier	100,000,000 m^3 109 deaths

Table 1, continued

Year	Location	Name and type	Triggering mechanism	Size, damage, and loss of human life
2001	El Salvador	MTD, lateral spreading, liquefaction	2 earthquakes; 1/13/2001: magnitude 7.7 2/13/2001: magnitude 6.6	The January earthquake caused MTD over a 25,000 km^2 area, (including parts of Guatemala). The February earthquake caused MTD over a 2,500 km^2 area. ~585 deaths
2002	Russia (North Ossetia)	Kolka Glacier debris flows	Detachment of large glacier, causing a debris flow	Travel distance: 19.5 km; 110,000,000 m^3 volume of glacial ice deposited 2,000,000−5,000,000 m^3 of ice debris at end of runout; 125 deaths
2003	Sri Lanka (Ratnapura and Hambantota)	MTD	Rainfall	24,000 homes and schools destroyed, 260 deaths
2003	United States (San Bernardino County, California)	Debris flows	Rainfall	>1,000,000 m^3 (total volume) 16 deaths
2005	Pakistan and India	MTD	Kashmir earthquake, magnitude 7.6	Thousands of MTD 25,500 deaths
2006	Philippines (Leyte)	MTD	Rainfall	15,000,000 m^3 1,100 deaths
2008	China (Sichuan)	MTD	Wenchuan earthquake, magnitude 8.0	15,000 MTD, and 20,000 deaths Still being assessed
2008	Egypt (East Cairo)	Al−Duwayqa MTD	Destabilization due to man-made construction	Affected area was 6,500 m^3 volume and rocks weighed about 18,000 tons. 107 deaths
2010	Uganda (Bududa)	Debris flows	Heavy rainfall	400+ deaths Still being assessed
2010	Brazil (Rio De Janeiro)	Debris flows	Heavy rainfall	350 deaths Still being assessed

Table 2 Comparison of large-volume (> 100 km^3) mass-transport deposits (MTD) in submarine environments with four of the largest MTD in subaerial environments. Note that the world′s largest submarine MTD (20,331 km^3) is 10 times volumetrically larger than the world′s largest subaerial MTD (2000 km^3). The term "landslide" was used to describe many of these examples by the original authors. Locations of selected examples are shown in Figure 1. Compiled from several sources.

MTD (Reference)	Volume in km^3	Environment (Age)	Comments
1. Agulhas slump SE African margin (Dingle, 1977)	20,331	Submarine (Post-Pliocene)	The world′s largest submarine MTD triggered by earthquakes
2. Chamais slump SE African margin (Dingle, 1980)	17,433	Submarine (Neogene)	Triggered by earthquakes
3. Nuuanu debris avalanche, NE Oahu, Hawaii (Normark *et al.*, 1993; Moore *et al.*, 1994)	5000	Submarine (2.7 Ma, Ward, 2001)	Triggered by volcanic activity; Debris avalanche is a velocity-based term (see text).
4. Storegga slide Offshore Norway (Bugge *et al.*, 1987; Haflidason *et al.*, 2005)	2400−3200	Submarine (8100 yrs BP)	Triggered by earthquakes

Table 2, continued

MTD (Reference)	Volume in km^3	Environment (Age)	Comments
5. WMTD, Amazon fan Equatorial Atlantic (Piper *et al.*, 1997)	2000	Submarine (Late Pleistocene)	WMTD: Western mass-transport deposits. Possibly triggered during falling sea level (Damuth *et al.*, 1988)
6. Insular slope slide Puerto Rico (Schwab *et al.*, 1993)	1500	Submarine (Quaternary?)	Triggered by earthquakes
7. Brunei slide NW Borneo (Gee *et al.*, 2007)	1200	Submarine (Quaternary?)	Triggered by sediment loading, gas hydrates, and earthquakes
8. Saharan debris flow NW African Margin (Embley, 1976; Embley and Jacobi, 1977; Gee *et al.*, 1999)	600−1100	Submarine (60,000 yrs BP)	Long-runout volcaniclastic debris flows of over 400 km on gentle slopes that decrease to as little as 0.05º
9. Orotava−Icod−Tino debris avalanche, NW African slope (Wynn *et al.*, 2000)	1000	Submarine (Pleistocene)	Debris avalanche is a velocity-based term (see text).
10. Slump complex, Israel (Frey-Martinez *et al.*, 2005)	1000	Submarine (Plio−Quaternary)	Triggered by earthquakes
11. Bassein slide Sunda Arc, NE Indian Ocean (Moore *et al.*, 1976)	900	Submarine (Late Quaternary)	Triggered by earthquakes
12. Alika 1 and 2 debris avalanches, NE Oahu, Hawaii (Normark *et al.*, 1993)	200−800	Submarine (300,000−105,000 yrs BP))	Triggered by volcanic activity; Debris avalanche is a velocity-based term (see text).
13. Nile MTC offshore Egypt (Newton *et al.*, 2004)	670	Submarine (Quaternary)	MTC = Mass-transport complex; triggered by rapid sedimentation
14. Copper River slide Kayak Trough Northern Gulf of Alaska (Carlson and Molnia, 1977)	590	Submarine (Holocene)	Possibly triggered by earthquakes and rapid sedimentation
15. MTC 1, Trinidad (Moscardelli *et al.*, 2006)	242	Submarine (Plio−Pleistocene)	MTC 1 = Mass-transport complex 1; triggered by tectonic activity and rapid sedimentation
16. Cape Fear MTD The Carolina Trough U.S. Atlantic Margin (Popenoe *et al.*, 1993; Lee, 2009)	200	Submarine (Pleistocene)	Triggered by salt tectonism and gas hydrate decomposition
17. The 1929 Grand Banks MTD, off the U.S. Atlantic coast and Canada (Heezen and Ewing, 1952; Piper and Aksu, 1987; Driscoll *et al.*, 2000; Bornhold *et al.*, 2003)	185−200	Submarine (1929)	Triggered by earthquakes, magnitude 7.2
18. Currituck slide U.S. Atlantic Margin (Locat *et al.*, 2009)	165	Submarine (24−50 ka)	Triggered by earthquakes and high pore pressure
19. East Breaks slide (western lobe) NW Gulf of Mexico (McGregor *et al.*, 1993)	~160	Submarine (15−20 ka)	Possibly triggered by salt tectonism

Table 2, continued

MTD (Reference)	Volume in km^3	Environment (Age)	Comments
20. MTD, Mississippi Canyon area Gulf of Mexico (McAdoo *et al.*, 2000)	152	Submarine (Holocene)	Triggered by salt tectonism and rapid sedimentation
21. Jan Mayen Ridge Norwegian−Greenland Sea (Laberg *et al.*, 2014)	60	Submarine (Pliocene and Pleistocene)	Retrogressive movement
22. Owen Ridge Oman coast, Arabian Sea (Rodriguez *et al.*, 2013)	40	Submarine (Holocene)	Retrogressive slumps
23. Markagunt gravity slide, SW Utah (USA) (Hacker *et al.*, 2014)	1700−2000	Subaerial 21−22 Ma	The world′s largest prehistoric subaerial volcanic MTD
24. Saidmarreh Slide Kabir Kuh anticline, SW Iran (Harrison and Falcon, 1938)	20	Subaerial (10,370+/−120 years BP, Shoaei and Ghayoumian, 1998)	The world′s second largest prehistoric subaerial MTD triggered by earthquakes
25. Mount St. Helens, USA (Schuster, 1983; Tilling *et al.*, 1990)	2.8	Subaerial (May 18, 1980)	The world′s largest historic subaerial MTD triggered by volcanic eruption (USGS, 2004)
26. Usoy, Tadzhik Republic (Formerly USSR) (Bolt *et al.*, 1975)	2.0	Subaerial (1911)	The world′s second largest historic subaerial MTD triggered by earthquakes, magnitude = 7.4 (USGS, 2010)

Oligocene strata (Gamboa *et al.*, 2010). Because the petroleum industry is moving exploration increasingly into the deep-marine realm to meet the growing demand for oil and gas, a clear understanding of deep-marine MTD is of great economic interest. For this reason, detailed descriptions of 7,832 meters of conventional cores from 123 wells, representing 32 petroleum fields worldwide (Table 3), provide the empirical data in this review.

1.2 Description of the problem

The basic problem stems from our failure to follow a sound and commonly applied concept for classifying MTD. In acknowledging this chronic problem, Camerlenghi *et al.* (2010, p. 506) state, "*For typology, we selected the following terms according to the terminology in the original manuscripts*: *Debris Avalanche*; *debris flow*; *deep-seated failure* (*when recognized mainly in deep penetration seismic profiles rather than bathymetric maps*); *glide*; *gravitational collapse*; *mass failure*; *mass transport*; *mass wasting*; *megaturbidite*; *slide*; *slump*. *Such terms often describe similar deposits. For the time being we have not modified the terminology. It is obvious that a unified terminology is needed for correct understanding and comparison of sedimentary deposits originated from submarine sediment mass transport*." There is absolutely no sedimentological basis for equating large turbidites (*i.e.*, megaturbidites) with slumps, slides, or debris avalanches. The current complacent usage of superfluous nomenclature is not only confusing but unnecessary. Clearly, there is a need for conceptual clarity, which is one of the objectives of this article.

The conceptual and nomenclatural problems are not unique to MTD. Similar problems are associated with turbidites (Sanders, 1965; Shanmugam, 1996) and tsunamites (Shanmugam, 2006b). What is troubling is that the problems of MTD are tightly intertwined with those of turbidites and tsunamites. This conceptual interconnection has led to a long lexicon of 79 types of MTD, which include normal turbidites, high-density turbidites, seismoturbidites, megaturbidites, fluxoturbidites, atypical turbidites, and tsuamites (Table 4).

Since the first use of the term "landslide" by James Dwight Dana in 1838 (Cruden, 2003), it has been adopted for a number of different downslope mass-transport processes that operate not only in subaerial (Shreve, 1968; Coates, 1977; Cruden, 1991; Highland and Bobrowsky, 2008), sublacustrine (Moernaut and De Batist, 2011), and submarine (Prior and Coleman, 1979; Schwab *et al.*, 1993;

Table 3 Summary of deep-water case studies, based on description of core and outcrop, carried out by the present author on MTD and SMTD (1974–2011). Note that most SMTD examples are petroleum-bearing deep-water reservoirs. Modified after Shanmugam (2014b).

Location symbol and number in Figure 1	Case studies	Thickness of core and outcrop described*	Comments (This paper)
1. Gulf of Mexico, U.S. (Shanmugam *et al.*, 1988b)	1. Mississippi fan, Quaternary, DSDP Leg 96	~ 500 m DSDP core (selected intervals described)	Mass-transport deposits, turbidites, bottom-current reworked sands
1. Gulf of Mexico, U.S. (Shanmugam *et al.*, 1993a, 1993b; Shanmugam and Zimbrick, 1996)	2. Green Canyon, Late Pliocene, 3. Garden Banks, Middle Pleistocene 4. Ewing Bank 826, Pliocene–Pleistocene 5. South Marsh Island, Late Pliocene 6. South Timbalier, Middle Pleistocene 7. High Island, Late Pliocene 8. East Breaks, Late Pliocene–Holocene	1067 m Conventional core and piston core 25 wells	Sandy mass-transport deposits and bottom-current reworked sands common
2. California (Shanmugam and Clayton, 1989; Shanmugam, 2006a, 2012a)	9. Midway Sunset Field, upper Miocene, onshore	650 m Conventional core 3 wells	Sandy mass-transport deposits and bottom-current reworked sands
3. Ouachita Mountains, Arkansas and Oklahoma, U.S. (Shanmugam and Moiola, 1995)	10. Jackfork Group, Pennsylvanian	369 m 2 outcrop sections	Sandy mass-transport deposits and bottom-current reworked sands common
4. Southern Appalachians, Tennessee, U.S. (Shanmugam, 1978; Shanmugam and Benedict, 1978)	11. Sevier Basin, Middle Ordovician	2152 m 5 outcrop sections	Mass-transport deposits, turbidites, bottom-current reworked sands
5. Brazil (Shanmugam, 2006a, 2012a)	12. Lagoa Parda Field, lower Eocene, Espirito Santo Basin, onshore 13. Fazenda Alegre Field, upper Cretaceous, Espirito Santo Basin, onshore 14. Cangoa Field, upper Eocene, Espirito Santo Basin, offshore 15. Peroá Field, lower Eocene to upper Oligocene, Espirito Santo Basin, offshore 16. Marlim Field, Oligocene, Campos Basin, offshore 17. Marimba Field, upper Cretaceous, Campos Basin, offshore 18. Roncador Field, upper Cretaceous, Campos Basin, offshore	200 m Conventional core 10 wells	Sandy mass-transport deposits and bottom-current reworked sands common
6. North Sea (Shanmugam *et al.*, 1995)	19. Frigg Field, lower Eocene, Norwegian North Sea 20. Harding Field (formerly Forth Field), lower Eocene, U.K. North Sea 21. Alba Field, Eocene, U.K. North Sea 22. Fyne Field, Eocene, U.K. North Sea 23. Gannet Field, Paleocene, U.K. North Sea 24. Andrew Field, Paleocene, U.K. North Sea 25. Gryphon Field, upper Paleocene–lower Eocene, U.K. North Sea	3658 m Conventional core 50 wells	Sandy mass-transport deposits and bottom-current reworked sands common
7. U.K. Atlantic Margin (Shanmugam *et al.*, 1995)	26. Faeroe area, Paleocene, west of the Shetland Islands 27. Foinaven Field, Paleocene, west of the Shetland Islands	Thickness included in the North Sea count 1 well Conventional core 1 well	Sandy mass-transport deposits and bottom-current reworked sands common

Table 3, continued

Location symbol and number in Figure 1	Case studies	Thickness of core and outcrop described*	Comments (This paper)
8. Norwegian Sea and vicinity (Shanmugam *et al.*, 1994)	28. Mid-Norway region, Cretaceous, Norwegian Sea 29. Agat region, Cretaceous, Norwegian North Sea	500 m Conventional core 14 wells	Sandy mass-transport deposits and bottom-current reworked sands common
9. French Maritime Alps, southeastern France (Shanmugam, 2002, 2003)	30. Annot Sandstone, Eocene−Oligocene	610 m** 1 outcrop section (12 units described)	Sandy mass-transport deposits and bottom-current reworked sands common (deep tidal currents)
10. Nigeria (Shanmugam, 1997, 2006a, 2012a)	31. Edop Field, Pliocene, offshore	875 m Conventional core 6 wells	Sandy mass-transport deposits and bottom-current reworked sands common (deep tidal currents)
11. Equatorial Guinea (Famakinwa *et al.*, 1996; ; Shanmugam, 2006a, 2012b)	32. Zafiro Field, Pliocene, offshore 33. Opalo Field, Pliocene, offshore	294 m Conventional core 2 wells	Sandy mass-transport deposits and bottom-current reworked sands common
12. Gabon (Shanmugam, 2006a, 2012a)	34. Melania Formation, lower Cretaceous, offshore (includes four fields)	275 m Conventional core 8 wells	Sandy mass-transport deposits and bottom-current reworked sands common
13. Bay of Bengal, India (Shanmugam *et al.*, 2009)	35. Krishna−Godavari Basin, Pliocene	313 m Conventional core 3 wells	Sandy debrites and tidalites common
Kutei Basin , Makassar Strait (Saller *et al.*, 2006)	Kutei Basin, Miocene	2 wells? (Saller *et al.*, 2006, 2008a, 2008b)	Discussion of problematic turbidites (Shanmugam, 2008a, 2013c, 2014a)
Total thickness of rocks described by the author		11,463 m	

* The rock description of 35 case studies of deep-water systems comprises 32 petroleum-producing massive sands worldwide. Description of core and outcrop was carried out at a scale of 1:20 to 1:50, totaling 11,463 m, during 1974−2011, by G. Shanmugam as a Ph.D. student (1974−1978), as an employee of Mobil Oil Corporation (1978−2000), and as a consultant (2000−2011). Global studies of cores and outcrops include a total of 7832 meters of conventional cores from 123 wells, representing 32 petroleum fields worldwide (Shanmugam, 2013d).These modern and ancient deep-water systems include both marine and lacustrine settings.

** The Peira Cava outcrop section was originally described by Bouma (1962), and later by Pickering and Hilton (1988, their Figure 62), among others.

Table 4 Nomenclature of 79 different types of mass-transport processes and their deposits with overlapping and confusing meanings. Compiled from several sources. Updated after Shanmugam (2012a).

Nomenclature	Characteristics	Reference	Comments
1. Landslide: Type 1 (First classification by J. D. Dana in 1862) (see Cruden, 2003)	Refers to three processes: rock slides, earth spreads, and debris flows	Cruden (2003)	Impractical * (MTD or SMTD)**
2. Landslide: Type 2 (GSA Thematic Volume)	A general term used for various moderately rapid gravity-induced mass movements, which exclude creep and solifluction	Coates (1977)	Impractical (MTD or SMTD)
3. Landslide: Type 3 (AGI Glossary)	A general term for a variety of gravity-induced downslope mass movements, which include creep and solifluction	Bates and Jackson (1980)	Impractical (MTD or SMTD)

Table 4, continued

Nomenclature	Characteristics	Reference	Comments
4. Landslide: Type 4 (NATO Workshop)	A sudden movement of earth and rocks down a steep slope	Saxov (1982) (See also Cruden, 1991)	Impractical (MTD or SMTD)
5. Landslide: Type 5 (USGS Handbook)	A downslope movement of rock or soil, or both, occurring on the surface of rupture in which much of the material often moves as a coherent or semi-coherent mass with little internal deformation	Highland and Bobrowsky (2008) (See also Eckel, 1958)	Impractical (MTD or SMTD)
6. Fall or rockfall	Freefall of material from steep slopes	Varnes (1978)	Impractical (MTD or SMTD)
7. Sand fall	Freefall of material at submarine canyon heads	Shepard and Dill (1966)	Impractical (SMTD)
8. Topple	Tilting without collapse	Varnes (1978)	Impractical (MTD or SMTD)
9. Slide	Coherent mass with translational movement	Dott (1963)	Slide
10. Slump	Coherent mass with rotational movement and internal deformation	Dott (1963)	Slump
11. Translational slump	Translational movement	Milia *et al.* (2006)	Translational movements associated with slides (Dott., 1963), MTD
12. Drained slump	Slumping without excess pore pressure	Morgenstern (1967)	Impractical (MTD)
13. Undrained slump	Slumping with excess pore pressure	Morgenstern (1967)	Impractical (MTD)
14. Toreva-block (Named after the village of Toreva in Arizona, USA)	Backward rotational slip	Reiche (1937)	Impractical (MTD or SMTD)
15. Spread	Lateral extension accommodated by shear or tensile fractures	Varnes (1978)	Impractical (MTD or SMTD)
16. Debris flow	Plastic (en masse) flow with laminar state	Dott (1963), Hampton (1972)	Debrite
17. Debris avalanche	Extremely fast-moving debris flows	Varnes (1978)	Impractical (MTD or SMTD)
18. Cohesionless debris avalanche	Rolling, cascading, and collision of rock fragments on steep underwater slopes	Prior and Bornhold (1990)	Impractical (SMTD)
19. Rock-fragment flow	Large extremely rapid “rock fall-debris flows”	Varnes (1958, 1978)	Impractical (MTD)
20. Debris slide	Slow-moving mass that breaks up into smaller blocks	Varnes (1978)	Impractical (MTD or SMTD)
21. Flow slide (two words)	Disintegrating subaerial slide in coarse material where a temporary transfer of part of the normal stress onto the fluids of the void space, with a consequent sudden decrease in strength	Koppejan *et al.* (1948) (see also Rouse, 1984)	Impractical (MTD or SMTD)
22. Flow slide (two words)	High-velocity, transitional type between slumps and debris lows	Shreve (1968)	Impractical (MTD or SMTD)
23. Flowslide (one word)	Basal dense layer with viscoplastic behavior in stratified submarine sediment flows	Norem *et al.* (1990)	SMTD and associated turbidite

Table 4, continued

Nomenclature	Characteristics	Reference	Comments
24. Marine flow slide	Liquefied marine sand with high porosity and high pore-water pressure	Koning (1982)	Impractical (SMTD)
25. Retrogressive flow slide	Occurring along banks of noncohesive clean sand or silt and showing repeated fluctuations in porewater pressure	Andresen and Bjerrum (1967)	Impractical (SMTD)
26. Deep creep	Slow moving mass of bedrock (Synonym: rock flow)	Varnes (1978, his Figure 2.2)	Impractical (MTD or SMTD)
27. Soil creep	Slow moving mass of fine soil	Varnes (1978, his Figure 2.2)	Impractical (MTD or SMTD)
28. Seasonal creep	Slow moving mass within the soil horizon affected by seasonal changes in soil moisture and temperature	Hansen (1984)	Impractical (MTD or SMTD)
29. Continuous creep	Slow moving mass where shear sress continuously exceeds the material strength	Hansen (1984) (USGS, 2004)	Impractical (MTD or SMTD)
30. Progressive creep	Slow moving mass associated with slopes reaching point of failure by other mass movements	Hansen (1984)	Impractical (MTD or SMTD)
31. Talus creep	Slow moving large angular rock fragments on a gentle slope (Synonym: scree creep)	Sharpe (1938)	Impractical (MTD or SMTD)
32. Slump-creep	Slow moving multiple processes	Carter and Lindqvist (1975)	Impractical (MTD or SMTD)
33. Mass creep	Slow moving submarine slope sediments due to repeated loading effects by earthquakes	Almagor and Wiseman (1982)	Impractical (MTD or SMTD)
34. Rock-glacier creep	Slow moving tongue of the rock glacier	Sharpe (1938)	Impractical (MTD or SMTD)
35. Solifluction (Soil flow of Varnes, 1978)	Slow moving waterlogged soil over permafrost layers	Anderson (1906)	Impractical (MTD)
36. Earth flows	Slow-to fast-moving fine soil	Varnes (1978)	Impractical (MTD)
37. Sturzstrom (Synonym: rock avalanche)	Fast-moving debris flows	Hsü (1975, 2004)	Impractical (MTD or SMTD)
38. Inertia flow	Grain avalanching	Bagnold (1954)	SMTD
39. Grain flow	Sediment support by grain collision	Middleton and Hampton (1973)	SMTD
40. Fluidized flow	Full sediment support by upward intergranular flow	Middleton and Hampton (1973)	Impractical (SMTD)
41. Liquefied flow	Partial sediment support by upward intergranular flow	Lowe (1976)	Impractical (SMTD)
42. Turbidity current	Sediment support by fluid turbulence	Middleton and Hampton (1973)	Turbidite, not MTD
43. Sand flow	A flow of wet sand that is subjected to fluctuations in pore-water pressure	Varnes (1958)	Impractical (SMTD)
44. Loess flow	Intermediate stage between “liquefaction flow” and “sand flow” with increasing grain size	Coates (1977)	Impractical (MTD)

Table 4, continued

Nomenclature	Characteristics	Reference	Comments
45. "High-density turbidity current"	Stratified lower debris flow and upper turbidity current	Kuenen (1951)	Debrite and turbidite (Shanmugam, 1996)
46. Sandy debris flow	Sandy flow with plastic rheology and laminar state	Shanmugam (1996)	Sandy debrite
47. Cohesionless liquefied sandflow	Sliding-related sandy mass flows	Nemec (1990, his Figure 32)	Impractical SMTD
48. Hyperconcentrated flow	Sediment concentration: 20−60 by volume %	Pierson and Costa (1987)	Impractical SMTD
49. Slurry flow	Cohesive debris flows	Carter (1975a)	Impractical MTD
50. Slurry flow	Synonym for "High-density turbidity current"	Lowe and Guy (2000)	Impractical MTD or SMTD
51. Lahar	Volcaniclastic debris flow	Bates and Jackson (1980)	MTD or SMTD
52. Nuée ardente	Decoupling of pyroclastic flows (*i.e.*, stratified flows)	Fisher (1995)	Impractical MTD
53. Cascading dense water event	Analogous to "sand fall" of Shepard and Dill (1966)	Gaudin *et al.* (2006)	Impractical (SMTD)
54. Dense flow	Basal high-concentration layer in stratified sediment flows	Norem *et al.* (1990)	SMTD and associated turbidite
55. Fluidized cohesionless-particle flow	Basal high-concentration layer in stratified sediment flows	Friedman *et al.* (1992)	SMTD and associated turbidite
56. Liquefied cohesionless coarse-particle flow	Basal high-concentration layer in stratified sediment flows	Sanders and Friedman (1997)	SMTD and associated turbidite
57. Slide	Basal high-concentration layer in stratified sediment flows	Kuenen (1951)	Impractical MTD or SMTD
58. Flowing-grain layer	Basal high-concentration layer in stratified sediment flows	Sanders (1965)	SMTD and associated turbidite
59. Laminar inertia-flow	Basal high-concentration layer in stratified sediment flows	Postma *et al.* (1988)	SMTD and associated turbidite
60. Laminar sheared layer	Basal high-concentration layer in stratified sediment flows	Vrolijk and Southard (1997)	SMTD and associated turbidite
61. Traction carpet	Basal high-concentration layer in stratified sediment flows	Dzulynski and Sanders (1962)	SMTD and associated turbidite
62. Avalanching flow	Basal high-concentration layer in stratified sediment flows	Sanders (1965)	SMTD and associated turbidite
63. Mass flow	Basal high-concentration layer in stratified sediment flows	Friedman *et al.* (1992)	SMTD and associated turbidite
64. Mass flow	Plastic flow with shear stress distributed throughout the mass	Nardin *et al.*, (1979)	MTD or SMTD
65. Laminar mass flow	Gradational processes involving sand flows, slumping, sliding, and spontaneous liquefaction	Carter (1975b)	SMTD
66. Granular mass flow	Concentrated grain (> 0.06 mm)-fluid mixtures in rock avalanches, debris flows, and pyroclastic flows	Iverson and Vallance (2001)	Impractical SMTD

Table 4, continued

Nomenclature	Characteristics	Reference	Comments
67. Hyperpycnal flow	Sinking river water that has higher density than basin water	Bates (1953), Mulder *et al.* (2003)	Impractical MTD
68. Dense flow	Multiple processes	Gani (2004)	SMTD and associated turbidite
69. Hybrid flow	Multiple processes	Houghton *et al.* (2009)	SMTD and associated turbidite
70. Tsunamite (deposit)	"Rope-ladder texture" and multiple processes	Michalik (1997)	Impractical Shanmugam (2006b)
71. Homogenite (deposit, Kastens and Cita, 1981)	Uniform texture, considered synonymous with submarine landslide and megaturbidite	Camerlenghi *et al.* (2010)	Turbidite, not MTD (Shanmugam, 2006b)
72. Olistostrome (deposit)	Submarine gravity sliding or slumping	Flores (1955); Hsü (1974)	Impractical (MTD or SMTD)
73. Gravitite (deposit)	Debris flows	Natland (1967)	Impractical (MTD or SMTD)
74. Gravite (deposit)	Slide, slump, debris flow, dense flow, and turbidity current	Gani (2004)	Impractical (MTD or SMTD)
75. Fluxoturbidite (deposit) (See Hsü, 2004 for a critique of this term)	Sand avalanche	Dzulynski *et al.* 1959	Impractical (SMTD)
76. Seismoturbidite (deposit)	Large-scale mass flows	Mutti *et al.* (1984)	Impractical (SMTD)
77. Megaturbidite (deposit)	Large-scale debris flows	Labaume *et al.* (1987)	Impractical (SMTD)
78. Atypical turbidite (deposit)	Slumps, debris flows, and sand flows	Stanley *et al.* (1978)	Impractical (SMTD)
79. Duplex-like structures (deposit)	Slumps and debris flows	Shanmugam *et al.* (1988a)	Impractical (MTD)

* In some cases, it is impractical to interpret a specific process from the rock record. In such cases, a non-specific term of MTD or SMTD is preferred.
**MTD = Mass-transport deposits. SMTD = Sandy mass-transport deposits.

Hampton *et al.*, 1996; Locat and Lee, 2000, 2002; Masson *et al.*, 2006; Feeley, 2007; Twichell *et al.*, 2009) environments on Earth, but also in extraterrestrial environments on Venus (Malin, 1992), Mars (Lucchitta, 1979; McEwen, 1989; Montgomery *et al.*, 2009), and Saturn′s satellite Iapetus (Singer *et al.*, 2012), among others. At present, the literal meaning of the word landslide is totally lost in the geologic and engineering literature. For example, (1) Hungr (1995, p. 610) states, "*…rapid landslides such as debris flows, debris avalanches, rock slide avalanches, large scale liquefaction failures, and slides…*" in describing subaerial mass-transport processes. (2) Twichell *et al.* (2009, their Figure 2d) labeled the toe of the "Currituck landslide" as "Debris flow deposit" on a 3.5 kHz seismic profile from the U.S. Atlantic margin. (3) Singer *et al.* (2012, p. 574) state that "*Here we analyse images from the Cassini mission and report numerous long-runout landslides on Iapetus, an icy satellite of exceptional topographic relief…We use the ratio of drop height to runout length as an approximation for the friction coefficient of landslide material*." The above three examples, selected among many other similar ones, reveal the following fundamental problems:

- The use of the term landslide, with a built-in reference to a sliding motion, to represent topples without a sliding motion or debris flows with a flowing motion is er-

roneous (Varnes, 1978). In acknowledging this basic problem, Brabb (1991, p. 52) state "*Note that Varnes prefers the term* '*slope movements*'. *I will use the more familiar* '*landslides*' *in this paper, even though many processes are loosely termed* '*landslides*' *involve little or no true sliding*." This practice of postponing conceptual problems is chronic in this domain. For example, Hansen (1984, p. 1) states that "*Demands for standardized terminology are common, and certainly moves have been made to improve definition* (*Varnes*, 1978). *As yet the move towards what might be called an impossible ideal is slow, but it still remains a worthy aim*." Disappointingly, Varnes (1984) himself abandoned his own valuable aim and reverted back to the popular and confusing usage of the term "landslide" for a variety of mass-transport processes that involve little or no sliding motion.

- Aspects of sediment failure and related sliding can be measured in modern subaerial environments by installing piezometers and inclinometers (Duncan and Wright, 2005, their Figure 2.7), but such measurements are impractical in modern deep-marine and extraterrestrial environments.
- Motion types can be determined by direct examination of ancient strata in core or outcrop, but the distinction between sliding and flowing motions cannot be ascertained from seismic or radar images.
- The synonymous use of the term landslide for high-velocity debris avalanches is indefensible. This is because there are no objective criteria to distinguish low-velocity flows from high-velocity flows in the depositional record on Earth (Shanmugam, 2006a, 2012a). Nor is there any technique to measure velocity of mass movements on other planets.
- The measure of *H*/*L* (fall height/runout length) ratios of MTD on other planets using radar images and comparison of such data with *H*/*L* ratios of MTD on Earth derived from outcrop or seismic data is incompatible.
- Although MTD on the U.S. Atlantic margin have been described as submarine landslides by Twichell *et al.* (2009), cores from some of these landslides are indeed composed of debrites (Embley, 1980).

The current landslide problem, somewhat analogous to the turbidite problem (Van der Lingen, 1969) and the tsunamite problem (Shanmugam, 2006b; Luczyński, 2012) encountered earlier, requires a rigorous scrutiny of fundamental issues. Therefore, the primary objective here is to bring clarity to the classification of subaerial and submarine downslope processes by combining sound principles of fluid mechanics, soil mechanics, laboratory experiments, study of modern deep-marine systems, and detailed examination of core and outcrop worldwide (Figure 1, Table 3). Specific objectives are: (1) to review the first principles of soil strength and slope stability; (2) to critically evaluate existing nomenclature and classification of downslope processes and select a meaningful scheme; (3) to establish criteria for recognizing process-specific depositional facies in the stratigraphic record using core and outcrop; (4) to classify types of triggering mechanisms of sediment failures and to demonstrate their relevance in discarding popular sea-level models; (5) to discuss problems associated with long-runout mass movements; and finally (6) to emphasize the importance of recognizing process-specific depositional facies in characterizing deep-water petroleum reservoir sands. This review with 403 references is intended for a broad international readership that includes students (both undergraduate and graduate), academic scholars, petroleum geoscientists, engineers, and managers.

1.3 Limitations and organization

There are limitations in organizing this paper in a conventional format with a coherent theme. First, this review is a blend of nomenclatural, conceptual, theoretical, experimental, observational, and interpretational issues. As such, it is difficult to devote the same rigorous attention to details on each issue. For example, unlike sedimentological studies of landslides on Earth, rock-based sedimentological data of landslides on Mars and Venus are totally lacking. Second, the emphasis of submarine MTD in this article is intentional because of their global economic importance in petroleum exploration and production. Third, contrary to the popular usage of the term "landslide" for all types of MTD by other researchers, this paper advocates the strict application of the term solely to a single MTD type. Fourth, in minimizing a tedious text, portions of the paper are organized using numbered or bulleted pithy statements. Fifth, in maintaining some continuity and clarity, selected text and figures are reused from the author′s previous publications.

By necessity, this iconoclastic review is organized, rather unorthodoxly and disjointedly, under the following main headings:

- Mechanics of sediment failure and sliding
- Nomenclature and classification
- Recognition of the three basic types of MTD
- Triggering mechanisms
- Long-runout mechanisms
- Reservoir characterization

2 Mechanics of sediment failure and sliding

Sediment failures on continental margins are controlled by the pull of gravity, the source of the material (bedrock vs. regolith), the strength of the soil (grain size, mineralogy, compaction, cementation, *etc.*), the weight of the material, the slope angle, the pore-water pressure, and the planes of weaknesses. In order to evaluate sediment failures in general, one needs to conduct a slope stability analysis for describing the sediment behavior and sediment strength during loading or deformation.

2.1 Soil strength and slope stability

The most fundamental requirement of slope stability is that the shear strength of the soil must be greater than the shear stress required for equilibrium (Duncan and Wright, 2005; Shanmugam, 2014a). The two conditions that result in slope instability are (1) a decrease in the shear strength of the soil and (2) an increase in the shear stress required for equilibrium. The decrease in the shear strength of the soil is caused by various *in situ* processes, such as an increase in pore-water pressure, cracking of the soil, swelling of clays, leaching of salt, *etc.* The increase in shear stress is induced by loads at the top of the slope, an increase in soil weight due to increased water content, seismic shaking, *etc.*

A common method for calculating the slope stability is the 'Limit equilibrium analyses' in soil mechanics. A stable slope can be maintained only when the factor of safety for slope stability (F) is larger than or equal to 1 (Duncan and Wright, 2005, their equations 6.1 and 13.2):

$$F = \frac{S}{\tau} = \frac{\text{Shear strength of the soil}}{\text{Shear stress required for equilibrium}} \geqslant 1$$

where

S = Available shear strength, which depends on the soil weight, cohesion, friction angle, and pore-water pressure.

τ = Equilibrium shear stress, which is the shear stress required to maintain a just-stable slope. It depends on the soil weight, pore-water pressure, and slope angle.

The shear strength is equal to the maximum shear stress which can be absorbed by the slope without failure and can be defined by the Mohr-Coulomb failure criterion:

$$S = c + \sigma \tan \varphi$$

where

S = Available shear strength (Figure 4A)

c = Cohesion (nonfrictional) component of the soil strength

σ = Total normal stress acting on the failure surface

φ = Angle of internal friction of the soil

By combining the equations of shear strength and Mohr-Coulomb failure criterion, the factor of safety (F) can be expressed as:

$$F = \frac{c + \sigma \tan \varphi}{\tau}$$

A sediment failure is initiated when the factor of safety for slope stability (F) is less than 1 (Figure 4B). In other words, the sliding motion along the shear surface commences only when the driving gravitational force exceeds the sum of resisting frictional and cohesive forces. Initial porosity of the sediment plays a critical factor in controlling the behavior of the shear surface (Anderson and Riemer, 1995). Based on an experimental study on landslides initiated by rising pore-water pressures, Iverson *et al.* (2000) reported that even small differences in initial porosity had caused major differences in mobility. For example, wet sandy soil with 50% porosity contracted during slope failure, partially liquefied, and accelerated to a speed of over 1 m s^{-1}, whereas the same soil with 40% porosity dilated during failure, slipped episodically, and traveled at a slow velocity of 0.2 cm s^{-1}. Finally, soil strength differs between drained and undrained conditions (Terzaghi *et al.*, 1996; USACE, 2003; Duncan and Wright, 2005).

Slides occur commonly on modern slopes of 1−4° (Booth *et al.*, 1993) (Figure 5). Contrary to the popular belief, most submarine slides occur on gentle slopes of less than 4°, sometimes even at 0.25°. Submarine slides on slopes greater than 10° are rare (Figure 5).

2.2 The role of excess pore-water pressure

Terzaghi (1936) first recognized that pore-water pressure controls the frictional resistance of slopes, which has remained the most important concept in understanding landslide behaviour. A founding principle of slope stability is that a rise in pore-water pressure reduces the shear strength of the soil (Skempton, 1960). The shear strength of soil, in particular clays, is controlled by the frictional resistance and interlocking between particles (*i.e.*, physical component), and interparticle forces (*i.e.*, physicochemical component) (Karcz and Shanmugam, 1974; Parchure, 1980; Hayter *et al.*, 2006). Furthermore, bed density and shear strength of soil increase with increasing consolidation (Hanzawa and Kishida, 1981; Dixit, 1982). A rise in pore-water pressure occurs when the saturated soil is stressed, and when the porosity cannot increase or the pore fluid cannot expand or escape through fractures. The ex-

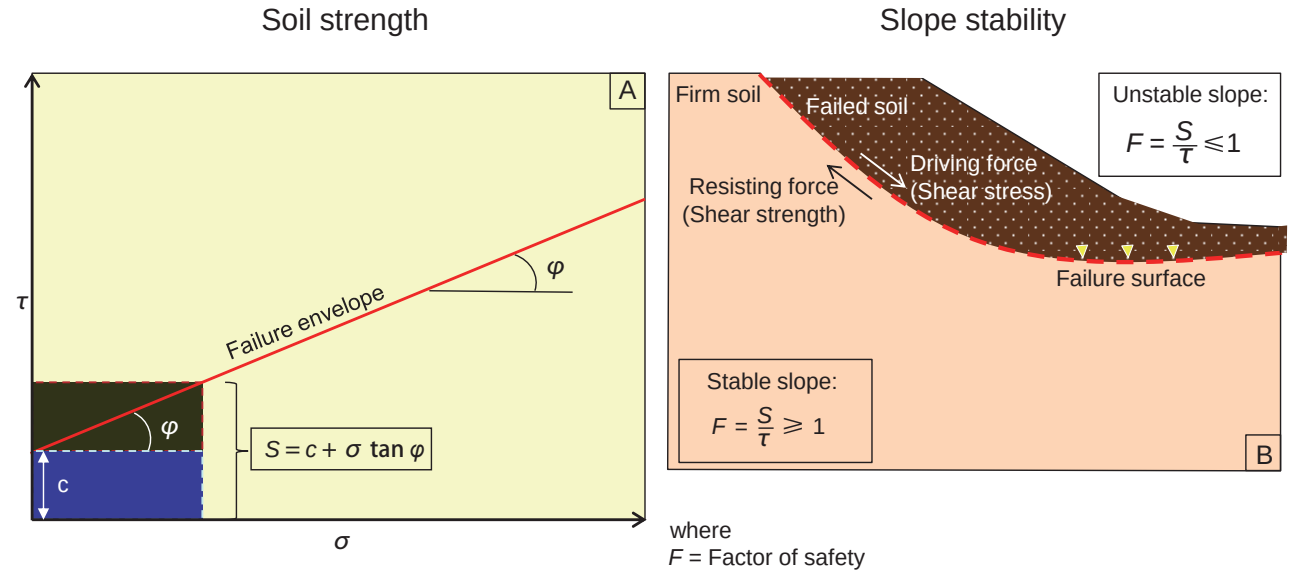

where
S = Shear strength
τ = Shear stress
c = Cohesive component of the soil strength
σ = Total normal stress acting on the failure surface
φ = Frictional component of the soil strength

where
F = Factor of safety
S = Shear strength
τ = Shear stress

Figure 4 A−Plot showing that the shear strength of the soil (*s*) is composed of frictional (φ) and cohesive (*c*) components; B−Conceptual diagram showing that a stable slope can be maintained only when the factor of safety for slope stability (*F*) is larger than or equal to 1 (Duncan and Wright, 2005). The sliding motion of failed soil mass commences along the shear surface when the factor of safety (*F*) is less than 1. Synonyms: Failure surface = slip surface = shear surface = primary glide plane. Compiled from several sources (*e.g.*, USACE, 2003; Duncan and Wright, 2005). From Shanmugam (2014a).With permission from AAPG.

cess pore-water pressure has been considered a vital factor in explaining the origin of subaerial mass-transport processes (Johnson, 1984; Anderson and Sitar, 1995; Iverson, 1997, 2000; Iverson *et al.*, 1997; Jakob and Hungr, 2005). Iverson (1997), based on studies of coarse-grained subaerial debris flows, has developed a model in which excess pore-water pressure causes liquefaction of the sediment and thereby strongly reduces internal friction and increases sediment mobility or runout distances.

Excess pore-water pressures have also been considered a characteristic property in explaining long-runout submarine MTD (Suhayda and Prior, 1978; Hampton *et al.*, 1996; Iverson *et al.*, 1997; Gee *et al.* 1999; Major and Iverson, 1999). Submarine debris flows have lower yield strengths than subaerial debris flows due to entrainment of sea water (Pickering *et al.*, 1989) and elevated pore-water pressure (Pierson, 1981).

Laboratory measurements of pore-water pressure have shown that the front of the subaqueous clayey debris flow exhibits hydroplaning (Mohrig *et al.*, 1998) on a thin layer of water, which causes low bed friction. Fronts of sandy debris flows show a fluidized head where bed friction is minimal (Ilstad *et al.*, 2004). A 5-m thick submarine sandy debris flow, with a long-runout distance of over 400 km downslope of the Canary Islands, has been attributed to the development of excess pore-water pressure due to loading induced by a pelagic debrite package (Gee *et al.*, 1999, their Figure 12). Problems associated with long-runout MTDs are discussed below (Section 6).

3 Nomenclature and classification

3.1 Landslide versus mass transport

Although the term landslide is deeply entrenched in the literature, there are inherent problems associated with the usage.

1) For his first paper, Varnes (1958) used the title "*Landslide types and processes*" that included fall, topple, spread, translational slide, rotational slide, and flow. But for his second paper, Varnes (1978) changed the paper title to "Slope movement types and processes" to represent the same six processes, namely (a) fall, (b) topple, (c) spread, (d) translational slide, (e) rotational slide, and (f) flow (Figure 6). In abandoning the term landslide, Varnes (1978, p. 11) eloquently explained that "*One obvious change is the*

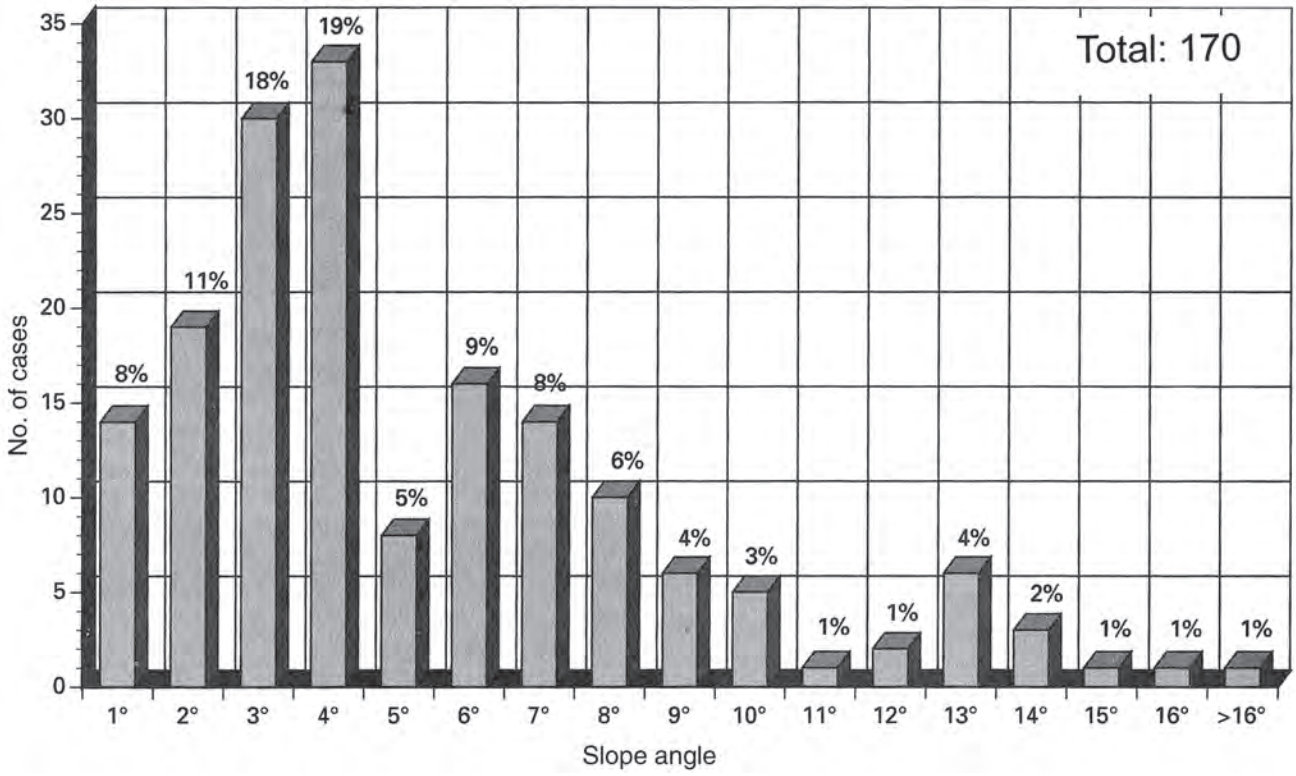

Figure 5 Histogram showing frequency distribution of submarine slides with increasing slope angle, U.S. Atlantic Continental Slope. Note most slides occur on gentle slopes of less than 4°. This compilation of empirical data from modern examples is helpful to the petroleum industry for understanding ancient slides and palaeogeography. From Booth *et al.* (1993). With permission from USGS.

term slope movements, rather than landslides, in the title of this paper and in the classification chart. The term landslide is widely used, and no doubt, will continue to be used as an all inclusive term for almost all varieties of slope movements, including some that involve little or no true sliding. Nevertheless, improvements in technical communication require a deliberate and sustained effort to increase the precision associated with the meaning of words, and therefore the term slide will not be used to refer to movements that do not include sliding." This cautionary note, which has been obviously ignored by other researchers, is the underpinning principle of this paper.

2) The term landslide literally implies sliding motion of a rigid body of earth or land along a shear surface. But debris flows, considered to be a part of the landslide family in some classifications (Cruden, 1991), are characterized by intergranular movements, not shear-surface movements (Shanmugam *et al.*, 1994; Iverson *et al.*, 1997).

3) The AGI Glossary of Geology (Bates and Jackson, 1980, p. 349) defined a landslide as "*A general term covering a wide variety of mass movement landforms and processes involving the downslope transport, under gravitational influence, of soil and rock material en masse. Usually the displaced material moves over a relatively confined zone or surface of shear*." This definition, although implies that the shear-surface movement is a critical factor (see Figure 4B), includes a variety of mass movements.

4) According to Cruden (1991), "*A landslide is the movement of a mass of rock, earth or debris down a slope*". This broad definition includes not only slides, but also debris flows. There are at least five different definitions of the term landslide with conflicting meanings (Table 4).

5) Geertsema *et al.* (2009, p. 59) state that "*Landslides include debris flows and slides, earth flows and flowslides, rock falls, slides, and avalanches, and complex landslides involving both rock and soil*." On the one extreme, the term landslide has been applied without any implication for a specific process (Gee *et al.*, 2007; Camerlenghi *et al.*, 2010), but on the other extreme, the term landslide represents only one category within a larger phenomenon called mass movements (Coates, 1977).

6) The U.S. Geological Survey uses the term landslide to include debris avalanche and creep with velocity connotations (Highland and Bobrowsky, 2008). However, velocities of transport processes cannot be interpreted from bathymetric images of modern seafloor or by examining the ancient rock record in core and outcrop (see Section 3.4 on 'Classification based on transport velocity' below).

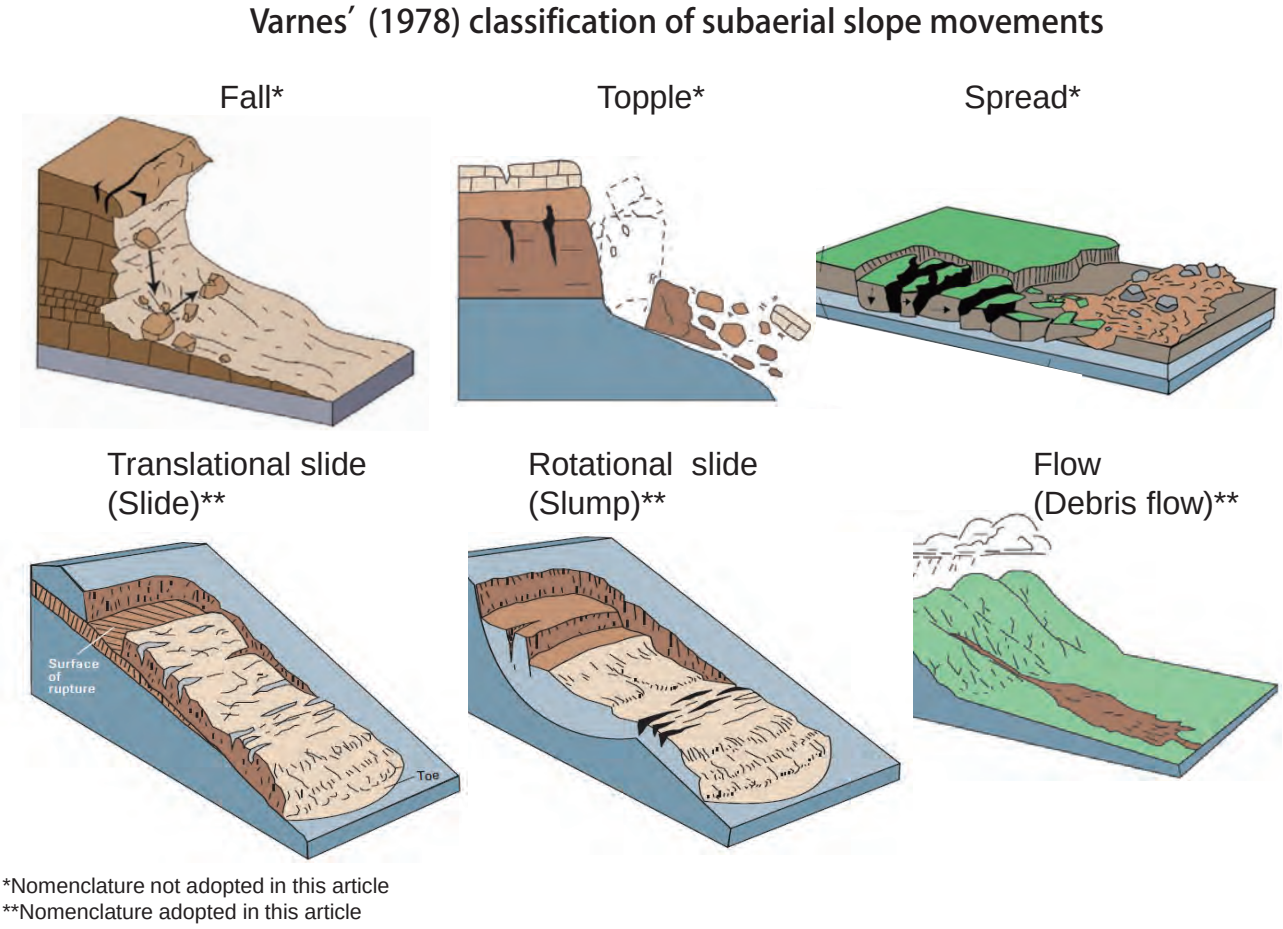

Figure 6 Classification of subaerial slope movements into six types by Varnes (1978). Note that the term "landslide" was not used in his 1978 classification, but was used by Varnes (1958) in his previous classification. Also note that the processes fall, topple, and spread are not adopted in this article because deposits of these processes are difficult to distinguish from deposits of debris flows (*i.e.*, debrites). See Cruden and Varnes (1996) and Wieczorek and Snyder (2009) for an expanded classification of Varnes (1978) with four additional types: (1) debris avalanche, (2) earthflow, (3) creep, and (4) lateral spread. See text for a critique of these additional terms. Diagram modified after Highland and Bobrowsky (2008). With permission from USGS.

7) Even the International Geoscience Programme (IGCP−585), now called E-MARSHAL (Earth′s continental margins: assessing the geohazard from submarine landslides) uses the word landslide for all submarine mass movements (E-MARSHAL, 2013).

8) Similarly, the Springer journal "Landslides" (Editor-in-Chief: Kyoji Sassa) defines that "*Landslides are gravitational mass movements of rock, debris or earth*", without a distinction between landslides and mass movement. Credit: http://www.springer.com/earth+sciences+and+geography/natural+hazards/journal/10346 (accessed December 27, 2014).

The use of the term landslide is inappropriate as a general term to represent both the shear-surface 'sliding' motion of a rigid body and the intergranular 'flowing' motion of a plastic mass (Shanmugam *et al.*, 1994). A more appropriate general term is "mass transport" or "mass movement", which represents the failure, dislodgement, and downslope movement of either sediment or glacier under the influence of gravity. The advantage of the general term "mass transport" is that there is no built-in reference to a sliding motion. Nor is there any reference to sediment or glacier.

3.2 Classification based on types of movement and material

Varnes (1978, his Figure 2.1) classified subaerial mass-transport processes into six movement-based types: (1) falls (2) topples, (3) translational slides, (4) rotational kinds, (5) spreads, and (6) flows (Figure 6). Further, Varnes (1978) added the prefix "rock" to the process names and established the material-based types: (1) rock fall (2) rock topple, (3) rock slide, (4) rock slump, (5) rock spread, and (6) rock flow or deep creep. Although the spreads,

topples, and falls could be observed in modern subaerial environments, the deposits of these three processes in the ancient rock record would not have any distinguishing attributes. This is because deposits of spreads, topples, and falls would resemble debrites (*i.e.*, deposits of debris flows). Therefore, these three types are not adopted in the present article (Figure 6).

3.3 Classification based on mechanical behavior

Dott (1963, his Figure 7) proposed the most meaningful and practical classification of subaqueous mass-transport processes. It is somewhat analogous to the most widely accepted classification of subaerial mass-transport processes by Varnes (1958). In this scheme, subaqueous processes are broadly classified into (1) elastic, (2) elastic and plastic, (3) plastic, and (4) viscous fluid types based on mechanical behavior (Figure 7). The elastic behavior represents rockfall; the elastic and plastic behavior comprises slide and slump; the plastic behavior represents debris flow, and the viscous fluid represents Newtonian turbidity current. The importance of Dott′s (1963) classification is that mass-transport processes do not include turbidity currents (Figure 7C). In this classification, a rockfall refers to sudden falling of rock fragments on steep slopes, such as submarine canyonheads. Because recognition of rockfall in the ancient record is impractical, it is not considered here as a separate type. In short, mass-transport processes are composed of three basic types: (1) slide, (2) slump, and (3) debris flow (Figure 7). I have adopted Dott′s (1963) classification in this review because theoretical analysis (Shanmugam, 1996), experimental observations (Shanmugam, 2000; Marr *et al.*, 2001), and empirical data (Table 3) overwhelmingly show that turbidity currents are not mass-transport processes.

The underpinning principle of Dott′s (1963) classification is the separation of solid from fluid mode of transport based on sediment concentration. In the solid (elastic and plastic) mode of transport, high sediment concentration is the norm (25%−100% by volume, Figure 7B). Mass-transport mechanisms are characterized by solid blocks or aggregate of particles (mass). In contrast, individual particles are held in suspension by fluid turbulence in turbidity currents (Dott, 1963; Sanders, 1965). Turbidity currents are characterized by low sediment concentration of 1%−23% by volume (Figure 7B). In other words, turbidity currents are innately low in flow density. A simple analogy to high-volume sediment transport by mass-transport processes is the human transport by a double-decker bus with a capacity to carry 73 passengers at a time (Figure 8A). In contrast, low-volume sediment transport by turbidity currents is analogous to human transport by a microcar with a capacity to carry only two passengers at a time (Figure 8B). Clearly, mass transport is a much more efficient mechanism for moving sediment downslope than a turbidity current. Mass transport can operate in both subaerial and subaqueous environments, whereas turbidity currents can operate only in subaqueous environments. The advantage of this classification is that physical features preserved in a deposit directly represent the physics of sediment movement that existed at the final moments of deposition.

3.4 Classification based on transport velocity

The concept of velocity-based classification was first introduced by Sharpe (1938) and later adopted by Varnes (1958, 1978) for subaerial processes. There are at least 10 different factors that are commonly used in classifying landslides by various authors (Hansen, 1984, Table 1.1). These factors are: (1) climate, (2) material moved, (3) coherence of material, (4) size of material, (5) geology, (6) type of movement, (7) speed of movement, (8) medium of movement: water/air/ice, (9) triggering mechanisms, and (10) morphological attributes. These 10 conflicting philosophies and related classifications have resulted in the current conceptual and nomenclatural crisis (Table 4). The velocity-based terms, such as avalanches, have also been adopted for downslope subaqueous processes when interpreting seismic and bathymetric data (Wynn *et al.*, 2000; Lewis and Collot, 2001; Masson *et al.*, 2006). Examples of velocity-based terms are as follows:

1) The term flow slide has been used for high-velocity subaerial processes that could be considered a transitional type between slumps and debris flows (Shreve, 1968; Rouse, 1984).

2) A slow-moving mass that breaks up into smaller blocks as it advances is called debris slide, whereas a fast-moving mass that breaks up into smaller blocks as it advances is called debris avalanche (Varnes, 1978). The velocity of debris avalanches is 5 $m \cdot s^{-1}$ (Cruden and Varnes, 1996; see also Hungr *et al.*, 2001).

3) Catastrophic (fast-moving) debris flows are called sturzstrom (Hsü, 1975, 2004).

4) The term creep refers to a slow-moving mass movement (Bates and Jackson, 1980). There are nine kinds of creep depending on material and movement: (a) deep creep, (b) soil creep, (c) seasonal creep, (d) continuous creep, (e) progressive creep, (f) talus creep, (g) slump creep, (h) mass creep, and (i) rock-glacier creep (Shan-

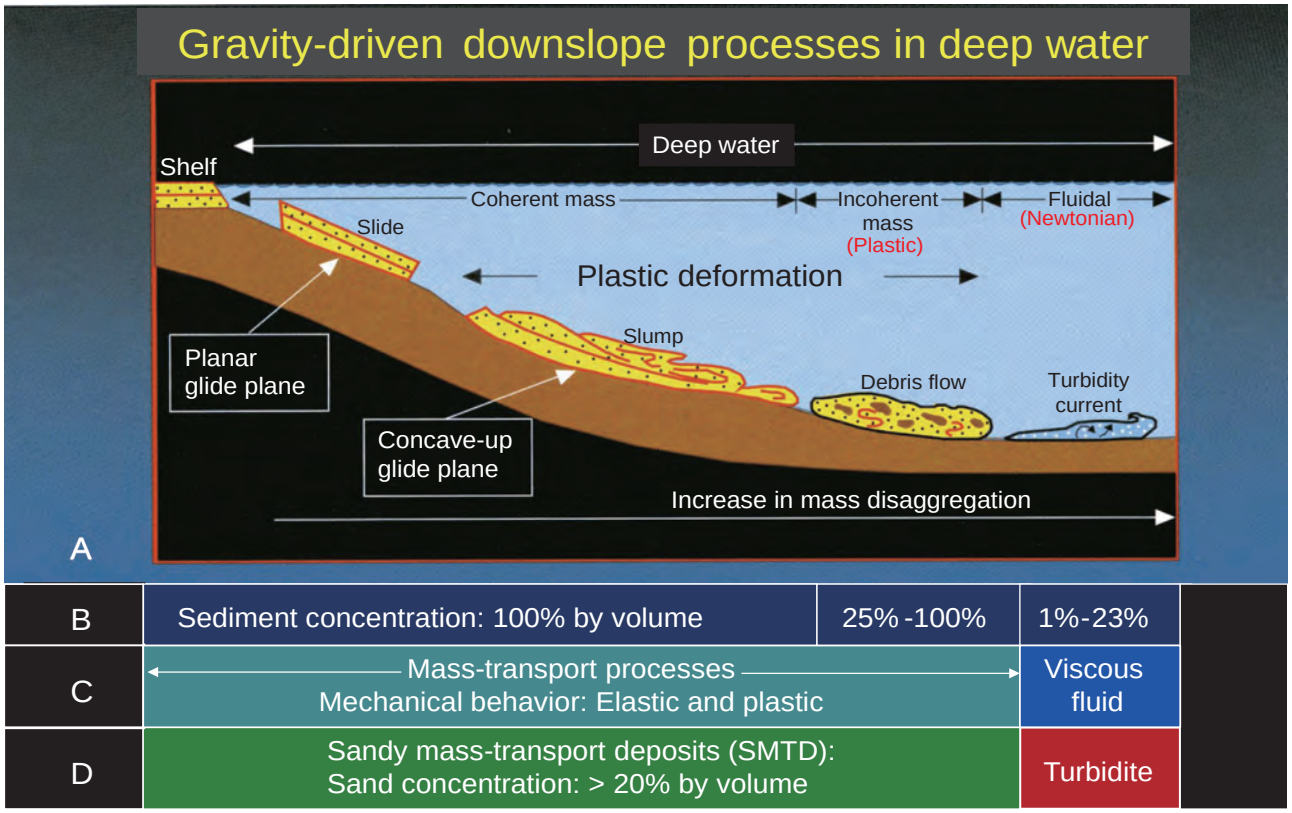

Figure 7 A−Schematic diagram showing four common types of gravity-driven downslope processes that transport sediment into deep-marine environments. A slide represents a coherent translational mass transport of a block or strata on a planar glide plane (shear surface) without internal deformation. A slide may be transformed into a slump, which represents a coherent rotational mass transport of a block or strata on a concave-up glide plane (shear surface) with internal deformation. Upon addition of fluid during downslope movement, slumped material may transform into a debris flow, which transports sediment as an incoherent mass in which intergranular movements predominate over shear-surface movements. A debris flow behaves as a plastic laminar flow with strength. As fluid content increases in debris flow, the flow may evolve into Newtonian turbidity current. Not all turbidity currents, however, evolve from debris flows. Some turbidity currents may evolve directly from sediment failures. Turbidity currents can develop near the shelf edge, on the slope, or in distal basinal settings. From Shanmugam *et al.* (1994); B−Sediment concentration (% by volume) in gravity-driven processes. Slides and slumps are composed entirely of sediment (100% by volume). Debris flows show a range of sediment concentration from 25% to 100% by volume. Note that turbidity currents are low in sediment concentration (1%−23% by volume); implying low-density flows. These concentration values are based on published data by various authors (see Shanmugam, 2000, his Figure 4 for details); C−Based on mechanical behavior of gravity-driven downslope processes, mass-transport processes include slide, slump, and debris flow, but not turbidity currents (Dott, 1963); D−The prefix "sandy" is used for mass-transport deposits that have grain (>0.06 mm: sand and gravel) concentration value equal to or above 20% by volume. The 20% value is adopted from the original field classification of sedimentary rocks by Krynine (1948). See Shanmugam (1996) for discussion on high-density turbidity currents. Modified after Shanmugam *et al.* (1994). With permission from AAPG. Modified after Shanmugam (2012a). With permission from Elsevier Copyright Clearance Center's RightsLink: Licensee: G. Shanmugam. License Number: 3567880649113. License Date: February 14, 2015.

mugam, 2012a).

Although fast-moving and slow-moving mass-transport processes have been classified using absolute velocity values (Cruden and Varnes, 1996; Hungr *et al.*, 2001), these velocity-based terms are not based on empirical data. For example, it is difficult to measure velocities of processes in modern deep-water environments because of common destruction of velocity meters by catastrophic mass-transport events (Inman *et al.*, 1976; Shepard and Marshall, 1978). Cable breaks were used to estimate velocity of submarine mass-transport processes, triggered by the 1929 Grand Banks earthquake in offshore Newfoundland, Canada, which traveled at a speed of 67 km·h^{-1} (Piper *et al.*, 1988). But such velocity values are not based on direct measurements. Therefore, we do not know whether those cables were broken by slumps, debris flows, or turbidity currents. More importantly, there are no sedimentological criteria to determine the absolute velocities of sediment movement

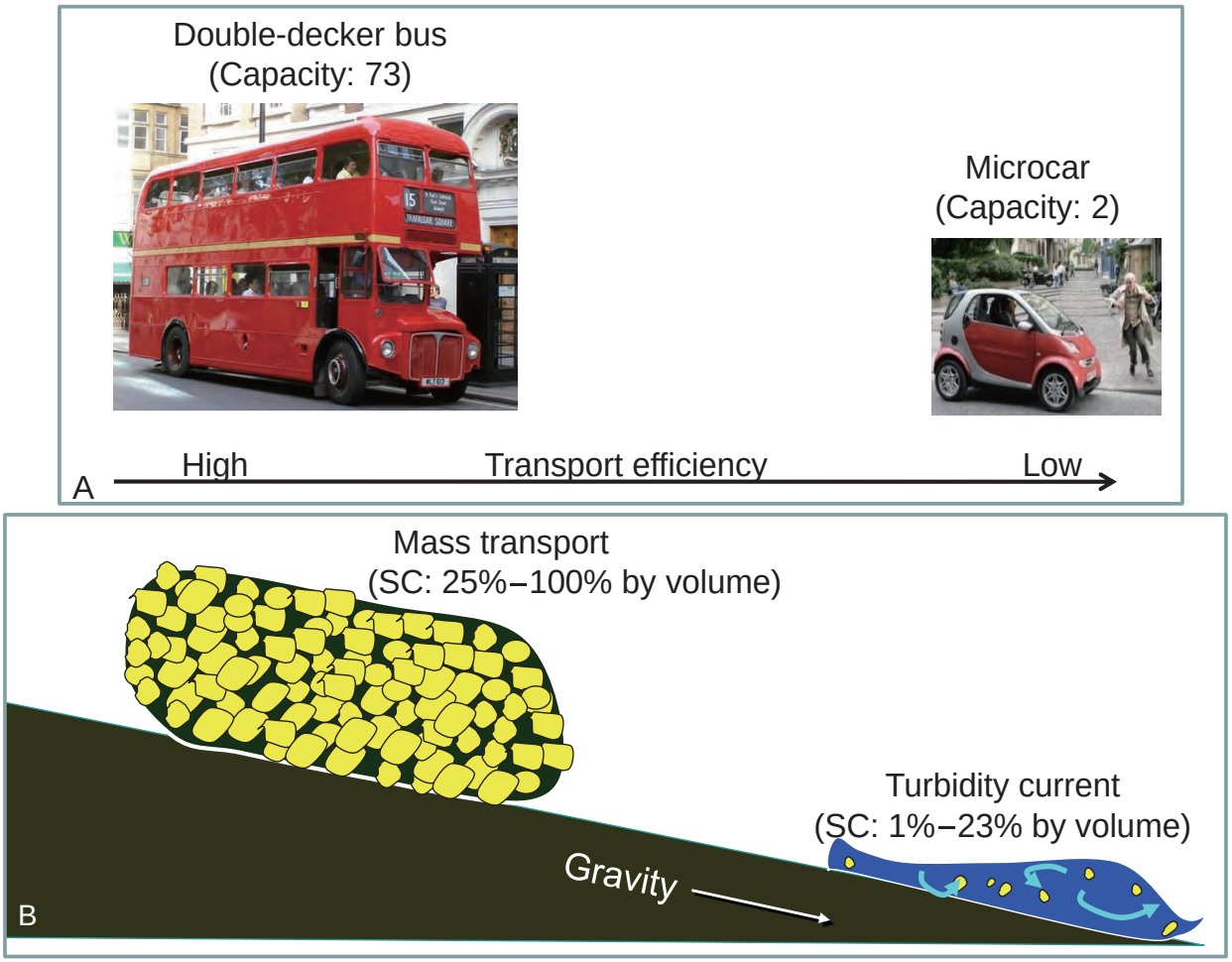

Figure 8 Comparison of human transport on land with gravity-driven sediment transport under water in illustrating the importance of sediment concentration. A−Difference between a double-decker bus with a capacity to carry at least 73 passengers and a microcar with a capacity for only two passengers; B−Difference between mass-transport processes with high sediment concentration (25%−100% by volume) and turbidity currents with low sediment concentration (1%−23% by volume). Sediment mass transport = bus transport. Turbidity current transport = microcar transport. Both bus and mass transport are extremely efficient systems for high-volume transport (long arrow). SC = Sediment concentration. Reproduced from Shanmugam (2012a). With permission from Elsevier Copyright Clearance Center's RightsLink: Licensee: G. Shanmugam. License Number: 3567880649113. License Date: February 14, 2015.

in the ancient rock record. This is because sedimentary features preserved in the deposits cannot and do not reflect absolute transport velocities. The practice of determining flow velocity from grain size using the Hjulström Diagram, meant for fluvial processes (Sundborg, 1956), is inapplicable to MTD. This is because grain size is not proportional to flow velocity in mass-transport processes. In California, for example, it has been well documented that a slow-moving (at velocities of a few centimeter per day) debris flow with strength can detach a house from its foundation and transport it downslope. The other complication is that a debris flow can transform into turbidity current (Hampton, 1972), which is called surface transformation (Fisher, 1983). But there are no objective sedimentological criteria for interpreting flow transformation from the depositional record. In other words, the velocity-based terms are impractical and therefore meaningless for interpreting the ancient geologic record.

3.5 Classifications with emphasis on turbidity currents

A plethora of classifications on deep-water processes and facies models, with a skewed emphasis on turbidity currents, exists (Bouma, 1962; Mutti and Ricci Lucchi, 1972; Middleton and Hampton, 1973; Lowe, 1982; Stow, 1985; Pickering *et al.*, 1989; Mutti, 1992; Mulder, 2011; Talling *et al.*, 2012). Middleton and Hampton (1973) proposed a classification, based on sediment-support mechanisms, in which turbidity currents were considered as mass flows. Some authors (Nardin *et al.*, 1979, their Table 3; Nemec,

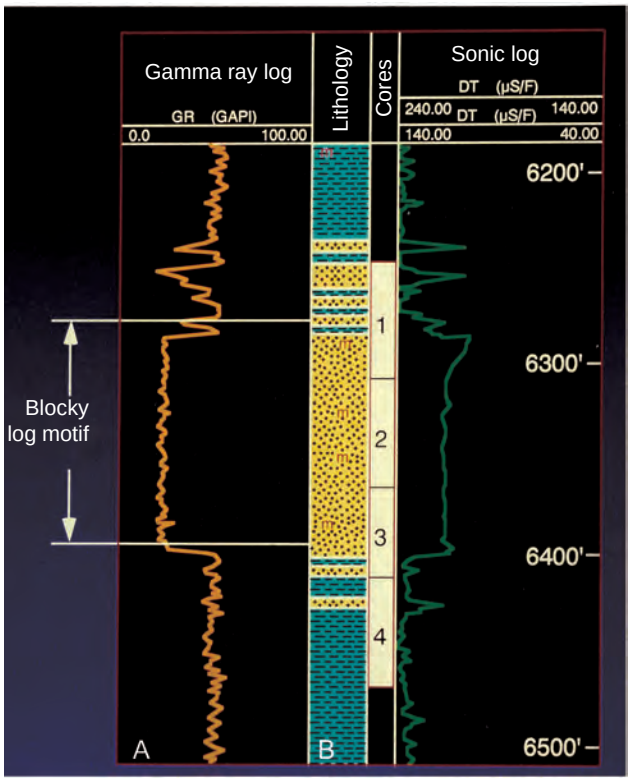

Figure 9 A−Gamma ray log showing blocky motif of a real-world subsurface cored Eocene interval, North Sea; B−Cored intervals (cores 1, 2, 3, and 4) showing distribution of muddy and sandy lithologies. Based on detailed core description, sedimentological features of the cored intervals (cores 1, 2, 3, and 4) are illustrated in Figure 10B. Compare this motif with blocky log motifs in Figures 10, 11 and 24. After Shanmugam (2012a). With permission from Elsevier Copyright Clearance Center's RightsLink: Licensee: G. Shanmugam. License Number: 3575381333515. License Date: February 24, 2015.

1990, his Figure 6; Martinsen, 1994, his Figure5.1; Mulder and Cochonat, 1996, their Figure11 and 13; Locat and Lee, 2002, their Figure 2) have included turbidity currents as a type of mass movement or mass flow following the classification of Middleton and Hampton (1973), whereas others (Shanmugam, 2006a; Moscardelli and Wood, 2008) have excluded turbidity currents from mass-transport processes following the classification of Dott (1963). I have already emphasized the theoretical, experimental, and empirical basis for adopting the Dott's (1963) classification. In confusing the issue further, some authors have even classified debris flows as turbidity currents (Mutti *et al.*, 1999).

Of significance in the above compilation is the vertical facies model for deposits of high-density turbidity currents (HDTC) with R1, R2, R3, S1, S2, and S3 internal divisions for sands and gravels in ascending order (Lowe, 1982). This model was derived solely from the study of ancient rock record using outcrops. The primary attraction to this model in the petroleum industry is that it allows one to interpret ancient deep-water coarse sandstone and conglomerate deposits as turbidites (Mutti, 1992; Mulder, 2011). Despite some recent cosmetic changes in nomenclature (Talling *et al.*, 2012, their Figure 3) and other attempts to explain the basic turbidite facies models (Postma *et al.*, 2014, their Figure 13), there is absolutely no empirical evidence (*i.e.*, vertical sediment concentration profiles and grain-size measurements) for the existence of sandy and gravelly turbidity currents in modern oceans (Shanmugam, 2012a). Thus far, none of the published claims of turbidity currents in modern environments (Heezen and Ewing, 1952; Inman *et al.*, 1976; Hay *et al.*, 1982; Dengler and Wilde, 1987; Normark, 1989; Piper *et al.*, 1999; Khripounoff *et al.*, 2003; Parsons *et al.*, 2003; Xu *et al.*, 2004; Crookshanks and Gilbert, 2008) has offered verifiable empirical data on natural sandy and gravelly turbidity currents (Shanmugam, 2012a). Nor has anyone ever documented the complete vertical Lowe Sequence with R1, R2, R3, S1, S2, and S3 divisions in modern deep-sea sands and gravels in DSDP and ODP sediment cores. When the very existence of natural sandy and gravelly turbidity currents is in doubt, outcrop-based facies models of HDTC (Lowe, 1982; Postma *et al.*, 2014) are irrelevant in understanding the true origin of deep-water sandy deposits. In terms of fluid rheology and flow state, the concept of HDTC is a euphemism for sandy debris flows (Shanmugam, 1996). Unlike HDTC, however, sandy mass-transport processes and their deposits have been documented extensively by direct observations, underwater photographs, and remote sensing techniques in modern submarine canyons (Shepard and Dill, 1966), on modern submarine fan lobes (Gardner *et al.*, 1996), and on modern continental rise (USGS, 1994). In short, any classification of deep-water medium-coarse sands and gravels as turbidites is dubious.

3.6 Excessive synonyms

Various classifications have given birth to a surplus of synonyms for mass-transport processes and their deposits (Reiche, 1937; Varnes, 1958, 1978; Hsü, 1974; Nardin *et al.*, 1979; Bates and Jackson, 1980; Nemec, 1990; Palanques *et al.*, 2006; Gaudin *et al.*, 2006; Shanmugam, 1996, 2006b; Camerlenghi *et al.*, 2010; Tappin, 2010; Festa *et al.*, 2014). Selected examples are:

- Landslide = slope movement = mass movement = mass transport = mass wasting
- Submarine landslide = megaturbidite = homogenite
- Mass-transport complex (MTC) = mass-transport de-

posit (MTD) = submarine mass failure (SMF)

- Translational landslide = translational slip = block slide = glide = slide
- Rotational landslide = rotational slip = toreva block = slump
- Muddy debris flow = mud flow = cohesive debris flow = slurry flow = mass flow
- Debrite = olistostrome = sedimentary mélange
- Sandy debris flow = granular flow = cohesionless debris flow = density-modified grain flow = cohesionless liquefied sandflow = grain flow = mass flow = high-density turbidity current = hyperconcentrated flow = slurry flow = hybrid flow
- Flow slide = liquefaction slide
- Rock avalanche = debris avalanche = sturzstrom
- Sand fall = cascading densewater event = sand avalanche = grain flow = mass flow.

This excessive use of synonyms is, obviously, not only not necessary but even a reason for much confusion.

4 Recognition of the three basic types of MTD

Subaerial "landslides" were recognized as early as in 186 BC in China (Li, 1989). Neveretheless, only during the past few decades, techniques of systematic recognition and mapping have been developed (Brabb, 1991; Lee, 2005). Also, Geographical Information Systems (GIS) have become an important part of databases on landslide research (*e.g.*, Dikau *et al.*, 1996). However, the ultimate recognition of individual types of MTD in the rock record must be based on principles of process sedimentology.

4.1 Process sedimentology

Process sedimentology is the key to recognizing the basic MTD types in core and outcrop. Sanders (1963) published the pioneering paper on process sedimentology entitled 'Concepts of fluid mechanics provided by primary sedimentary structures'. The discipline is concerned with the detailed bed-by-bed description of siliciclastic (and calciclastic) sedimentary rocks for establishing the link between the deposit and the physics and hydrodynamics of the depositional process. Basic requirements, principles, and methods of this discipline are: (1) a knowledge of *physics*, with emphasis on *soil mechanics* and *fluid mechanics* (Sanders, 1963; Brush, 1965), (2) the application of uniformitarianism principle, (3) the pragmatic, accurate, precise, and consistent description of the rock, (4) the preservation of absolute distinction between description and interpretation, (5) the documentation of excruciating details in sedimentological logs, (6) the interpretation of processes using exclusively primary sedimentary structures, (7) the mandatory consideration of alternative process interpretations, (8) the total exclusion of facies models, (9) the quantification of depositional facies, and (10) the routine use of common sense. A major problem in sedimentological studies is the failure to adopt the basic principles of process sedimentology, which has prompted lively debates on the deep-water petroleum-producing reservoirs of the Kutei Basin, Indonesia (Figure 1) (Dunham and Saller, 2014; Saller *et al.*, 2006; Shanmugam, 2008a, 2014a).

Of the three basic types of mass-transport processes, namely slides, slumps, and debris flows (Figure 7), the terms slide and slump are used for both a process and a deposit. The term debrite is used for deposit of a debris flow. The prefix 'sandy' is used for lithofacies that have grain size values greater than 0.06 mm (sand and gravel) and have concentration value equal to or above 20% by volume (Figure 7D). The three sandy SMTD types are emphasized here because of their reservoir potential. Criteria for recognizing MTD and SMTD types in core and outcrop have been developed by integrating my rock description (Table 3) with published information by other researchers (Dott, 1963; Helwig, 1970; Johnson, 1970; Fisher, 1971; Hampton, 1972; Middleton and Hampton, 1973; Enos, 1977; Dingle, 1977; Woodcock, 1976, 1979; Cook, 1979; Lowe, 1982; Maltman, 1987, 1994; Pickering *et al.*, 1989; Collinson, 1994). Numerous outcrop and core photographs of features associated with sandy slides, sandy slumps, and sandy debrites were published elsewhere (Shanmugam, 2012a).

4.2 Slides

A slide is a coherent mass of sediment or a rigid body that moves along a planar glide plane and shows no internal deformation (Figure 7A). Slides represent translational shear-surface movements. Such sliding movements are also common in glaciers (Easterbrook, 1999). Submarine slides can travel hundreds of kilometers on continental slopes. Long-runout distances of up to 810 km for slides have been documented for submarine MTD (Table 5).

Some of the best studied seismic examples of submarine MTD are in the area of the Storegga Slide on the mid-Norwegian continental margin (Solheim *et al.*, 2005b). Even in these cases, the authors acknowledged the practical difficulties in distinguishing slides from debrites on seismic profiles. This is because both slides and debrites

Table 5 Comparison of long-runout MTD on Earth (submarine and subaerial) with Venus, Iapetus, and Mars (extraterrestrial). The term "landslide" was used to describe many of these examples by the original authors. Locations of selected examples are shown in Figure 1. Long-runout MTD provide empirical data for developing depositional models for deep-water sandstone petroleum reservoirs. The change in numbering is to reflect the change in type of environment (subaerial, submarine, and extraterrestrial). Compiled from several sources.

Name and location	Runout distance (km)	Environment	Data	Process
1. Storegga slide, Norwegian continental margin (Bugge *et al.*, 1987; Jansen *et al.*, 1987; Haflidason *et al.*, 2005)	810	Submarine	Seismic and GLORIA side-scan sonar images, and core	Slide, slump, and debris flow
2. Agulhas, SE Africa (Dingle, 1977)	750	Submarine	Seismic	Slide and slump
3. Saharan debris flow, NW African Margin (Embley, 1982)	700	Submarine	Seismic	Debris flow
4. Canary debris flow, NW African Margin (Masson *et al.*, 1997)	600	Submarine	Seismic and core	Debris flow
5. Hatteras, U.S. Atlantic Margin (Embley, 1980)	~500	Submarine	Seismic and core	Slump and debris flow
6. Mauritania−Senegal, NW African Margin (Jacobi, 1976)	~300	Submarine	Seismic and core	Slump and debris flow
7. Nuuanu, NE Oahu (Hawaii) (Normark *et al.*, 1993; Moore *et al.*, 1994)	235	Submarine	GLORIA side-scan sonar images	Mass transport
8. Wailau, N Molakai (Hawaii) (Normark *et al.*, 1993)	<195	Submarine	GLORIA side-scan sonar images	Mass transport
9. Rockall, NE Atlantic (Prior and Coleman, 1979, 1984)	160	Submarine	Seismic	Mass transport
10. Clark, SW Maui, Hawaii (Normark *et al.*, 1993)	150	Submarine	GLORIA side-scan sonar images	Mass transport
11. N Kauai, N Kauai, Hawaii (Normark *et al.*, 1993)	140	Submarine	GLORIA side-scan sonar images	Mass transport
12. East Breaks (West), Gulf of Mexico (McGregor *et al.*, 1993)	110	Submarine	Seismic and core	Slump and debris flow
13. Grand Banks, Newfoundland (Heezen and Ewing, 1952; Driscoll *et al.*, 2000; Bornhold *et al.*, 2003)	>100	Submarine	Seismic and core	Mass transport and turbidity current*
14. Ruatoria, New Zealand (Collot *et al.*, 2001)	100	Submarine	Seismic	Mass transport
15. Alika−2, W Hawaii (Hawaii) (Normark *et al.*, 1993)	95	Submarine	GLORIA side-scan sonar images	Mass transport
16. Kaena, NE Oahu (Hawaii) (Normark *et al.*, 1993)	80	Submarine	GLORIA side-scan sonar images	Mass transport
17. El Golfo, western Canary Islands (Masson *et al.*, 2002)	65	Submarine	Seismic	Mass transport
18. Bassein, Bay of Bengal (Moore *et al.*, 1976)	55	Submarine	Seismic	Slide and debris flow
19. Kidnappers, New Zealand (Lewis, 1971)	45	Submarine	Seismic	Slump and slide
20. Munson−Nygen, New England (O'Leary, 1993)	45	Submarine	Seismic	Slump and debris flow

Table 5, continued

Name and location	Runout distance (km)	Environment	Data	Process
21. Ranger, Baja California (Prior and Coleman, 1984)	35	Submarine	Seismic	Mass transport
1. Osceola mudflow, Mount Rainier (Vallance and Scott, 1997)	120	Subaerial	Outcrop	Mass transport
2. Nevado del Ruiz, Colombia (Pierson, 1990)	103	Subaerial	Outcrop	Mass transport
3. Pine Creek and Muddy River lahars, Mount St. Helens (Pierson, 1985)	31	Subaerial	Outcrop	Mass transport (The world′s largest historical subaerial MTD)
4. Saidmarreh slide, Zagros fold-thrust belt, SW Iran (Roberts and Evans, 2009)	19	Subaerial	Outcrop	Mass transport (The world′s second largest prehistoric subaerial MTD)
1. Venus (Malin, 1992)	5−50	Extraterrestrial (Venus)	Radar images by the Magaellan spacecraft	Mass transport
2. Iapetus, a satellite of Saturn (Singer *et al.*, 2012, their Figure 5)	7−80	Extraterrestrial (Iapetus)	Cassini mission images	Mass transport
3. Thaumasia Plateau (Montgomery *et al.*, 2009, their Figure 9)	2500	Extraterrestrial (Mars)	Thermal Emission Imaging System infrared [THEMIS IR]	Mass transport

* See Shanmugam (2012a) for discussion on the evidence for turbidity currents

exhibit homogeneous (*i.e.*, transparent) to chaotic reflections (Figure 3). In distinguishing slides from debrites, Solheim *et al.* (2005b) used additional criteria, such as the existence of a headwall as well as sidewalls. Similar problems of recognizing individual depositional facies (*e.g.*, slides vs. debrites) on seismic profiles have been acknowledged by Tripsanas *et al.* (2008) and Twichell *et al.* (2009). In recognizing slides, McAdoo *et al.* (2000) used bathymetry and GLORIA (Geological Long-Range Inclined Asdic) side-scan sonar data. But such large-scale images are unreliable for distinguishing the sliding motion from flowing motion. These real-world examples reveal the limitations of relying on seismic data for distinguishing specific types of deep-water depositional facies. The solution is to examine the rocks directly by using core or outcrop.

Slides are capable of transporting gravel and coarse-grained sand because of their inherent strength. General characteristics of slides are:

- Blocky log motif (Figure 9A). Cored interval of this log motif (Figure 9B) reveals complex internal features in core (Figure 10B)
- Primary basal glide plane or décollement (core and outcrop) (Figure 10B)
- Basal shear zone (core and outcrop) (Figure 10C)
- Secondary internal glide planes (core and outcrop) (Figure 10B)
- Preservation of original strata from the provenance region (Figure 11)
- Multiple internal layers within a single slide unit (Figure 11)
- Subaerial to shallow-water facies encased in deep-water host muddy facies (Figure 11)
- Associated slumps (Figure 11)
- Sheet-like geometry (Figure 11)

In submarine environments, slides tend to occur on continental margins commonly near the shelf-slope breaks, in submarine canyons, and in fjords. However, long-runout slides may occur in basinal settings as well. Slides are commonly associated with triggering events such as earthquakes, meteorite impacts, volcanic activities, glacial loading, sediment loading, cyclones, and tsunamis.

4.3 Slumps

A slump is a coherent mass of sediment that moves on a concave-up glide plane and undergoes rotational move-

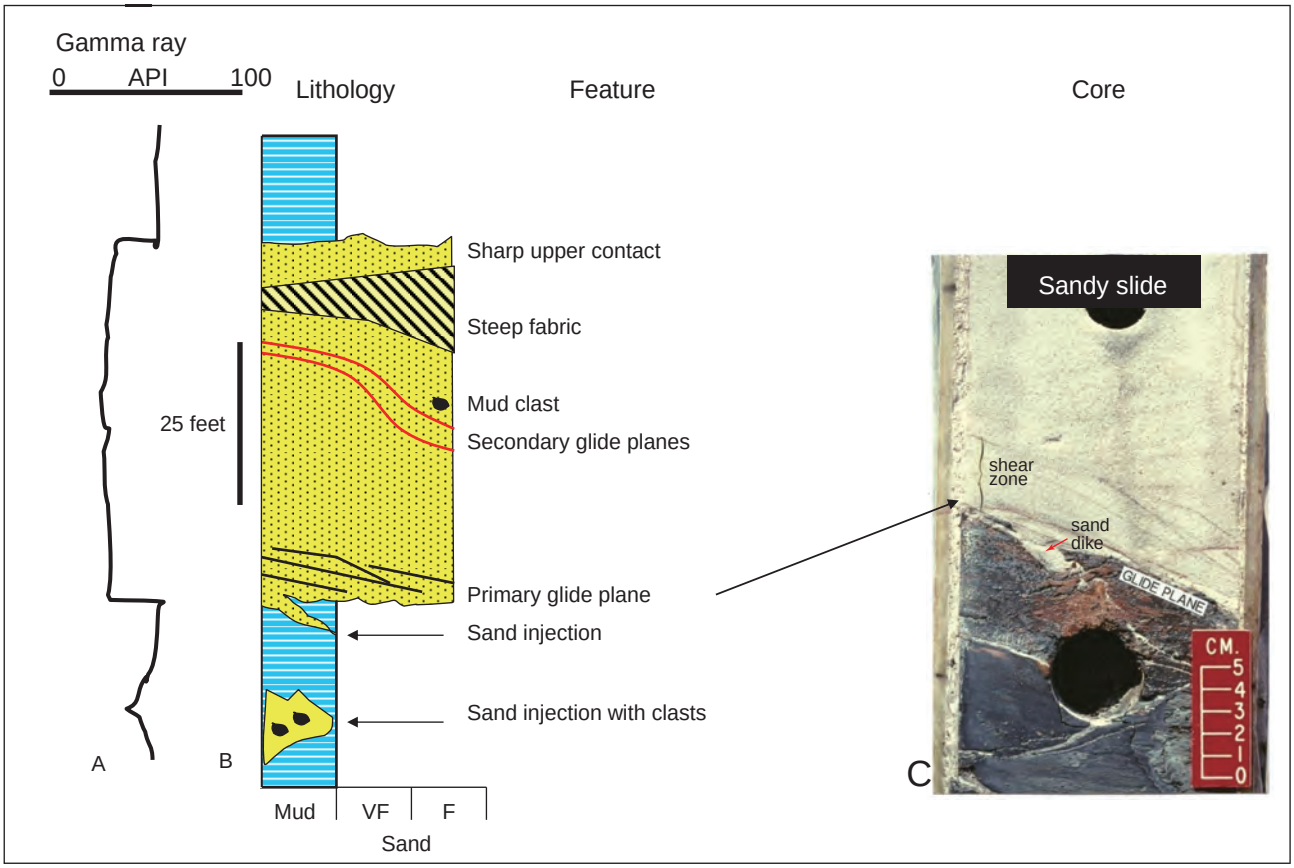

Figure 10 A−Sketched blocky wireline log motif of a sandy slide/slump unit (see Figure 9A for the genuine wireline log); B−Sedimentological log showing details. VF = very fine sand; F = fine sand; primary glide plane (décollement) = the basal primary slip surface along which major displacement occurs; secondary glide plane = internal slip surface along which minor displacement occurs; mud clasts = occurrence of mud clasts at some distance above the basal contact; C−Core photograph showing an upper sand interval (light color) and a lower mudstone interval (dark color). The basal contact (arrow) is interpreted as a primary glide plane (a décollement) of a sandy slide/slump. Additional core photographs of this cored interval are published elsewhere (Shanmugam, 2012a, his Figures 3.10, 3.12, 3.13, and 3.14). Shear zone = basal interval of a rock unit that has been crushed and brecciated by many subparallel fractures due to shear strain. Note a sand dike (*i.e.*, injectite) at the base of shear zone. Eocene, North Sea. Compare this small-scale slide (15 m thick) with a large-scale slide (50 m thick) in Figure 11. Modified after Shanmugam (2012a). With permission from Elsevier Copyright Clearance Center's RightsLink: Licensee: G. Shanmugam. License Number: 3575381333515. License Date: License Date: February 24, 2015.

ments causing internal deformation (Figure 7A). Slumps represent rotational shear-surface movements. Slumps are capable of transporting gravel and coarse-grained sand because of their inherent strength. General characteristics of slumps are:

- Basal zone of shearing (core and outcrop)
- Slump folds (Helwig, 1970) interbedded with undeformed layers (core and outcrop) (Figure 12)
- Irregular upper contact (core and outcrop)
- Chaotic bedding in heterolithic facies (core and outcrop)
- Rotated elongate grains (Maltman, 1987) (Microscopic)
- Steeply dipping and truncated layers (core and outcrop) (Figure 12)
- Associated slides (core and outcrop) (Figure 11)
- Chaotic facies in high-resolution seismic profiles.

In submarine environments, slumps tend to occur commonly on slope settings.

4.4 Debrites

A debris flow is a sediment flow with plastic rheology and laminar state from which deposition occurs through freezing *en masse*. The terms debris flow and mass flow are used interchangeably because each exhibits plastic flow behavior with shear stress distributed throughout the mass (Nardin *et al.*, 1979). In debris flows, inter-granular movements predominate over shear-surface movements.

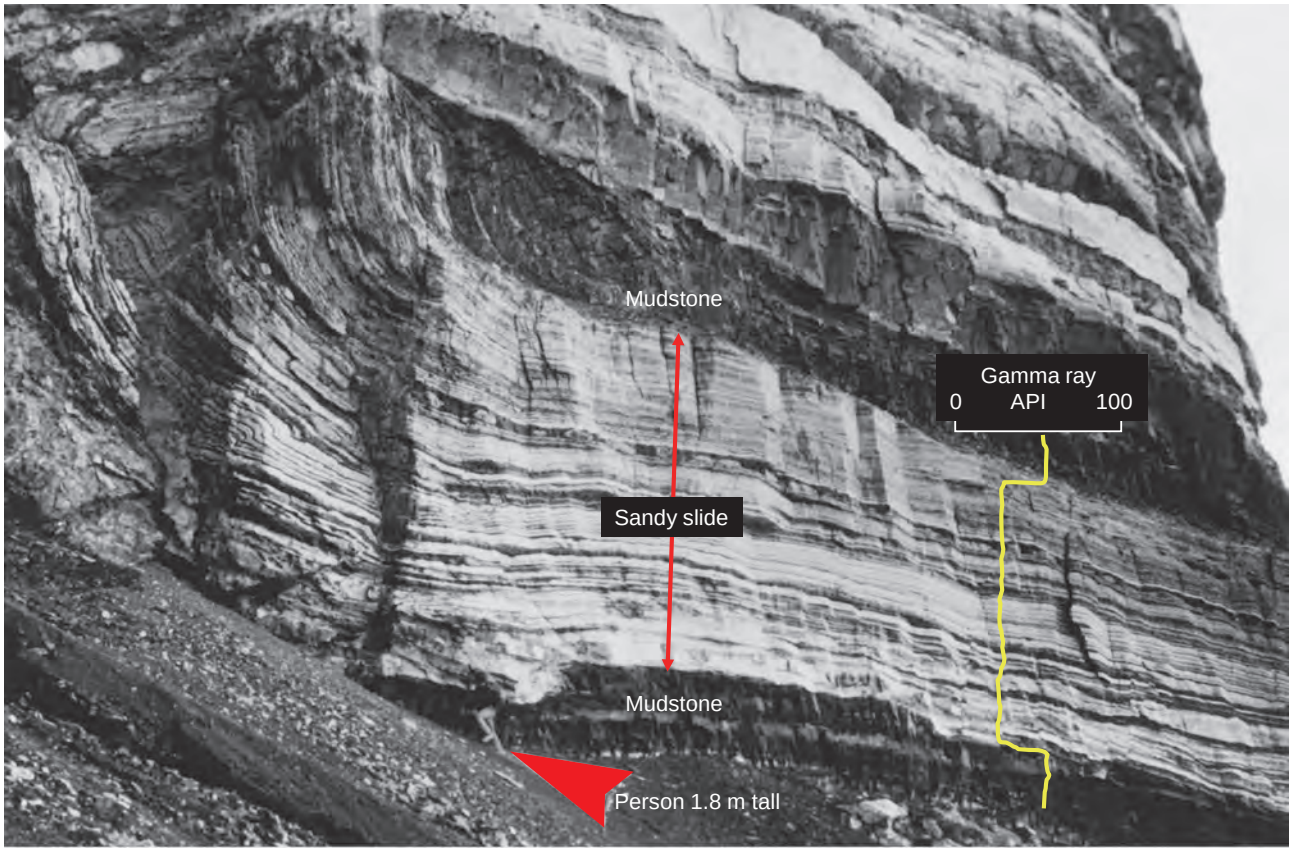

Figure 11 Outcrop photograph showing sheet-like geometry of an ancient sandy submarine slide (1000 m long and 50 m thick) encased in deep-water mudstone facies. Note the large sandstone sheet with rotated/slumped edge (left). Person (arrow): 1.8 m tall. Note multiple internal layers of the slide unit representing pre-transport disposition of strata in the provenance region. A hypothetical gamma ray log showing blocky motif for the sandy slide is inserted to illustrate how this sandy unit might appear in the subsurface on wireline logs (compare with Figure 10A and Figure 24A). Ablation Point Formation, Kimmeridgian (Jurassic), Alexander Island, Antarctica. Photo courtesy of D. J. M. Macdonald. From Macdonald *et al.* (1993). With permission from GSA.

Although most debris flows move as incoherent mass, some plastic flows may be transitional in behavior between coherent mass movements and incoherent sediment flows (Marr *et al.*, 2001). Debris flows may be mud-rich (*i.e.*, muddy debris flows), sand-rich (*i.e.*, sandy debris flows), or mixed types.

For the first time, to understand mechanics of sandy debris flows (SDF) and their deposits and to distinguish them from turbidites, a Mobil-funded experimental flume study was carried out at St. Anthony Falls Laboratory (SAFL), University of Minnesota (1996−1998). Experiments clearly showed that SDF transport coarse sediment as plastic laminar flow (basal layer), emplacing massive sands (Shanmugam, 2000; Marr *et al.*, 2001). Debris flows are capable of transporting gravel and coarse-grained sand because of their inherent strength. In contrast, turbidity currents cannot transport coarse sand and gravel in turbulent suspension (Shanmugam, 2012a). These experimental studies yielded diagnostic depositional features that are the key to recognizing deep-water massive sands as sandy debrites (Shanmugam, 2000).

General characteristics of muddy and sandy debrites are:

- Floating or rafted mudstone clasts near the tops of sandy beds (core and outcrop) (Figure 13); clasts can also be dispersed throughout the sediment interval
- Floating armored mudstone balls in sandy matrix (core and outcrop)
- Planar clast fabric (core and outcrop) (Figure 13). Planar clast fabric can be used to infer laminar flow conditions (Fisher, 1971; Enos, 1977; Shanmugam and Benedict, 1978), a flow state common to debris flow.
- Projected clasts (core and outcrop) (Shanmugam and Benedit, 1978)
- Imbricate clasts in outcrop (van Loon, 1972; Shanmugam and Benedict, 1978; Brown and Bell, 2007) and in experiment (Major, 1998)
- Brecciated mudstone clasts in sandy matrix (core and

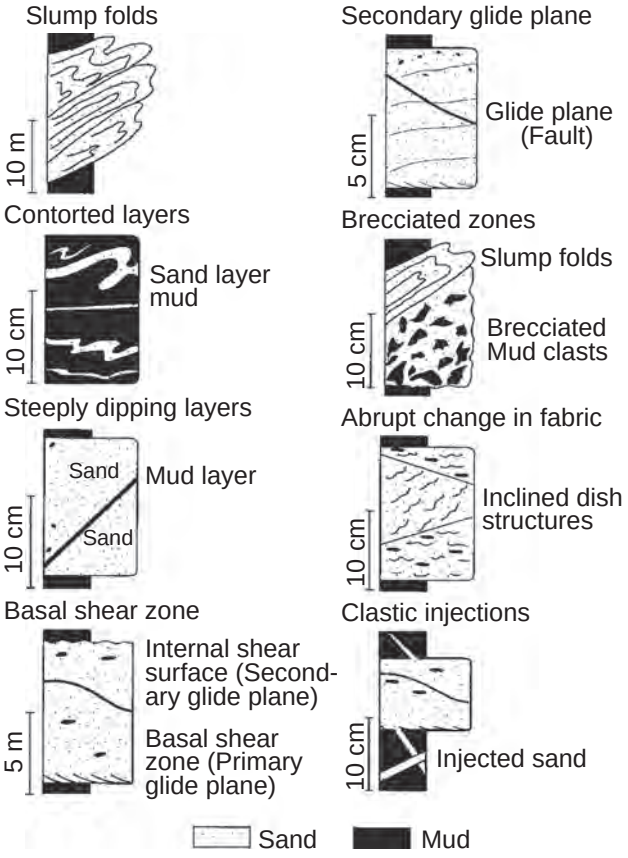

Figure 12 Summary of sedimentological features associated with sandy slumps and associated debrites observed in core and outcrop. These features, compiled from real-world examples, are useful in recognizing MTD types in the rock record. From Shanmugam *et al.* (1995). With permission from AAPG.

outcrop) (Figure 12)

- Inverse grading, normal grading, inverse to normal grading, and absence of any grading of matrix (core and outcrop)
- Floating quartz granules in fine-grained sandy matrix (core and outcrop), suggesting flow strength (Shanmugam, 2012a)
- Pockets of gravels in sandy matrix (core and outcrop)
- Preservation of delicate mud fragments with planar fabric in sandy matrix (core and outcrop). Delicate features and constituents have been cited as evidence of laminar flow in debris-flow deposits (Enos, 1977; Johnson, 1970).
- Irregular and sharp upper contacts (core and outcrop) are considered evidence for deposition by *en masse* freezing of flows with plastic rheology (*i.e.*, flow strength).
- Side-by-side occurrence of garnet granules (density: 3.5−4.3) and quartz granules (density: 2.65) (core and outcrop), indicating flow strength (Shanmugam, 2012a)
- Lenticular to sheet in geometry

In submarine environments, debrites tend to occur both on slope and basinal settings. Debrites are also common in submarine canyons. Debrites are commonly associated with triggering events such as earthquakes, volcanic eruptions, monsoonal floods, cyclones, and tsunamis.

5 Triggering mechanisms

A critical analysis of types of triggering mechanisms is important in understanding the timing of sediment failures that control emplacement of deep-water reservoirs. In the petroleum industry, most deep-water sands are believed to be deposited during periods of sea-level lowstands (Figure 19A) (Vail *et al.*, 1991). However, such conceptual models are not supported by empirical data (Shanmugam, 2008b, 2012a). Because deep-water SMTD constitute important petroleum reservoirs worldwide (Table 3), this topic is pertinent in this review.

A triggering mechanism is defined here as the primary process that causes the necessary changes in the physical, chemical, and geotechnical properties of the soil, which results in the loss of shear strength that initiates the sediment failure and movement. Commonly, triggering processes are considered "external" with respect to the site of failure. Wieczorek and Snyder (2009, p. 245), for example, state that "*The term landslide trigger refers specifically to an external stimulus, such as intense rainfall, rapid snowmelt, earthquake, volcanic eruption, or stream or coastal erosion. These stimuli initiate an immediate or near-immediate landslide movement by rapidly increasing shear stresses or porewater pressures, by ground acceleration due to seismic activity, by removing lateral support, by reducing the strength of slope materials, or by initiating debris-fl ow activity*."

In continental margins, several triggering mechanisms may work concurrently or in tandem (*e.g.*, earthquake-triggered tsunamis). Sowers (1979) articulated the challenge of identifying the single mechanism that is solely responsible for the failure as follows: "*In most cases, several 'causes' exist simultaneously; therefore, attempting to decide which one finally produced failure is not only difficult but also technically incorrect. Often the final factor is nothing more than a trigger that sets a body of earth in motion that was already on the verge of failure. Calling the final factor the cause is like calling the match that lit the fuse that detonated the dynamite that destroyed the building the cause of the disaster*."

5.1 Classification based on duration

Although more than one triggering mechanism can

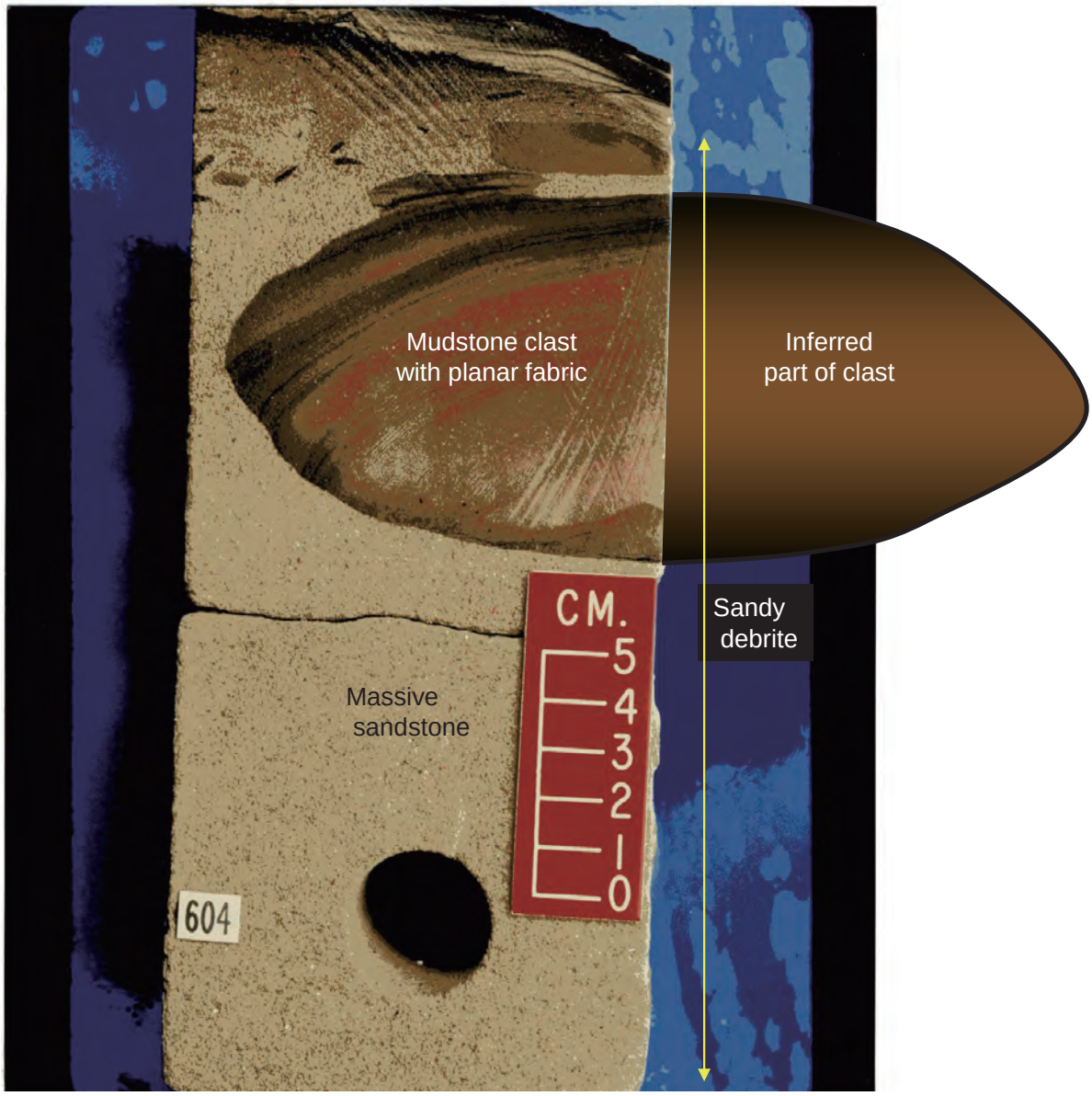

Figure 13 Core photograph of a massive fine-grained sandstone unit showing a large floating mudstone clast (above the scale). Note planar clast fabric (*i.e.*, long axis of clast is aligned parallel to bedding surface), revealed by the inferred part of the clast, suggesting deposition from a laminar sandy debris flow. Note the occurrence of other mudstone clasts of different sizes immediately adjacent to the large clast. Also note sharp and irregular upper bedding contact (top of photo). Such features are indicative of flow strength and deposition from freezing of laminar plastic flows (Enos, 1977; Shanmugam and Benedict, 1978; Fisher, 1971). Paleocene, North Sea. Modified after Shanmugam (20012a). With permission from Elsevier.

cause a single process (*e.g.*, debris flow) at a given site, there are no objective criteria yet to distinguish either the triggering mechanism or the transport process from the depositional record (Shanmugam, 2006b, 2012b; Mulder *et al.*, 2011). This is because what is preserved in the deposit reflects the final moment of deposition, not transport (Middleton and Hampton, 1973). During the long transport history, a sediment-gravity flow can and does undergo flow transformation (Fisher, 1983; Shanmugam, 1996; Talling *et al.*, 2007). For example, sediment of a turbidite bed on the seafloor could have been transported as a debris flow and underwent flow transformation into a turbidity current at the time of deposition (see experiments by Hampton, 1972). Therefore, one cannot interpret transport mechanism from the depositional record using either seismic data or core data. Nevertheless, an understanding of different triggering mechanisms is necessary in evaluating sediment failures (Locat and Lee, 2005; Masson *et al.*, 2006; Feeley, 2007; Piper *et al.*, 2012a). There are at least 21 triggering mechanisms that can initiate sediment

failures in subaerial and submarine environments on Earth (Table 6). These mechanisms are grouped into three major categories based on their duration of activity (Table 6): (1) short-term events that last for only a few minutes to several hours, days or months (*e.g.*, earthquakes, volcanic eruptions, meteorite impacts, tsunamis, tropical cyclones, monsoon floods, *etc.*), (2) intermediate-term events that last for hundreds to thousands of years (*e.g.*, tectonic events, glacial maxima and loading, depositional loading, gas hydrate decomposition, *etc.*), and (3) long-term events that last for thousands to millions of years, such as lowstands of sea level (Shanmugam, 2012a, 2012b). Conceivably, some intermediate-term events may last for a longer duration. The point here is that short-term events and long-term events are markedly different in their duration.

Brönnimann (2011) has recognized seven triggering mechanisms associated with hydrogeology: (1) suction, (2) rising pore-water pressure, (3) seepage forces, (4) inner erosion, (5) liquefaction, (6) over pressure, and (7) mechanisms related to high plasticity. Although these processes are important in affecting slope stability, they are not considered here as principal triggering mechanisms, with the exception of groundwater seepage (Table 6). The reason is that the excess pore-water pressure, for example, is a piezometric response *in situ* to external forces, such as rainfall, glacial loading, human activity, *etc.* Furthermore, the in-situ lithologic properties are closely tied to controlling pore-water pressures and related sediment failures. These complications are evident in the 1979 sediment failure that occurred at the Nice international airport in southern France. The 1979 Nice incident has been attributed to a combination of both external and internal factors (Dan *et al.*, 2007, their Figure 20). These complications are illustrated in Figure 14.

1) Internal lithologic factor (Figure 14A): The presence of a high-permeability sand layer, which served as a freshwater conduit, was significant in increasing the sensitivity of the surrounding clay by leaching.

2) External human factor (Figure 14B): The international airport was constructed on a platform enlarged by land-filling material. The 1979 expansion of the airport apparently resulted in local loading beneath the embankment, which was responsible for softening of the mechanical properties of the sensitive clay layer and for its 'creeping' movement.

3) External meteorological factor (Figure 14C): Intense rainfall over the entire Var drainage basin and the Nice coast in southern France two weeks before the 1979 event was vital in pre-conditioning the site for a potential slope failure.

Table 6 Types and duration of triggering mechanisms of sediment failures. Compiled from several sources. Updated after Shanmugam (2012a, 2012b, 2013a). The change in numbering is to reflect the change in duration of triggering events.

Types of triggering	Environment of sediment emplacement	Duration
1. Earthquake (Heezen and Ewing, 1952; Henstock *et al.*, 2006)	Subaerial & submarine	
2. Meteorite impact (Claeys *et al.* 2002; Barton *et al.*, 2009/2010)	Subaerial & submarine	
3. Volcanic activity (Tilling *et al.*, 1990)	Subaerial & submarine	
4. Tsunami waves (Shanmugam, 2006b)	Subaerial & submarine	
5. Rogue waves (Dysthe *et al.*, 2008)	Submarine	
6. Cyclonic waves (Bea *et al.*, 1983; Prior *et al.*, 1989; Shanmugam, 2008b)	Subaerial & submarine	Short-term events: a few minutes to several hours, days or months
7. Internal waves and tides (Shanmugam, 2013b, 2013c, 2013d, 2014b)	Submarine	
8. Ebb tidal current (Boyd *et al.*, 2008)	Submarine	
9. Monsoonal rainfall (Petley, 2012)	Subaerial	
10. Groundwater seepage (Brönnimann, 2011)	Subaerial & submarine	
11. Wildfire (Cannon *et al.*, 2001)	Subaerial	
12. *Human activity (Dan *et al.*, 2007)	Subaerial & submarine	

Table 6, continued

Types of triggering	Environment of sediment emplacement	Duration
1. **Tectonic events: (a) tectonic oversteepening (Greene *et al.*, 2006); (b) tensional stresses on the rift zones (Urgeles *et al.*, 1997); (c) oblique seamount subduction (Collot *et al.*, 2001), among others	Subaerial & submarine	Intermediate-term events: hundreds to thousands of years
2. Glacial maxima, loading (Elverhoi *et al.*, 1997, 2002); glacial meltwater (Piper *et al.*, 2012b)	Submarine	
3. Salt movement (Prior and Hooper, 1999)	Submarine	
4. Depositional loading (Coleman and Prior, 1982; Behrmann *et al.*, 2006)	Submarine	
5. Hydrostatic loading (Trincardi *et al.*, 2003)	Submarine	
6. Ocean-bottom currents (Locat and Lee, 2002)	Submarine	
7. Biological erosion in submarine canyons (Dillon and Zimmerman, 1970; Warme *et al.*, 1978)	Submarine	
8. Gas hydrate decomposition (Popenoe *et al.*, 1993; Sultan *et al.*, 2004; Maslin *et al.*, 2004)	Submarine	
1. Sea-level lowstand (Damuth and Fairbridge, 1970; Shanmugam and Moiola, 1982, 1988; Vail *et al.*, 1991)	Submarine	Long-term events: thousands to millions of years

* Although human activity is considered to be the second most common triggering mechanism (next to earthquakes) for known historic submarine mass movements (Mosher *et al.*, 2010), it is irrelevant for interpreting ancient rock record.
* *Some tectonic events may extend over millions of years.
Note: Schuster and Wieczorek (2002) reviewed landslide triggers and types. Talling (2014) disussed triggers of subaqueous sediment density flows in various settings.

4) Internal geotechnical factor (Figure 14C): After a period of rainfall, seepage of fresh ground water through the high-permeability sand layer into the surrounding clay had caused an increase in the pore-water pressure, which led to the reduction of the effective shear strength that resulted in the Nice sediment failure on October 16, 1979. As a result, a part of the airport extension, which was built to be a harbor, collapsed into the Mediterranean Sea. Although the pore-water pressure was the last factor involved in a long-line of processes that caused the sediment failure, it was not the sole triggering mechanism.

5.2 Sea-level lowstand model

In the petroleum industry, the sea-level lowstand model is the perceived norm for explaining the timing of deep-water sands. Saller *et al.* (2006), for example, attributed the timing of reservoir sands in the Kutei Basin in the Makassar Strait, Indonesian Seas (Figure 1, black triangle) to a lowstand of sea-level. Nevertheless, the location of the Kutei Basin (Figure 1, black triangle) is frequently affected by earthquakes, volcanoes, tsunamis, tropical cyclones, monsoon floods, the Indonesian throughflow, and M2 baroclinic tides (M2 represents the main lunar semidiurnal tidal constituent with a period of 12.42 h) (see Shanmugam, 2008a, 2012a, 2014a). These daily activities of the solar system (*e.g.*, earthquakes, meteorite impacts, tsunamis, cyclonic waves, *etc.*) do not come to a halt during sea-level lowstands. In tectonically and oceanographically tumultuous locations, such as the Indonesian Seas, the short-term events are the primary triggering mechanisms of deepwater sediment failures and they occur in a matter of hours or days during long periods of both highstands and lowstands (Shanmugam, 2008b).

Deep-water petroleum-bearing Paleocene sand (100 m thick) of the Lower Tertiary Wilcox trend, which occurs above the K−T boundary in the BAHA #2 wildcat test well, has been interpreted as “lowstand” turbidite fan in the northern Gulf of Mexico (Meyer *et al.*, 2007, their Figure 3). However, because of the opportune location of the Lower Tertiary Wilcox trend and the stratigraphic position and age, the drilled Paleocene sand could alternatively be attributed to the Chicxulub impact and related seismic shocks and tsunamis (Figure 15). Tsunami-related deposition on continental margins has been discussed by Shanmugam (2006b). Contrary to the conventional wisdom on the timing of deposition of deep-water sands during periods of sea-level lowstands, earthquakes, meteorite impacts (Barton *et al.*, 2009/2010), tsunamis (Figure 16), tropical cyclones (Figure 17), initiate SMTD suddenly in a matter of hours or days during the present sea-level highstand.

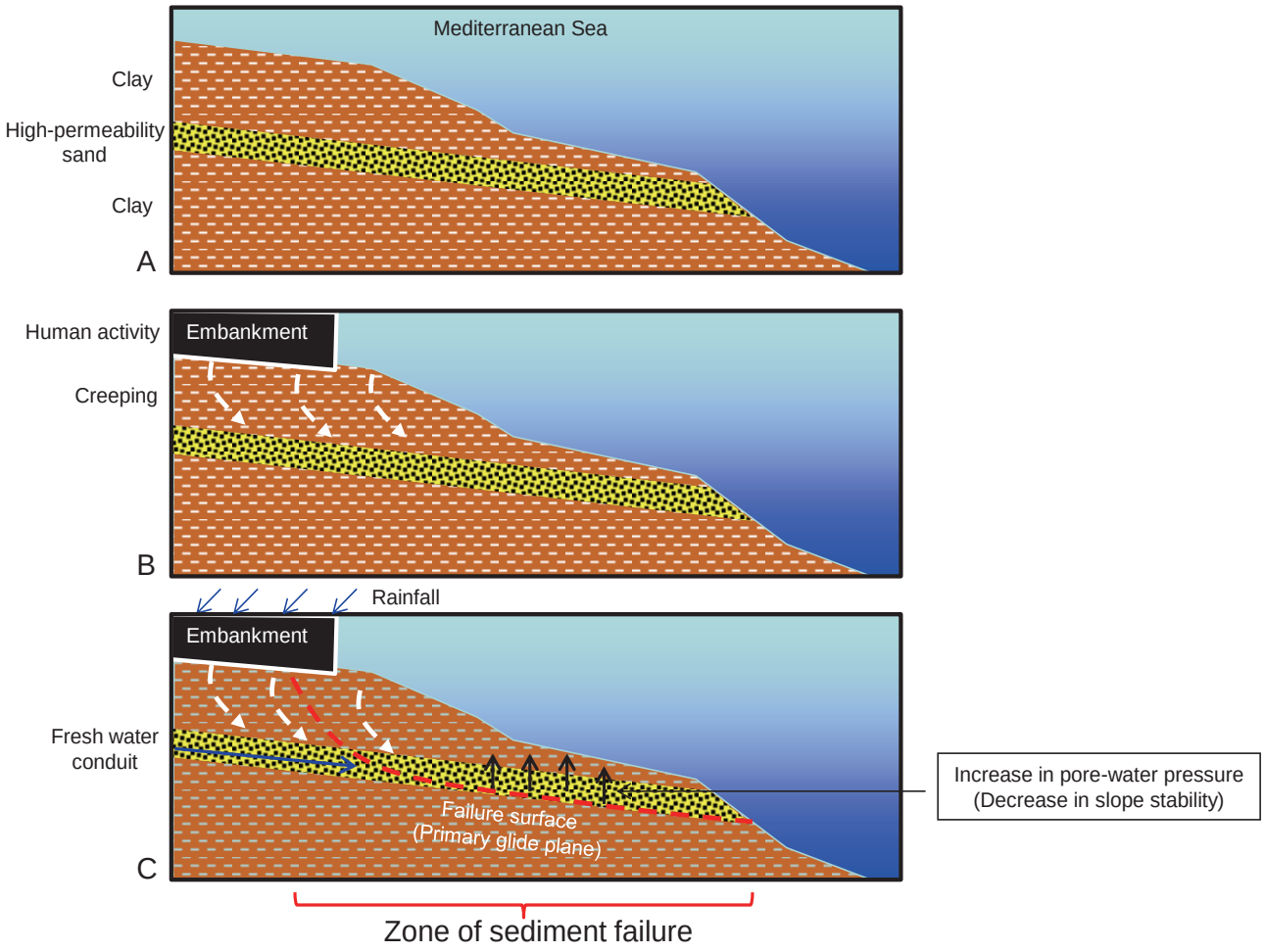

Figure 14 Illustration of the 1979 sediment failure that occurred at the Nice international airport in southern France. The Nice sediment failure has been attributed to a combination of both external and internal factors (Dan *et al.*, 2007). A−Internal (*in situ*) lithologic factor composed of clay and sand layers; B−Human factor involving the building of airport embankment; C−External meteorological and internal geotechnical factors. See text for details. Diagram is based on the concept of Dan *et al.*, (2007, their Figure 20). With permission from Elsevier Copyright Clearance Center's RightsLink: Licensee: G. Shanmugam. License Number: 3571710918661. License Date: February 18, 2015.

However, there are no established criteria to distinguish SMTD associated with tsunamis (Figure 18) from those associated with tropical cyclones (Shanmugam, 2012b). This is an important area of future research.

The Hurricane Hugo (Hubbard, 1992), which passed over St. Croix in the U.S. Virgin Islands on 17 September 1989, had generated winds in excess of 110 knots (204 km·h^{-1}, Category 3 in the Saffir-Simpson Scale) and waves 6−7 m in height. In the Salt River submarine canyon (>100 m deep), offshore St. Croix, a current meter measured net down-canyon currents reaching velocities of 2 m·s^{-1} and oscillatory flows up to 4 m·s^{-1}. Hurricane Hugo had caused erosion of 2 m of sand in the Salt River Canyon at a depth of about 30 m. A minimum of 2 million kg of sediment were flushed down the Salt River Canyon into deep water (Hubbard, 1992). The transport rate associated with Hurricane Hugo was 11 orders of magnitude greater than that measured during fair-weather period. In the Salt River Canyon, much of the soft reef cover (*e.g.*, sponges) had been eroded away by the power of the hurricane. Debris composed of palm fronds, trash, and pieces of boats found in the canyon were the evidence for storm-generated debris flows. Storm-induced sediment flows during the present highstand have also been reported in a submarine canyon off Bangladesh (Kudrass *et al.*, 1998), in the Capbreton Canyon, Bay of Biscay in SW France (Mulder *et al.*, 2001), in the Cap de Creus Canyon in the Gulf of Lions (Palanques *et al.*, 2006), and in the Eel Canyon, California (Puig *et al.*, 2003), among others. These alternative real-world highstand possibilities are often overlooked because of the prevailing mindset of the sea-level lowstand model.

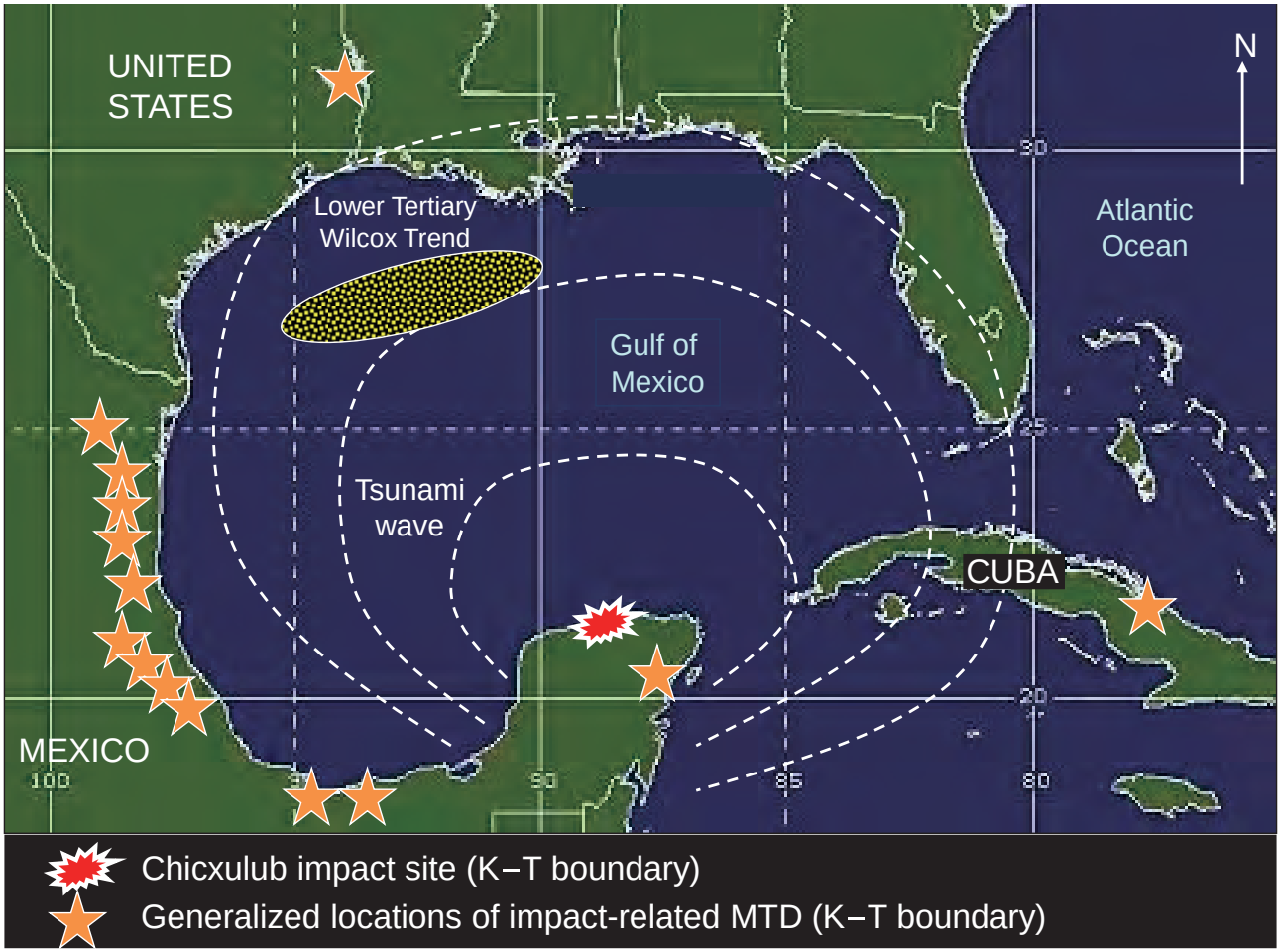

Figure 15 Map showing the site of Chicxulub meteorite impact at the K−T boundary in Yucatan, Mexico, and the inferred link between impact-related tsunami waves and deep-water petroleum reservoirs in the Gulf of Mexico (see text for details). Note northward propagation of tsunami waves away from the impact site. Generalized outline of petroleum-producing Lower Tertiary Wilcox Trend is from several sources (*e.g.*, Meyer *et al.*, 2007). Stars represent locations of mass-transport deposits and tsunami-related deposits associated with the Chicxulub impact at the K−T boundary (Bourgeois *et al.*, 1988; Smit *et al.*, 1996; Grajales-Nishimura *et al.*, 2000; Takayama *et al.*, 2000; Claeys *et al.*, 2002; Lawton *et al.*, 2005). After Shanmugam (2012a). With permission from Elsevier Copyright Clearance Center's RightsLink: Licensee: G. Shanmugam. License Number: 3577110946798. License Date: February 27, 2015.

The reasons for sand deposition in the deep sea during highstands are: (1) narrow shelf width and headward erosion of submarine canyons (Schwalbach *et al.*, 1996); (2) increasing monsoon intensity (Goodbred, 2003) and related deep-water sedimentation (Weber *et al.*, 1997); (3) sediment bypassing of the shelf (Kuehl *et al.*, 1989); (4) rates of delta progradation and formation of highstand shelfedge deltas (Burgess and Hovius, 1998); (5) high sediment supply (Carvajal and Steel, 2006); (6) cyclones (Kudrass *et al.*, 1998; Shanmugam, 2008b); and (7) tsunamis (Shanmugam, 2006a, 2006b). In discussing the La Jolla highstand fan in the California borderland, Covault *et al.* (2007, p. 786) state, "*Contrary to widely used sequence stratigraphic models, lowstand fans are only part of the turbidite depositional record, and this analysis reveals that a comparable volume of coarse clastic sediment has been deposited in California borderland deep-water basins regardless of sea level*."

At the rate of 10 cyclones per year during 1891−2000 in the Bay of Bengal (Mascarenhas, 2004), 200,000 cyclones would have occurred during the present highstand (Figure 19). Empirical data also show that 140,000 tsunamis would have occurred during the present highstand interval in the Pacific Ocean alone (Figure 19). In other words, sand deposition can and does occur during periods of sea-level highstands (Figure 19). For these reasons, the lowstand model is obsolete for explaining the triggering of deep-water SMTD worldwide (Shanmugam, 2007, 2008b).

In light of the existing wealth of empirical data associ-

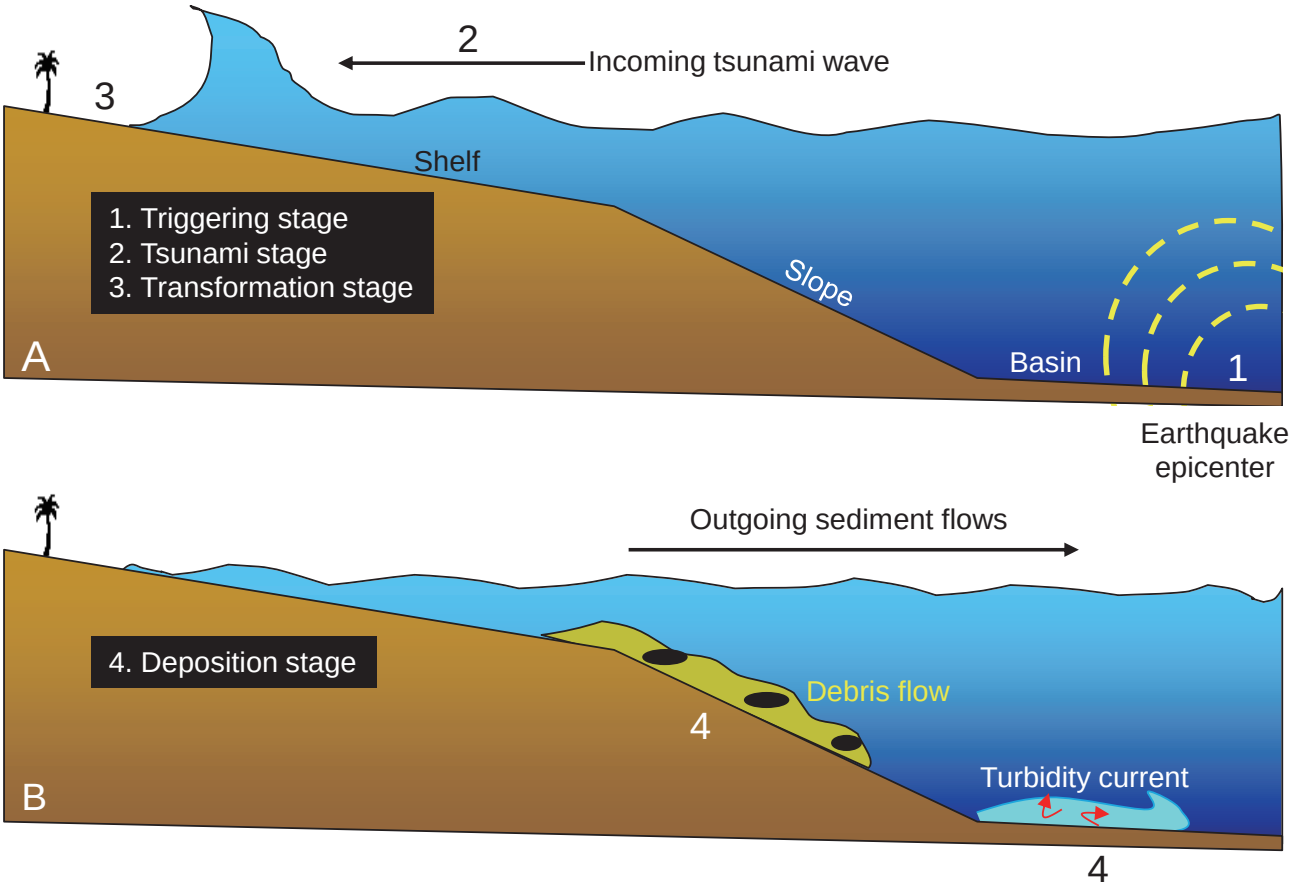

Figure 16 Depositional model showing the link between tsunamis and deep-water deposition. A−1−Triggering stage in which earthquakes trigger tsunami waves. 2−Tsunami stage in which an incoming (up-run) tsunami wave increases in wave height as it approaches the coast. 3−Transformation stage in which an incoming tsunami wave erodes and incorporates sediment, and transforms into sediment flows; B−4−Deposition stage in which outgoing (backwash) sediment flows (*i.e.*, debris flows and turbidity currents) deposit sediment in deep-water environments. Suspended mud created by tsunami-related events would be deposited via hemipelagic setting. After Shanmugam (2006b). With permission from SEPM.

ated with tsunamis, tropical cyclones, meteorite impacts, earthquakes, *etc.*, future petroleum exploration cannot afford to continue the application of obsolete sea-level models in understanding the timing and emplacements of deep-water sands (Shanmugam, 2007).

6 Long-runout mechanisms

An understanding of long-runout mechanisms is important not only for academic reasons, but also for economic reasons. For example, long-runout MTD (Table 5) provide empirical data for developing predictive depositional models for deep-water sandstone petroleum reservoirs in the subsurface.

6.1 Basic concept

The basic premise of long-runout MTD is that they travel further than the distance predicted by simple frictional models. Heim's (1932) study of the subaerial 'Elm Slide' in the Swiss Alps has been the source of the following basic equations for understanding the mobility of MTD:

1) $H/L = \tan \varphi$, where H represents the vertical fall height, L represents the runout distance, and φ is the Coulomb angle of sliding friction (*e.g.*, Griswold and Iverson, 2008).

2) $H/L \alpha\ 1/V$, where V is the initial volume of the moving mass (*e.g.*, McEwen, 1989).

3) $H/L = 1$, where L is the normal-runout distance (Figure 20A) (*e.g.*, Collins and Melosh, 2003).

4) $H/L \leqslant 1$, where L is the long-runout distance (Figure 20B) (*e.g.*, Hampton *et al.*, 1996).

Although there are many documented cases of long-runout MTD in both subaerial (Table 5) and submarine (*e.g.*, submarine slides in Hawaii with more than 200 km of runout distances, Moore *et al.*, 1989) environments with

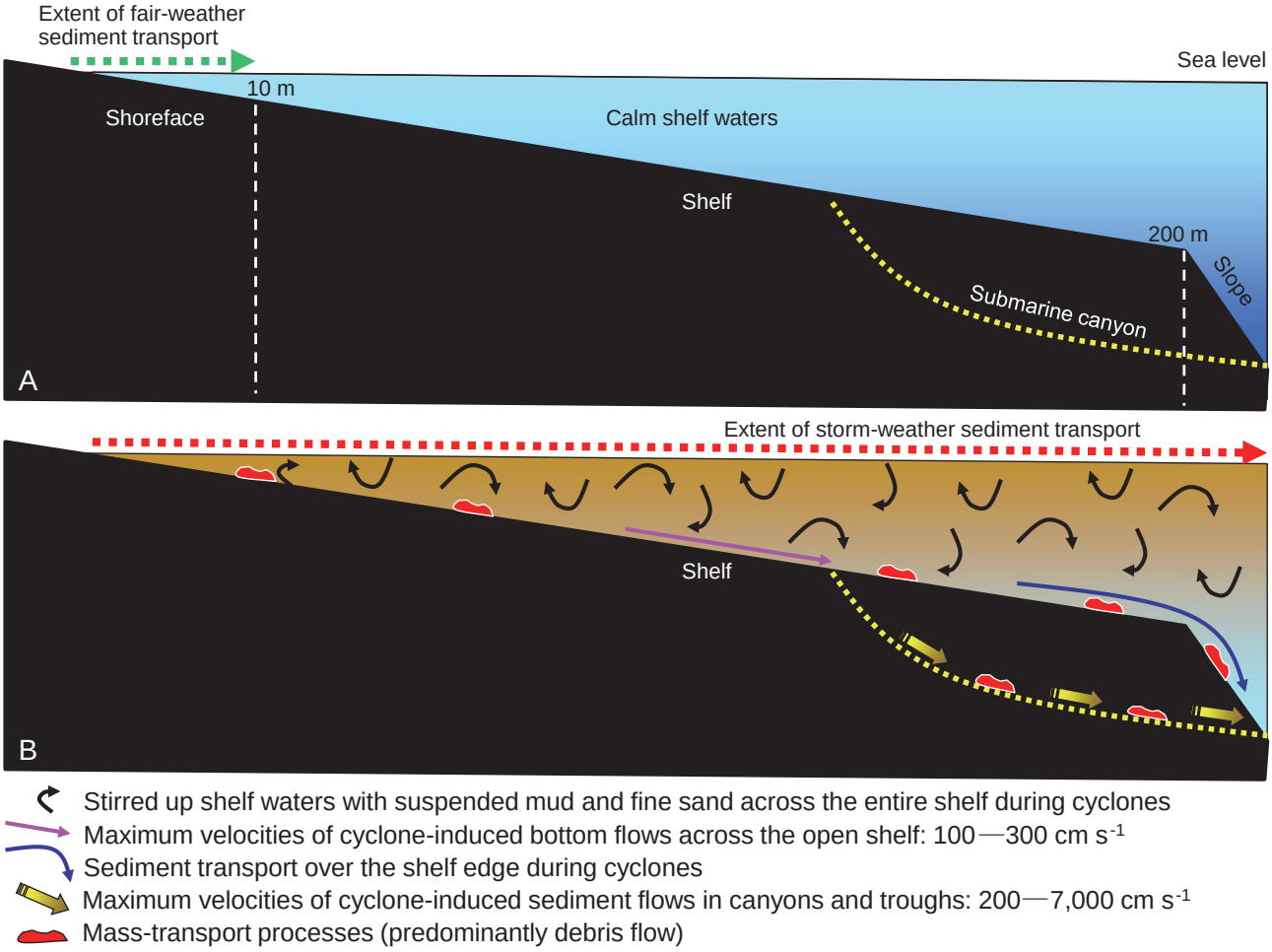

Figure 17 A−Highstand sedimentological model showing calm shelf waters and limited extent of sediment transport in the shoreface zone (short green arrow) during fair-weather periods. Shoreface bottom-current velocities during fair weather are in the range of 10−20 cm s^{-1} (Snedden *et al.*, 1988). The shelf edge at 200 m water depth separates shallow-water (shelf) from deep-water (slope) environments; B−Highstand sedimentological model showing sediment transport on the open shelf, over the shelf edge, and in submarine canyons during periods of tropical cyclones (storm weather) into deep water (long red arrow). Mass-transport processes are commonly induced by intense hurricanes (*e.g.*, 2005 Hurricane Katrina in the U.S. Gulf Coast). Modified after Shanmugam (2008b). With permission from AAPG.

runout distances measuring up to 100 times their vertical fall height and high speeds of up to 500 km·h^{-1} (Martinsen, 1994), the geologic community was reluctant to accept mechanisms that attempted to explain MTD that travel farther and faster than expected. A major turning point on the skepticism over long-runout MTD occurred on May 18, 1980 when the Eruption of Mount St. Helens in the U.S. generated impressive long runout subaerial MTD that were captured on videotapes (see The Learning Channel, 1997).

6.2 Subaerial environments

There are at least 20 potential mechanisms that could explain the mechanical paradox of long-runout MTD (Terzaghi, 1950; Brunsden, 1979; Schaller, 1991, among others). Selected examples of subaerial mechanisms are:

1) Lubrication by liquefied saturated soil entrained during transport (Heim, 1882; Hungr and Evans, 2004)

2) Dispersive pressure in grain flows (Bagnold, 1954)

3) Fluidization by entrapped air (Kent, 1966)

4) Cushion of compressed air beneath the slide (Shreve, 1968)

5) Fluidization by dust dispersions (Hsü, 1975), akin to grain flows (Bagnold, 1954)

6) Spontaneous reduction of friction angle at high rates of shearing (Scheidegger, 1975; Campbell, 1989)

7) Vaporization of water at the base and related excess pore-water pressure (Goguel, 1978)

8) Frictional heating along a basal fluid-saturated shear zone and related rise in pore-water pressure (Voight and

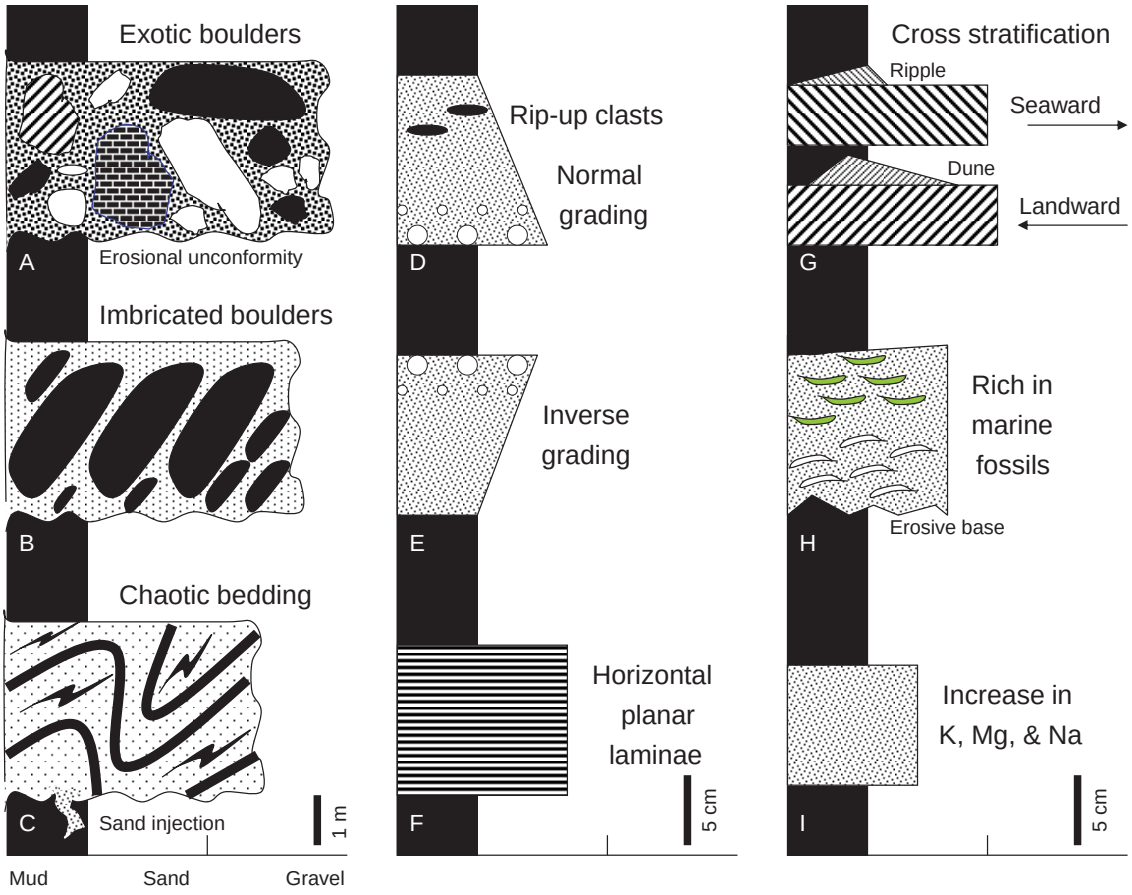

Figure 18 Published sedimentological features claimed to be associated with tsunami-related deposits by other authors. These features are also claimed to be associated with cyclone-related deposits by different authors. See review by Shanmugam (2012b). With permission from Springer Copyright Clearance Center's RightsLink: Licensee: G. Shanmugam. License Number: 3570270421988. License Date: February 15, 2015.

Faust, 1982; Goren and Aharonov, 2007)

9) Self-lubrication by frictionally generated basal melt layers (Erismann, 1979; De Blasio and Elverhøi, 2008; Weidinger and Korup, 2009)

10) Acoustic fluidization (Melosh, 1979)

11) Mechanical fluidization or inertial grain flow (Davies, 1982)

12) Fluidization by volcanic gases (Voight *et al.*, 1983).

13) Excess pore-water pressure (Cruden and Hungr, 1986; Iverson, 1997)

14) Self-lubrication by granular flows acting as basal shear zone (Cleary and Campbell, 1993)

15) Seismic energy released during meteorite impacts, proposed for Mars (Akers *et al.*, 2012), is also applicable to Earth.

6.3 Submarine environments

Submarine environments with long-runout MTD have been broadly grouped into five types: (1) fjords, (2) active river deltas on the continental margin, (3) submarine canyon-fan systems, (4) open continental slopes, and (5) oceanic volcanic islands and ridges by Hampton *et al.* (1996). To this list, a sixth type 'glacially-influenced continental margins' (Elverhøi *et al.*, 1997) needs to be added. Submarine MTD with long-runout distances of over 100 km commonly occur on slopes of less than 2° on the U.S. Atlantic Continental Slope (Figure 5). Several potential mechanisms are available for explaining long-runout submarine MTD over low-angle slopes:

1) Hydroplaning (Mohrig *et al.*, 1998)

2) Excess pore-water pressure (Pierson, 1981; Gee *et al.*, 1999)

3) Elevated gas pressure (Coleman and Prior, 1988)

4) Dispersive pressure in grain flows (Bagnold, 1954; Norem *et al.*, 1990)

5) Self-lubrication by granular flows acting as basal shear zone (Cleary and Campbell, 1993)

6) Self-lubrication at the base of gas-hydrate stability window that coincides with the base of MTD (Bugge *et al.*, 1987; Cochonat *et al.*, 2002).

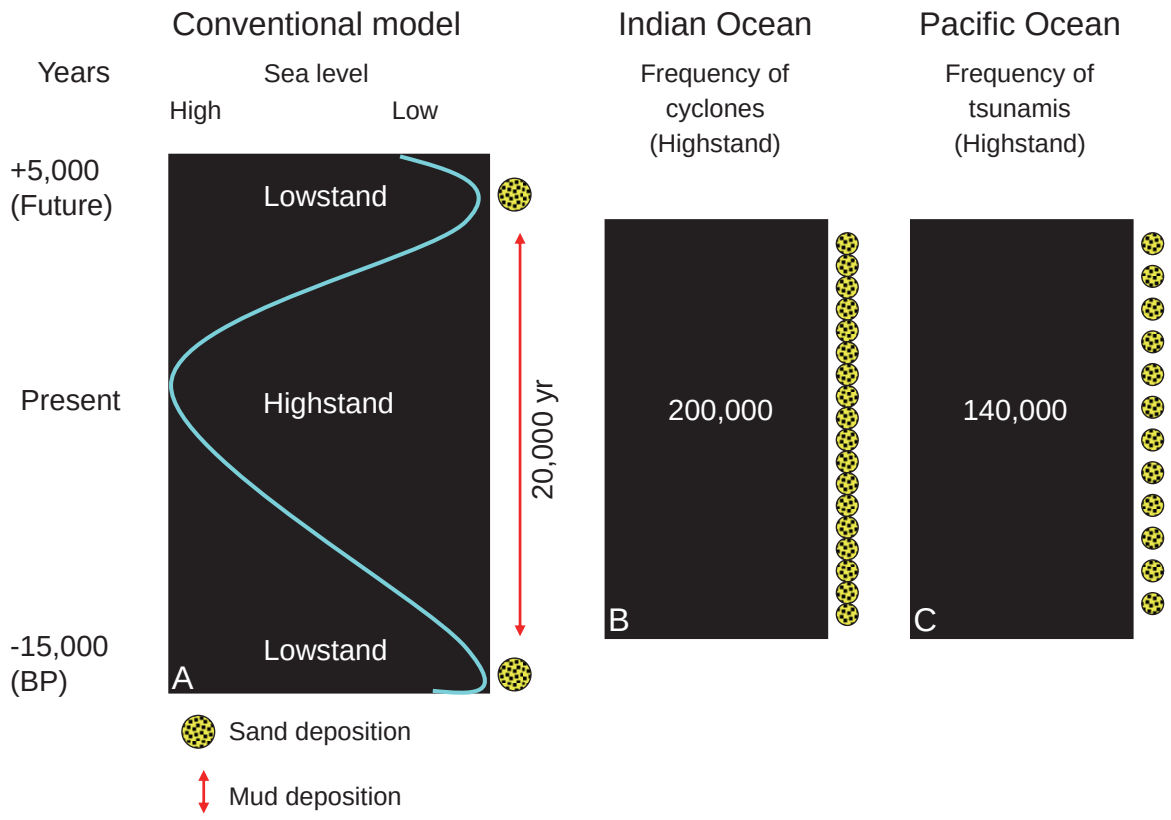

Figure 19 A−Conventional sea-level model showing deep-water deposition of sand during periods of lowstand and deposition of mud during periods of highstand. The present highstand is estimated to represent a period of 20,000 years. BP = before present; B−200,000 cyclones are estimated to occur during the present highstand in the Bay of Bengal (Indian Ocean) and in the Atlantic Ocean; C−140,000 tsunamis are estimated to occur during the present highstand in the Pacific Ocean. After Shanmugam (2008b). With permission from AAPG.

7) Flow transformation (Talling *et al.*, 2007)

8) Seismic energy released during meteorite impacts, proposed for Mars (Akers *et al.*, 2012), is also applicable to Earth.

Of various mechanisms listed above, the hydroplaning concept (Mohrig *et al.*, 1998) has gained acceptance (McAdoo *et al.*, 2000; Shanmugam, 2000; Marr *et al.*, 2001; Elverhøi *et al.*, 2002; Ilstad *et al.*, 2004; De Blasio *et al.*, 2006). Nevertheless, the hydroplaning mechanism is inapplicable to explaining long-runout debris flows in subaerial and extraterrestrial environments.

6.4 Extraterrestrial environments

Analogous to subaerial and submarine environments on Earth, there are numerous published examples of long-runout MTD on other planets of the Solar System (Table 5). Although submarine MTD show much longer runout distances than those of subaerial MTD on Earth, the longest runout distance of 2500 km has been documented for an extraterrestrial MTD on Mars (Montgomery *et al.*, 2009, their Figure 9). The following mechanisms have been offered for explaining long-runout MTD on extraterrestrial environments:

1) Self-lubrication by released groundwater, wet debris, or mud (Lucchitta, 1979, 1987)

2) Aqueous pore-pressure support (Harrison and Grimm, 2003)

3) Continental-scale salt tectonics coupled with overpressured fluids (Montgomery *et al.*, 2009)

4) Movement on ice (De Blasio, 2011)

5) Movement on evaporitic salt (De Blasio, 2011)

6) Friction reduction during flash heating (Singer *et al.*, 2012)

7) Seismic energy released during meteorite impacts (Akers *et al.*, 2012). Similar explanations were offered previously for landslides on the Moon (Guest, 1971; Howard, 1973).

6.5 *H/L* ratio problems

Although the *H/L* model has been influential for nearly a century, many problems still remain.

1) Because the original work by Heim (1932) was

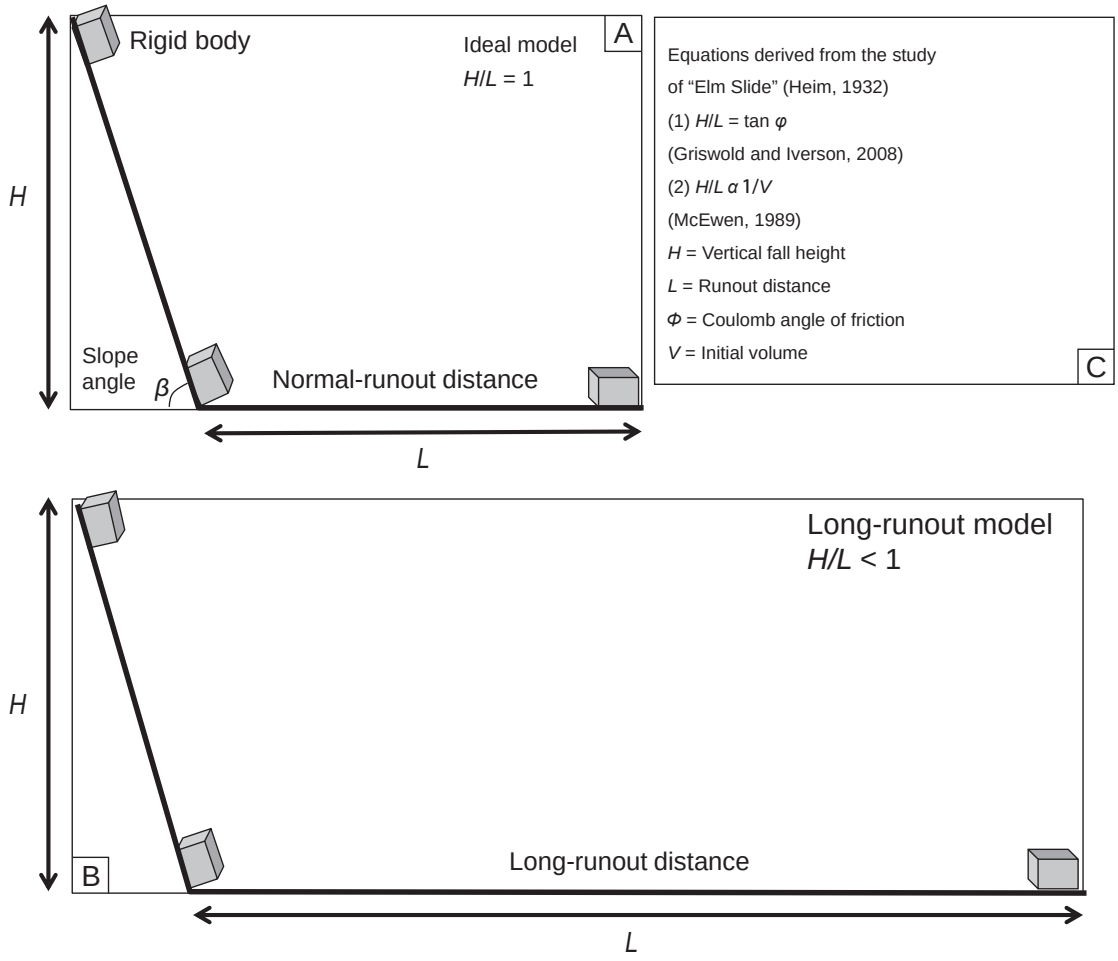

Figure 20 Conceptual models showing sliding movement of a rigid body in subaerial environments. A−An ideal model in which the predicted runout length (*L*) is equal to vertical fall height (*H*) (*e.g.*, Collins and Melosh, 2003); B−Long-runout model in which the runout length (*L*) exceeds the vertical fall height (*e.g.*, Hampton *et al.*, 1996); C−Basic equations derived from the work of Heim (1932) on the 'Elm Slide' in the Swiss Alps.

written in German, there have been differences of opinion among later workers as to the meaning of the German nomenclature used by Heim to describe the type of motion, ranging from sliding (Shreve, 1968) to flowing (Hsü, 1975).

2) The *H/L* ratios for submarine MTD are lower (0.001−0.3, Hampton *et al.*, 1996, their Table 5) than those for subaerial counterparts (1.6−21, Ritter *et al.*, 1995). The model underestimates the extent of runout distance (*L*) for water-saturated debris flows (Iverson, 1997; Griswold and Iverson, 2008) and if the volumes of moving mass exceed about 106 m^3 (Heim, 1932; Hsü, 1975; Scheidegger, 1973). Also, the model does not take into account the effect of runout-path topography on the distal or lateral limits of inundation (Griswold and Iverson, 2008).

3) At a given value of *H/L*, the Martian MTD are typically about 50 to 100 times more voluminous than the terrestrial counterparts (McEwen, 1989). However, there is no universally accepted physical basis for explaining the equation $H/L\alpha\ 1/V$ (Dade and Huppert, 1998).

4) Dade and Huppert (1998) have used *L/H* as a measure of the efficiency of MTD movement, which is the inverse of the friction coefficient (*H/L*).

5) On Earth, submarine MTD are much larger in size than subaerial MTD (Hampton *et al.*, 1996), and submarine MTD travel longer distances than subaerial MTD (Figure 21) (Hampton *et al.*, 1996, their Table 1; and Elverhøi *et al.*, 2002, their Table 1).

6) Venusian MTD (Malin, 1992, his Figure 11) and Martian MTD (Collins and Melosh, 2003, their Figure 1) travel longer distances than those on Earth′s subaerial environments (Figure 22).

7) The *H/L* model has been applied to both 'landslides' and 'debris flows' without acknowledging the basic differences in sediment movement between the two processes (McEwen, 1989; Malin, 1992; Hampton *et al.*, 1996; Ab-

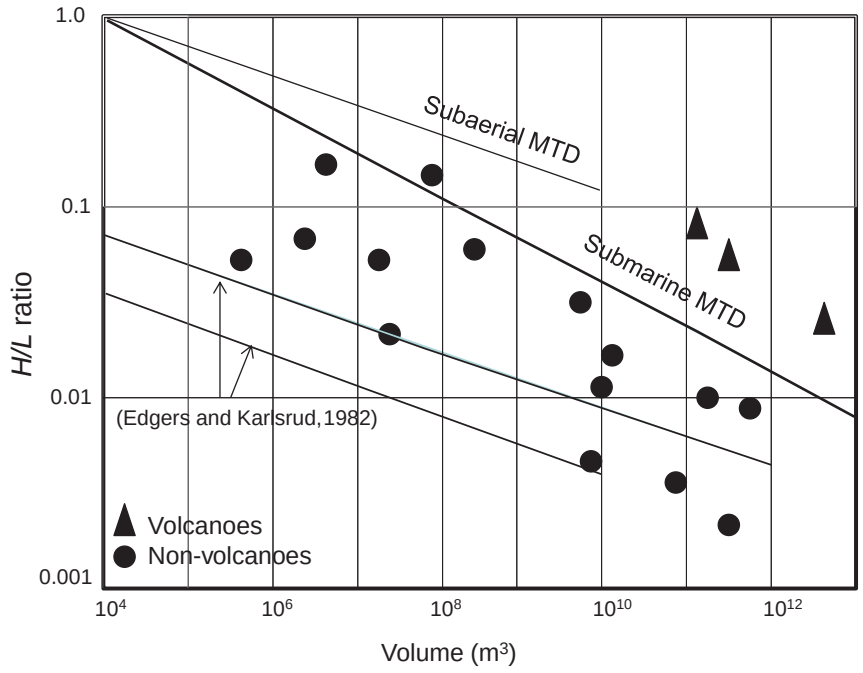

Figure 21 Plot of *H/L* (vertical fall height/length of runout) ratio versus volume of submarine MTD by Hampton *et al.* (1996). For comparison, the average value for subaerial MTD (upper curve) proposed by Scheidegger (1973) is shown. Note the upper-bound values from Edgers and Karlsrud (1982) for submarine (upper curve) and subaerial (lower curve) MTD. Redrawn from Hampton *et al.* (1996). With permission from American Geophysical Union.

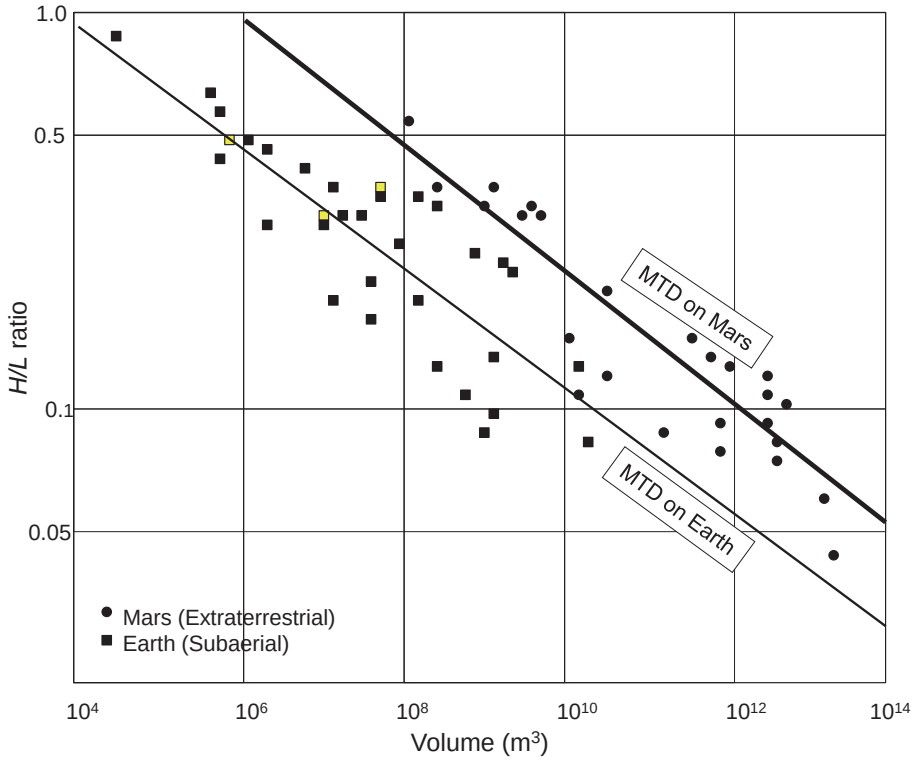

Figure 22 Plot of *H/L* (vertical fall height/length of runout) ratio vs. volume of MTD on Mars and Earth. Filled circles = Data points from Valles Marineris on Mars (McEwen, 1989, his Table 1). Filled squares = Data points for dry-rock avalanches of nonvolcanic origin on Earth (Scheidegger, 1973; Hsü, 1975). Lines are linear least-squares fits. Redrawn from McEwen (1989). With permission from Geological Society of America.

lay and Hürlimann, 2000; McAdoo *et al.*, 2000; Elverhøi *et al.*, 2002; Legros, 2002; Collins and Melosh, 2003; Geertsema *et al.*, 2009; Singer *et al.*, 2012). The problem is that slides represent a rigid-body sliding motion over a shear surface (Varnes, 1978; Dott, 1963), whereas debris flows represent an intergranular flowing motion (Shanmugam *et al.*, 1994; Iverson *et al.*, 1997).

8) In subaerial environments on Earth, *H/L* ratios were measured from outcrops (Heim, 1932), but in submarine environments *H/L* ratios were measured using bathymetric and/or side-scan sonar images (McAdoo *et al.*, 2000). On Mars, *H/L* ratios were measured from the Viking Orbiter images (McEwen, 1989). Clearly, there is no consistency among these methodologies.

9) Unlike on Earth, field measurements of motion type and direct examination of the rock *in situ* are impractical in distinguishing slides from debris flows on other planets. Nevertheless, Malin (1992) interpreted slides and debris flows on Venus based on types of landforms seen on radar images acquired from the Magellan spacecraft. Costard *et al.* (2002) interpreted debris flows based on the observation of small gullies on Mars, seen on images obtained from the Mars Observer Camera (MOC) aboard the Mars Global Surveyor spacecraft, and using the similarities of Martian gullies with gullies in East Greenland. Miyamoto *et al.* (2004) interpreted debris flows on Mars using MOC images and numerical simulation. The problem is that debrite depositional facies should be interpreted using cm-scale primary sedimentary features in core or outcrop for establishing plastic rheology and laminar state of the debris flow (see 'Recognition of Depositional Facies' section above). Such detailed observations cannot be made using seismic data and radar images.

After over 130 years of research, since the work of Heim (1882), there is still no agreement on a unified scientific theory on long-runout MTD. The reason is that each case is unique. More importantly, there are no consistencies in concepts, nomenclatures, data sources, and methodologies when investigating MTD on different planets.

7 Reservoir characterization

An accurate depiction of depositional facies is crucial in reservoir characterization of deep-water MTD. However, there are cases in which the use of the term landslide has created unnecessary confusion. For example, Welbon *et al.* (2007, p. 49) state, "*Landslides can consist of rotational slips, translational slide blocks, topples, talus slopes, debris flows, mudslides and compressional toes which combine in different proportions to form complex landslides… Processes of landslide deformation include slip on discrete surfaces, distribution of shear within the landslide, vertical thinning and lateral spreading through shear, fluidization, porosity collapse and loss of material from the top or toe of the complex. These processes control the quality of the resultant reservoirs*." This reservoir characterization raises the following fundamental questions:

- What are the criteria for distinguishing deposits of topples with no sliding motion from those of debris flows with flowing motion in core or on seismic profiles?
- Does the porosity collapse occurs in deposits of topples?
- If so, what are the criteria to recognize porosity collapse in deposits of topples in the subsurface?
- What is the point in including a landform (talus slope) along with a process (debris flow) under the term landslide? For clarity, reservoir characterization of deep-water sands must identify the process-specific depositional facies, such as slides, slumps, debrites, *etc.*

In reservoir characterization, wireline (*e.g.*, gamma-ray) log motifs are the basic subsurface data that are routinely used by the petroleum industry. Interpreting a process-specific depositional facies (*e.g.*, slide vs. debrite) from a log motif, without corresponding sediment core, is impossible. For example, analogous to sandy slide blocks that are sandwiched between deep-water mudstones in outcrops (Figure 11), long runout sandy debrite bodies (Figure 23) are likely to generate blocky motifs on wireline logs in the subsurface (Figure 24A). In distinguishing sandy slides (Figure 24B) from sandy debrites (Figure 24C) in the ancient startigraphic record, direct examination of the rocks is crucial.

The other issue is the differences in reservoir quality between slides and debrites. Large sandy slides commonly contain multiple original strata (Figure 11). In cases where lithified strata are transported as sandy slides almost intact, the slided bodies are likely to represent original porosity and permeability (*i.e.*, pre-transport reservoir quality) from the provenance (Figure 24B). On the other hand, debrites are likely to represent post-transport depositional texture and reservoir quality (Figure 24C). Furthermore, if a sandy slide unit contains two sandstone reservoirs with an intervening shale layer, the shale layer could act as a permeability barrier (Figure 24B). In such cases, a single slide unit would have to be characterized as two separate petrophysical flow units. By contrast, a single debrite unit, without a permeability layer, would be characterized as a single petrophysical flow unit (Figure 24C).

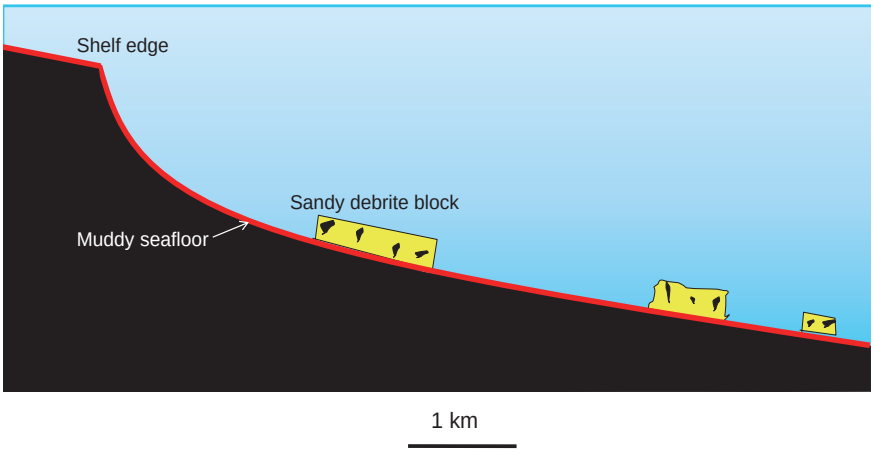

Figure 23 Conceptual model showing long-runout sandy debrite blocks away from the shelf edge. Based on studies of sandy debris flows and their deposits in flume experiments (Shanmugam, 2000; Marr *et al.*, 2001), documentation of long-runout sandy debris flows in modern oceans (Gee *et al.*, 1999) and interpretation of long-runout ancient "olistolith" (Teale and Young, 1987). This model is useful in developing deep-water depositional models for sandstone reservoirs of debrite origin. After Shanmugam (2012a). With permission from Elsevier Copyright Clearance Center's RightsLink: Licensee: G. Shanmugam. License Number: 3577110946798. License Date: February 27, 2015.

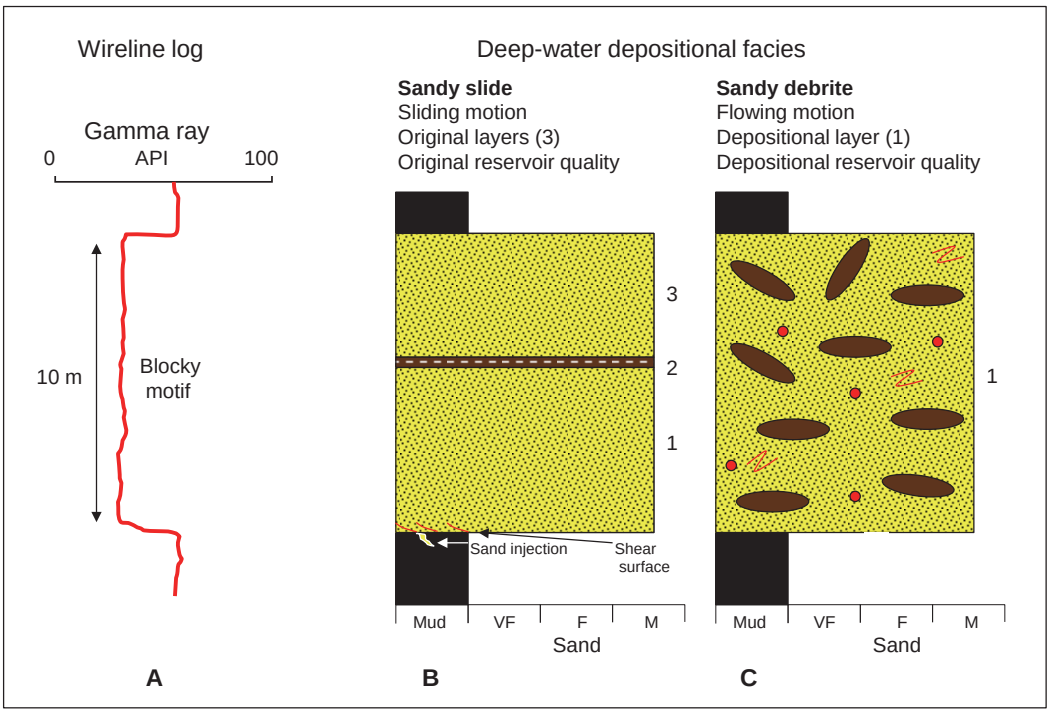

Figure 24 A−Hypothetical wireline log showing blocky motif for both sandy slide and sandy debrite units (compare with Figures 10A and 11). Blocky gamma ray (wireline) log motifs, among other motifs, are basic subsurface data that are routinely used by the petroleum industry (*e.g.* Shanmugam *et al.*, 1995). The primary control of log motif is sediment texture (*i.e.*, sand vs. mud), not individual primary sedimentary structures. Without direct examination of the rocks for sedimentary structures, distinguishing between a slide and a debrite facies is impossible from wireline log motifs alone; B−Hypothetical sedimentological log of a sandy slide unit, composed of three original layers representing pre-transport strata and texture from the provenance region, with basal shear surface and sand injection. 1. Sandstone. 2. Shale. 3. Sandstone. Note that layer 2 (shale) may act as a permeability barrier and that layer 3 (upper sandstone) and layer 1 (lower sandstone) may behave as two separate flow units during production; C−Hypothetical sedimentological log of a sandy debrite unit with floating mudstone clasts and quartz granules (red circles). This debrite sandstone without permeability barrier would behave as a single flow unit. VF = Very fine sand; F = Fine sand; M = Medium sand.

8 Ending the problem

The term "landslide" has been in use in a variety of scientific domains since 1838 without conceptual clarity. During the past 175 years, our failure to adopt a sound process-specific terminology has resulted in 79 superfluous MTD types in the geologic and engineering literature. This profligate period of "kicking the can down the road" must end now. Only slides, slumps, and debrites can be meaningfully interpreted in the sedimentary record. Therefore, the term "landslide" should be restricted solely to MTD in which a sliding motion can be empirically determined. A precise interpretation of a depositional facies (*e.g.*, sandy slide vs. sandy debrite) is vital not only for maintaining conceptual clarity but also for characterizing petroleum reservoirs. Clarity matters in science.

Acknowledgements

I thank Prof. Zeng-Zhao Feng (Editor-in-Chief) for his interest and Ms. Yuan Wang of the *Journal of Palaeogeography* for encouraging me to submit this review. I am grateful to the two anonymous journal reviewers for their critical and helpful comments. This paper is the culmination of gathering and analyzing empirical data on MTD during the past 40 years. My sedimentological research on deep-water mass-transport deposits began in 1974 as a part of my Ph.D. work on the Middle Ordovician of the Southern Appalachians in the USA (Shanmugam, 1978; Shanmugam and Benedict, 1978; Shanmugam and Walker, 1978, 1980) and has continued through my employment with Mobil Oil Company (Shanmugam, 1996, 1997; Shanmugam and Moiola, 1995; Shanmugam *et al.*, 1994, 1995) to the present as a consultant (Shanmugam, 2000, 2002, 2006a, 2012a, 2013a, 2014a). I thank R. J. Moiola and other geological managers for providing enthusiastic support for my research throughout my employment with Mobil (1978−2000). I am indebted to numerous colleagues at Mobil and other oil companies, petroleum-related service companies, academic institutions, and government agencies for assisting me in core and outcrop description worldwide. As always, I thank my wife Jean for her general comments. Finally, I am deeply indebted to Prof. Ian D. Somerville and Ms. Yuan Wang for their meticulous editing of this tome.

References

Ablay, G., Hürlimann, M., 2000. Evolution of the north flank of Tenerife by recurrent giant landslides. Journal of Volcanology and Geothermal Research, 103: 135−159.

Akers, C., Schedl, A. D., Mundy, L., 2012. What caused the landslides in Valles Marineris, Mars? The Woodlands, Texas: 43rd Lunar and Planetary Science Conference, March 19−23, 2012. http://search.aol.com/aol/search?q=What%20caused%20the%20landslides%20in%20Valles%20Marineris%2C%20Mars%3F&s_it=keyword_rollover&ie=UTF−8&VR=3430 (accessed December 27, 2014).

Almagor, G., Wiseman, G., 1982. Submarine slumping and mass movements on the slope of Israel. In: Saxov, S., Nieuwenhuis, J. K., (eds). Marine Slides and Other Mass Movements. New York and London: Plenum Press, 95−128.

Alves, T. M., Cartright, J. A., 2010. The effect of mass-transport deposits on the younger slope morphology, offshore Brazil. Marine and Petroleum Geology, 27: 2027−2036.

Anderson, J. G., 1906. Solifluction, a component of subaerial denudation. Journal of Geology, 14: 91−112.

Anderson, S. A., Riemer, M. F., 1995. Collapse of saturated soil due to reduction in confinement. Journal of Geotechnical Engineering, 121(2): 216−220.

Anderson, S. A., Sitar, N., 1995. Analysis of rainfall-induced debris flows. Journal of Geotechnical Engineering, 121(7): 544−552.

Andresen, A. Bjerrum, L., 1967. Slides in subaqueous slopes in loose sand and silt. In: Richards, A. F., (ed). Marine Geotechnique. Urbana: University of Illinois Press, 221−239.

Bagnold, R. A., 1954. Experiments on a gravity free dispersion of large solid spheres in a Newtonian fluid under shear. Royal Society of London, Proceedings (A), 225: 49−63.

Baltzer, A., 1875. "Uber einen neuerlichen felssturz am Rossberg, negst einigen allgemeinen Bermerkungen uber derartige Erscheinungen in den Alpen," (On a recent rockfall on Rossberg with a few observations on these phenomena in the Alps). Neues Jahrbuch fur Mineralogie, Geologie und Palaeontologie, 914−924.

Barton, R., Bird, K., Hernández, J. G., Grajales-Nishimura, J. M., Murillo-Muňetón, G., Herber, B., Weimer, P., Koeberl, C., Neumaier, M., Schenk, O., Stark, J., 2009/2010. High impact reservoirs. Oilfield Review, 21(4): 14−29.

Bates, C. C., 1953. Rational theory of delta formation. AAPG Bulletin, 37: 2119−2162.

Bates, R. L., Jackson, J. A., 1980. Glossary of Geology, Second Edition: Falls Church, Virginia, American Geological Institute, 751.

Bea, R. G., Wright, S. G., Sicar, P., Niedoroda, A. W., 1983. Wave-induced slides in South Pass Block 70, Mississippi delta. Journal of Geotechnical Engineering, 109: 619−644.

Beaubouef, R. T., Abreu, V., 2010. MTCs of the Brazos-Trinity slope system; thoughts on the sequence stratigraphy of MTCs and their possible roles in shaping hydrocarbon traps. In: Mosher, D. C., Shipp, R. C., Moscardelli, L., Chaytor, J. D., Baxter, C. D. P., Lee, H. J., and Urgeles, R., (eds). Submarine Mass Movements and Their Consequences: Advances in Natural and Technological Hazards Research, 28: 475−490.

Behrmann, J. H., Peter B. Flemings, Cédric, M. John, the IODP Ex-

pedition 308 Scientists, 2006. Rapid Sedimentation, Overpressure, and Focused Fluid Flow, Gulf of Mexico Continental Margin. Scientific Drilling, September 3, 1−17; DOI:10.2204/iodp.sd.3.03.2006.

Blong, R. J., 1973. A numerical classification of selected landslides of the debris slide-avalanche-flow type. Eng. Geol., 7: 99−114.

Bolt, B. A., Horn, W. L., Macdonald, G. A., Scott, R. F., 1975. Geological Hazards. New York: Springer-Verlag, 328.

Booth, J. S., O′Leary, D.W., Popenoe, P., Danforth, W.W., 1993. U.S. Atlantic continental slope landslides: Their distribution, general attributes, and implications. In: Schwab, W. C., Lee, H. J., Twichell, D.C., (eds). Submarine Landslides: Selected Studies in the U.S. Exclusive Economic Zone. U.S. Geological Survey Bulletin, 2002: 14−22.

Bornhold, B. D., Fine, I. V., Rabinovich, A. B., Thomson, R. E., Kulikov, E. A., 2003. The Grand Banks landslide-generated tsunami of November 18, 1929: Analysis and numerical modeling. Geophysical Research Abstracts, 5: 01775.

Bouma, A. H. 1962. Sedimentology of Some Flysch Deposits: A Graphic Approach to Facies Interpretation. Amsterdam: Elsevier, 168.

Bourgeois, J., Hansen, T. A., Wiberg, P. L., Kauffman, E. G., 1988. A tsunami deposit at the Cretaceous-Tertiary boundary in Texas. Science, 241: 567−570.

Boyd, R., Ruming, K., Goodwin, I., Sandstrom, M., Schröder-Adams, C., 2008. Highstand transport of coastal sand to the deep ocean: A case study from Fraser Island, southeast Australia. Geology, 36: 15−18.

Brabb, E. E., 1991. The world landslide problem. Episodes, 14(i): 52−61.

Brabb, E. E., Harrod, B. L., (eds). 1989. Landslides: Extent and economic significance. Proceedings of the 28th International Geological Congress: Symposium on Land Slides, Washington, DC, 17th July 1989. A. A. Balkema: Rotterdam and Brookfield (Vermont), 385.

Brönnimann, C. S., 2011. Effect of Groundwater on Landslide Triggering. Lausanne, Switzerland: École Polytechnique Fédérale de Lausanne. Ph. D. Dissertation. 239.

Brown, D. J., Bell, B. R., 2007. Debris flow deposits within the Palaeogene lava fields of NW Scotland: Evidence for mass wasting of the volcanic landscape during emplacement of the Ardnamurchan Central Complex. Bulletin of Volcanology, 69: 847−86.

Brunsden, D., 1979. Mass movements. In: Embleton, C., Thornes, J., (eds). Processes in Geomorphology. London: Arnold, 130−186.

Brush Jr., L. M., 1965. Experimental work on primary sedimentary structures. In: Middleton, G. V. (ed). Primary Sedimentary Structures and Their Hydrodynamic Interpretation. Tulsa, OK: SEPM Special Publication, 12: 17−24.

Bryn, P., Berg, K., Forsberg, C. F., Solheim, A., Kvalstad, T. J., 2005. Explaining the Storegga slide. Marine and Petroleum Geology, 22: 11−19.

Bugge, T., Befring, S., Belderson, R. H., Eidvin, T., Jansen, E., Kenyon, N. H., Holtedhal, H., Sejrup, H. P., 1987. A giant three-stage submarine slide off Norway. Geo-Marine Letters, 7: 191−198.

Burgess, P. M., Hovius, N., 1998. Rates of delta progradation during highstands: Consequences for timing of deposition in deep-marine systems. Journal of the Geological Society, London, 155: 217−222.

Camerlenghi, A., Urgeles, R., Fantoni, I., 2010. A Database on Submarine Landslides of the Mediterranean. In: Mosher, D. C., *et al.*, (eds). Submarine Mass Movements and Their Consequences, Advances in Natural and Technological Hazards Research, 28: 503−513.

Campbell, C. S., 1989. Self-lubrication for long runout landslides. The Journal of Geology, 97: 653−665.

Cannon, S. H., Kirkham, R. M., Parise, M., 2001. Wildfire-related debris-flow initiation processes, Storm King Mountain, Colorado. Geomorphology, 39: 171−188.

Carlson, P. R., Molnia, B. F., 1977. Submarine faults and slides on the continental shelf, northern Gulf of Alaska. In: Richards, A. F. (ed). Marine Geotechnology, Marine Slope Stability 2. New York: Crane, Russak & Company, 275−290.

Carter, R. M., 1975a. A discussion and classification of subaqueous mass-transport with particular application to grain-flow, slurry-low, and fluxoturbidites. Earth-Science Reviews, 11: 145−177.

Carter, R. M., 1975b. Mass-emplaced sand-fingers at Mararoa construction site, southern New Zealand. Sedimentology, 22: 275−288.

Carter, R. M., Lindqvist, J. K., 1975. Sealers Bay submarine fan complex, Oligocene, southern New Zealand. Sedimentology, 22: 465−483.

Carvajal, C. R., Steel, R. J., 2006. Thick turbidite successions from supply-dominated shelves during sea-level highstand. Geology, 34: 665−668.

Claeys, P., Kiessling, W., a Alvarez, W., 2002. Distribution of Chicxulub ejecta at the Cretaceous-Tertiary boundary. In: Koeberl, C., MacLeod, K. G., (eds). Catastrophic Events and Mass Extinctions: Impacts and Beyond. Boulder, Colorado: GSA Special Paper, 356: 55−68.

Clague, J. J., Stead, D., (eds). 2012. Landslides: Types, Mechanisms, and Modeling. Cambridge, UK: Cambridge University Press, 436.

Clarke, S., Hubble, T., Airey, D., Yu, P., Boyd, R., J Keene, J., Exon, N., Gardner, J., 2012. Submarine Landslides on the Upper Southeast Australian Passive Continental Margin—Preliminary Findings. In: Yamuda, Y., *et al.*, (eds). Submarine Mass Movements and Their Consequences·Advances in Natural and Technological Hazards Research, 31: 55−66.

Cleary, P. W., Campbell, C. S., 1993. Self-Lubrication for Long Runout Landslides′ Examination by Computer Simulation. Journal of Geophysical Research, 98(B12): 21, 911−21, 924.

Coates, D. R., 1977. Landslide prospective. In: Coates, D. R., (ed). Landslides. Boulder, Colorado: GSA, 3−38.

Cochonat, P., Cadet, J.−P., Lallemant, S. J., Mazzotti, S., Nouze, H., Fouchet, C., Foucher, J. P., 2002. Slope instabilities and gravity

processes in fluid migration and tectonically active environment in the eastern Nankai accretionary wedge (KAIKO-Tokai'96 cruise). Marine Geology, 187(1−2 SU): 193−202.

Coleman, J. M., Prior, D. B., 1982. Deltaic environments. In: Scholle, P. A., Spearing, D., (eds). Sandstone Depositional Environments. AAPG Memoir, 31: 139−178.

Coleman, J. M., Prior, D. B., 1988. Mass wasting on continental margins. Annual Review of Earth & Planetary Sciences, 16: 101−119.

Collins, G. S., Melosh, H. J., 2003. Acoustic fluidization and the extraordinary mobility of sturzstroms. Journal of Geophysical Research, 108, No. B10, 2473; DOI: 10.1029/2003JB002465, 2003.

Collinson, J., 1994. Sedimentary deformational structures. In: Maltman, A., (ed). The Geological Deformation of Sediments. London: Chapman & Hall, 95−125.

Collot, J.−Y., Lewis, K., Lamarche, G., Lallemand, S., 2001. The giant Ruatoria debris avalanche on the northern Hikurangi margin, New Zealand: Result of oblique seamount subduction. Journal of Geophysical Research, 106 (B9): 19, 271−19, 297; DOI: 10.1029/2001JB900004.

Cook, H. E., 1979. Ancient continental slope sequences and their value in understanding modern slope development. In: Doyle, L. J., Pilkey, O. H., (eds). Geology of Continental Slopes. Tulsa, OK: SEPM Special Publication, 27: 287−305.

Costard, F., Forget, F., Mangold, N., and Peulvast, J. P., 2002. Formation of recent Martian debris flows by melting of near-surface ground ice at high obliquity. Science, 295: 110−113.

Covault, J. A., Normark, W. R., Romans, B. W., Graham, S. A., 2007. Highstand fans in the California borderland: the overlooked deep-water depositional systems. Geology, 35: 783−786.

Crookshanks, S., Gilbert, R., 2008. Continuous, diurnally fluctuating turbidity currents in Kluane Lake, Yukon Territory. Canadian Journal of Earth Sciences, 45: 1123−1138.

Crozier, M. J., 1973. Techniques for the morphometric analysis of landslipe. Zeitschrift fur Geomophologie Dynamique, 17: 78−101.

Cruden, D. M., 1991. A simple definition of a landslide. Bulletin of the International Association of Engineering Geology, 43: 27−28.

Cruden, D. M., 2003. The first classification of landslides? Environmental & Engineering Geoscience, 9: 197−200.

Cruden, D. M., Hungr, O., 1986. The debris of the Frank slide and theories of rockslide-avalanche Mobility. Canadian Journal of Earth Sciences, 23: 425−432.

Cruden, D. M, Varnes, D. J., 1996. Landslides types and processes. In: Turner, A. K, Schuster, R. L., (eds). Landslides Investigation and Mitigation. Washington, D.C. Transportation Research Board National Research Council, Special Report, 247: 36−75.

Dade, W. B., Huppert, H. E., 1998. Long-runout rockfalls. Geology, 26(9): 803−806.

Damuth, J. E., Fairbridge, R. W., 1970. Equatorial Atlantic deep-sea sands and ice age aridity in tropical South America. GSA Bulletin, 81: 585−601.

Damuth, J. E., Flood, R. D., Kowsmann, R. O., Gorini, M. A., Belderson, R. H., Gorini, M. A., 1988. Anatomy and growth-pattern of Amazon deep-sea fan revealed by long-range side-scan sonar (GLORIA) and high-resolution seismic studies. AAPG Bulletin, 72: 885−911.

Dan, G., Sultan, N., Savoye, B., 2007. The 1979 Nice harbour catastrophe revisited: Trigger mechanism inferred from geotechnical measurements and numerical modeling. Marine Geology, 245: 40−64.

Davies, T. R. H., 1982. Spreading of rock avalanche debris by mechanical fluidization. Rock Mechanics and Rock Engineering, 15: 9−24.

De Blasio, F. V., 2011. Landslides in Valles Marineris (Mars): A possible role of basal lubrication by sub-surface ice. Planetary and Space Science, 59(13): 1384−1392.

De Blasio, F. V., Elverhøi, A., 2008. A model for frictional melt production beneath large rock avalanches. Journal of Geophysical Research: Earth Surface, 113, F02014; DOI:10.1029/2007JF000867.

De Blasio, F. V., Elverhøi, A., Engvik, L. E., Issler, D., Gauer, P., Harbitz, C., 2006. Understanding the high mobility of subaqueous debris flows. Norwegian Journal of Geology, 86: 275−284.

Dengler, A. T., Wilde, P., 1987. Turbidity currents on steep slopes: Application of an avalanche-type numeric model for ocean thermal energy conversion design. Ocean Engineering, 14: 409−433.

Dikau, R., Cavallin, A., Jäger, S., 1996. Databases and GIS for landslide research in Europe. Geomorphology, 15: 227−239.

Dillon, W. P., Zimmerman, H. P., 1970. Erosion by biological activity in two New England submarine canyons. Journal of Sedimentary Petrology, 40: 542−547.

Dingle, R. V., 1977. The anatomy of a large submarine slump on a sheared continental margin (SE Africa). Geological Society of London Journal, 134: 293−310.

Dingle, R. V., 1980. Large allochtonous sediment masses and their role in the construction of the continental slope and rise off southwestern Africa. Marine Geology, 37: 333−354.

Dixit, J. G., 1982. Resuspension Potential of Deposited Kaolinite Beds. Gainesville, FL: University of Florida. M.S. Thesis.

Dott, R. H., Jr., 1963. Dynamics of subaqueous gravity depositional processes. AAPG Bulletin, 47: 104−128.

Driscoll, N. W., Weissel, J. K., Goff, J. A., 2000. Potential for large-scale submarine slope failure and tsunami generation along the U.S. mid-Atlantic coast. Geology, 28: 407−410.

Duncan, J. M., Wright, S. G., 2005. Soil Strength and Slope Stability: Hoboken, New Jersey: John Wiley & Sons, Inc., 297.

Dunham, J., Saller, A. H., 2014. Modern internal waves and internal tides along oceanic pycnoclines: Challenges and implications for ancient deep-marine baroclinic sands: Discussion. AAPG Bulletin, 98: 851−857.

Duranti, D., Hurst, A., 2004. Fluidization and injection in the deep-water sandstones of the Eocene Alba Formation (U.K. North Sea). Sedimentology, 51: 503−529.

Dykstra, M. L., 2005. Dynamics of Submarine Sediment Mass-Transport, from the Shelf to the Deep Sea. Santa Barbara: The

University of California., Ph. D. dissertation., 159.

Dysthe, K., Krogstad, H. E., Műller, P., 2008. Oceanic rogue waves. Annual Reviews of Fluid Mechanics, 40: 287−310.

Dzulynski, S., Sanders, J. E., 1962. Current marks on firm mud bottoms. Connecticut Academy of Arts and Science, Transactions, 42: 57−96.

Dzulynski, S., Ksiazkiewicz, M., Kuenen, Ph. H., 1959. Turbidites in flysch of the Polish Carpathian Mountains. GSA Bulletin, 70: 1089−1118.

Easterbrook, D. J., 1999. Surface Processes and Landforms, 2nd Edition: New Jersey, Prentice Hall (Pearson Education Company), 546.

Eckel, E. B., 1958. Introduction. In: Eckel, E. B., (ed). Landslide and Engineering Practice. National Research Council, Highway Research Board Special Report, 29: 1−5.

Edgers, L., Karlsrud, K., 1982. Soil flows generated by submarine slides —— Case studies and consequences. In: Chryssostomidains, C., Connor, J. J., (eds). Proceedings of the Third International Conference on the Behavior of Offshore Structures. Bristol, PA: Hemisphere, 425−437.

Elverhøi, A., Norem, H., Anderson, E. S., Dowdeswell, J. A., Fossen, I., Haflidason, H., Kenyon, N. H., Laberg, J. S., King, E. L., Sejrup, H. P., Solheim, A., Vorren, T., 1997. On the origin and flow behavior of submarine slides on deep-sea fans along the Norwegian-Barents Sea continental margin. Geo-Marine Letters, 17: 119−125.

Elverhøi, A., F. De Blasio, F. A. Butt, D. Issler, C. B., Harbitz, L. Engvik, *et al.*, 2002. Submarine mass-wasting on glacially-influenced continental slopes: Processes and dynamics. In: Dowdeswell, J. A., O′Cofaigh, C., (eds). Glacier-Influenced Sedimentation on High-Latitude Continental Margins. London: Geological Society Special Publications, 203: 73−87.

E-MARSHAL (Earth′s continental margins: assessing the geohazard from submarine landslides), 2013. IGCP−511 Legacy. http://www.igcp585.org/ (accessed December 27, 2014).

Embley, R. W., 1976. New evidence for occurrence of debris flow deposits in the deep sea. Geology, 4: 371−374.

Embley, R. W., 1980. The role of mass transport in the distribution and character of deep-ocean sediments with special reference to the North Atlantic. Marine Geology, 38: 23−50.

Embley, R. W., 1982. Anatomy of some Atlantic margin sediment slides and some comments on ages and mechanisms. In: Saxov, S., Nieuwenhuis, J. K., (eds). Marine Slides and Other Mass Movements. New York: Plenum, 189−214.

Embley, R. W., Jacobi, R. D., 1977. Distribution and morphology of large submarine sediment slides and slumps on Atlantic Continental Margins. In: Richards, A. F., (ed). Marine Geotechnology, Marine Slope Stability. New York: Crane, Russak & Company, Inc., 2: 205−228.

Enos, P., 1977. Flow regimes in debris flow. Sedimentology, 24: 133−142.

Erismann, T. H., 1979. Mechanisms of large landslides. Rock Mechanics, 12: 15−46.

Famakinwa, S. B., Shanmugam, G., Hodgkinson, R. J., Blundell, L. C., 1996. Deep-water slump and debris flow dominated reservoirs of the Zafiro Field area, offshore Equatorial Guinea. In: Offshore West Africa Conference and Exhibition, Libreville, Gabon, November 5−7, 1−14.

Feeley K., 2007. Triggering Mechanisms of Submarine Landslides. Research Report: Boston, MA, Department of Civil and Environmental Engineering, Northeastern University, 45.

Festa, A., Dilek, Y., Gawlick, H-J., Missoni, S., 2014. Mass-transport deposits, olistostromes and soft-sediment deformation in modern and ancient continental margins, and associated natural hazards. Marine Geology, 356: 1−4.

Fisher, R. V., 1971. Features of coarse-grained, high-concentration fluids and their deposits. Journal of Sedimentary Petrology, 41: 916−927.

Fisher, R. V., 1983. Flow transformations in sediment gravity flows. Geology, 11: 273−274.

Fisher, R. V., 1995. Decoupling of pyroclastic currents: Hazards assessments. Journal of Volcanology and Geothermal Research, 66: 257−263.

Flores, G., 1955. Discussion in Beneo, E., −les Resultats des etudes pour la recherche petrolifere en Scile (Italie): Proc. 4th World Petrol. Congr. Rome, Sect. 1: 259−275.

Frey-Martinez, J., Cartwright, J., Hall, B., 2005. 3D seismic interpretation of slump complexes: Examples from the continental margin of Israel. Basin Research, 17: 83−108.

Friedman, G. M., Sanders, J. E., Kopaska-Merkel, D. C., 1992. Principles of Sedimentary Deposits: Stratigraphy and Sedimentology. New York: McMillan Publishing Company, 717.

Gales, J. A., Leat, P. T., Larter, R. D., Kuhn, G., Hillenbrand, C.−D., Graham, A. G. C.,.Mitchell, N. C., Tate, A. J., Buys, G. B., Jokat, W., 2014. Large-scale submarine landslides, channel and gully systems on the southern Weddell Sea margin, Antarctica. Marine Geology, 348: 73−87.

Gamboa, D., Alves, T., Cartwright, J., Terrinha, P., 2010. MTD distribution on a ‘passive’ continental margin: The Espírito Santo Basin (SE Brazil) during the Palaeogene. Marine and Petroleum Geology, 27: 1311−1324.

Gani, R., 2004. From turbid to lucid: A straightforward approach to sediment gravity flows and their deposits. The Sedimentary Record, 3: 4−8.

Gardner, J. V., Bohannon, R. G., Field, M. E., Masson, D. G., 1996. The morphology, processes, and evolution of Monterey Fan: A revisit. In: Gardner, J. V., Field, M. E., Twichell, D. C., (eds). Geology of the United States′ Sea Floor: The View from GLORIA. New York: Cambridge University Press, 193−220.

Gaudin, M., Berné, S., Jouanneau, J.−M., Palanques, A., Puig, P., Mulder, T., Cirac, P., Rabineau, M., Imbert, P., 2006. Massive sand beds deposited by dense water cascading in the Bourcart canyon head, Gulf of Lions (northwestern Mediterranean Sea). Marine Geology, 234: 111−128.

Gee, M. J. R., Masson, D. G., Watts, A. B., Allen, P. A., 1999. The Saharan debris fow: An insight into the mechanics of long runout

submarine debris flows. Sedimentology, 46: 317−335.

Gee, M. J. R., Gawthorpe, R. L., Friedmann, S. J., 2006. Triggering and evolution of a giant submarine landslide, offshore Angola, revealed by 3D seismic stratigraphy and geomorphology. Journal of Sedimentary Research, 76: 9−19.

Gee, M. J. R., Uy, H. S., Warren, J., Morley, C. K., Lambiase, J. J., 2007. The Brunei slide: A giant submarine landslide on the North West Borneo Margin revealed by 3D seismic data. Marine Geology, 246: 9−23.

Geertsema, M., Schwab, J. W., Blais-Stevens, A., Sakals, E., 2009. Landslides impacting linear infrastructure in west central British Columbia. Natural Hazards, 48: 59−72.

Glade, T., Anderson, M. G., Crozier, M. J., (eds). 2005. Landslide Hazard and Risk. West Sussex, UK: John Wiley & Sons, 824.

Goguel, J., 1978. Scale-dependent rockslide mechanisms, with emphasis on the role of pore fluid vaporization. In: Voight, B., (ed). Rockslides and Avalanches, 1, Natural Phenomena. Amsterdam: Elsevier, 693−705.

Goodbred, Jr., S. L., 2003. Response of the Ganges dispersal system to climate change: A source-to-sink view since the last interstade. Sedimentary Geology, 162: 83−104.

Goren, L., Aharonov, E., 2007. Long runout landslides: The role of frictional heating and hydraulic diffusivity. Geophysical Research Letters, 34, L07301; DOI:10.1029/2006GL028895, 2007.

Grajales-Nishimura, J. M., Cedillo-Pardo, E., Rosales-Domínguez, C., Morán-Zenteno, D., Alvarez, W., Claeys, P., Ruíz-Morales, J., García-Hernández, J., Padilla-Avila, P., Sánchez-Ríos, A., 2000. Chicxulub impact: The origin of reservoir and seal facies in the southeastern Mexico oil fields. Geology, 28: 307−310.

Greene, H. G., Murai, L. Y., Watts, P., Maher, N. A., Fisher, M. A., Paull, C. E., Eichhubl, P., 2006. Submarine landslides in the Santa Barbara Channel as potential tsunami sources. Natural Hazards and Earth System Sciences, 6: 63−88.

Griswold, J. P., Iverson, R. M., 2008. Mobility statistics and automated hazard mapping for debris flows and rock avalanches: Reston, Virginia, U.S. Geological Survey Scientific Investigations Report 2007−5276, 68.

Guest, J. E., 1971. Geology of the farside crater Tsiolkovsky. In: Fielder, G., (ed). Geology and Physics of the Moon. Amsterdam: Elsevier, 93−103.

Hacker, D. B., Biek, R. F., Rowley, P. D., 2014. Catastrophic emplacement of the gigantic Markagunt gravity slide, southwest Utah (USA): Implications for hazards associated with sector collapse of volcanic fields. Geology, 42(11): 943−946

Haflidason, H. L., Reidar Sejrup, H. P., Forsberg, C. F., Bryn, P., 2005. The dating and morphometry of the storegga slide. Marine and Petroleum Geology, 22: 123−136.

Hampton, M. A., 1972. The role of subaqueous debris flows in generating turbidity currents. Journal of Sedimentary Petrology, 42: 775−793.

Hampton, M. A., Lee, H. J., Locat, J., 1996. Submarine landslides. Reviews of Geophysics, 34: 33−59.

Hansen, M. J. 1984. Strategies for classification of landslides. In: Brunsden, D., Prior, D. B., (eds). Slope Instability. Chichester: John Wiley & Sons Ltd, 1−25.

Hanzawa, H., Kishida, T., 1981. Fundamental considerations of undrained strength characteristics of alluvial marine clays. Soils and Foundation, Japanese Society of Soil Mechanics and Foundation Engineering, 21(1): 39−50.

Harrison, J. V., Falcon, N. L., 1938. An ancient landslip at Saidmarreh in southwestern Iran. Journal of Geology, 46: 296−309.

Harrison, K. P., Grimm, R. E., 2003. Rheological constraints on martian landslides. Icarus, 163: 347−362.

Hart, B., Massé, M., Locat, J., Long, B., 2001. High-resolution three-dimensional seismic surveying of submarine landslides: Rationale and challenges: Calgary, Canada, 2001 An Earth Odyssey. 54th Canadian Geotechnical Conference, 738−742.

Hay, A., Burling, R. W., Murray, J. W., 1982. Remote acoustic detection of a turbidity current surge. Science, 217: 833−835.

Hayter, E. J., Mathew, ~R., Hallden, J., Garland, E., Salerno, H., Svirsky, S. C., 2006. Evaluation of the State-of-the-Art Contaminated Sediment Transport and Fate Modeling System. EPA/600/R−06/108 September 2006. National Exposure Research Laboratory, Office of Research and Development, U.S. Environmental Protection Agency: Research Triangle Park, NC 27711, 140.

Heezen, B. C, Ewing, M., 1952. Turbidity currents and submarine slumps and the 1929 Grand Banks earthquake. American Journal of Science, 250: 849−873.

Heim, A., 1882. Der Bergsturz von Elm. Zeitschrift der deutschen geologischen Gesellschaft, 34: 74−115.

Heim, A., 1932. Landslides and Human Lives (Bergsturz und Menschenleben): Vancouver. British Columbia, Bi-Tech Publishers, 196.

Helwig, J., 1970. Slump folds and early structures, northeastern Newfoundland and Appalachians. The Journal of Geology, 78: 172−187.

Henstock, T. J., McNeill, L. C., Tappin, D. R., 2006. Seafloor morphology of the Sumatran subduction zone: Surface rupture during megathrust earthquakes? Geology, 34: 485−488; DOI: 10.1130/22426.1

Highland, L. M., Bobrowsky, P., 2008. The landslide handbook—A guide to understanding landslides: Reston, Virginia. U.S. Geological Survey Circular, 1325: 129.

Houghton, P., Davis, C., McCaffrey, W., Barker, S., 2009. Hybrid sediment gravity flow deposits —— Classification, origin and significance. Marine and Petroleum Geology, 26: 1900−1918.

Howard, K. A., 1973. Avalanche mode of motion: Implications from Lunar examples. Science, 180: 1052−1055.

Howe, E., 1909. Landslides in the San Juan Mts. Colorado: including consideration of their causes and their classification. U.S. Geol. Survey Prof. Paper, 67: 58.

Hsü, K. J., 1974. Mélanges and their distinction from olistostromes. In: Dott, Jr. R. H. Shaver, R. H., (eds). Modern and Ancient Geosynclinal Sedimentation.Tulsa, OK: SEPM Special Publication, 19: 321−333.

Hsü, K. J., 1975. Catastrophic debris streams (sturzstromes) generated by rockfalls. GSA Bulletin, 86: 129−140.

Hsü, K. J., 2004. Physics of Sedimentology. 2nd Edition. Berlin: Springer, 240.

Hubbard, D. K., 1992. Hurricane-induced sediment transport in open shelf tropical systems —— An example from St. Croix, US Virgin islands. Journal of Sedimentary Petrology, 62: 946−960.

Hungr, O., 1995. A model for the runout analysis of rapid flow slides, debris flows and avalanches. Canadian Geotechnical Journal, 32: 610−623.

Hungr, O., Evans, S. G., 2004. Entrainment of debris in rock avalanches: An analysis of a long run-out mechanism. GSA Bulletin, 116: 1240−1252.

Hungr, O., Evans, S. G., Bovis, M., Hutchinson, J. N., 2001. Review of the classification of landslides of the flow type. Environmental and Engineering Geoscience, 7: 221−238.

Hutchinson, J. N., 1968. Mass movement. In: Fairbridge, R. W. (ed). Encyclopedia of Earth Sciences. New York: Reinhold, 688−695.

Ilstad, T., Marr, J. G., Elverhoi, A., Harbitz, C. B., 2004. Laboratory studies of subaqueous debris flows by measurements of pore-fluid pressure and total stress. Marine Geology, 213(1−4): 403−414.

Inman, D. L., Nordstrom, C. E., Flick, R. E., 1976. Currents in submarine canyons: An air-sea-land interaction. Annual Review of Fluid Mechanics, 8: 275−310.

Iverson, R. M., 1997. The physics of debris flows. Reviews of Geophysics, 35: 245−296.

Iverson, R. M., 2000. Landslide triggering by rain infiltration. Water Resources Research, 36 (7): 1897−1910.

Iverson, R. M., Vallance, R. W., 2001. New views of granular mass flows. Geology, 29: 115−118.

Iverson, R. M., Reid, M. E., LaHusen, R. G., 1997. Debris-Flow Mobilization from Landslides. Annual Review of Earth and Planetary Sciences, 25: 85−138.

Iverson, R. M., Reid, M. E., Iverson, N. R., LaHusen, R. G., Logan, M., Mann, J. E., Brien, D. L., 2000. Acute sensitivity of landslide rates to initial soil porosity. Science, 290 (5491): 513−516.

Jackson, B. A., 2004. Seismic evidence for gas hydrates in the north Makassar Basin, Indonesia. Petroleum Geoscience, 10: 227−238; DOI:10.1144/1354−079303−601.

Jacobi, R. D., 1976. Sediment slides on the northwestern continental margin of Africa. Marine Geology, 22: 157−173.

Jakob, M., Hungr, O., (eds), 2005. Debris-flow Hazards and Related Phenomena. Berlin: Heidelberg, Praxis-Springer, 739.

Jansen, E., Befring, S., Bugge, T., Eidvin, T., Holtedahl, H., Petter Sejrup, H., 1987. Large submarine slides on the Norwegian continental margin: Sediments, transport and timing. Marine Geology, 78: 77−107.

Johnson, A. M., 1970. Physical Processes in Geology. San Francisco: Freeman, Cooper and Co., 577.

Johnson, A. M., 1984. Debris Flow. In: Prior, D. B., (ed). Slope Instability. New York: John Wiley, 257−361.

Karcz, I., Shanmugam, G., 1974. Decrease in Scour Rate of Fresh Deposited Muds. Proc. American Society of Civil Engineers (ASCE). Journal of the Hydraulics Division, 100 (HY11): 1735−1738.

Karl, H. A., Carlson, P. R., Gardner, J. V., 1996. Aleutian basin of the Bering Sea: Styles of sedimentation and canyon development. In: Gardner, J. V., Field, M. E., and Twichell, D. C.,(eds). Geology of the United States′ Seafloor. New York: Cambridge University Press, 305−332.

Kent, P. E., 1966. The transport mechanism in catastrophic rock falls. The Journal of Geology, 74: 79−83.

Khripounoff, A., Vangriesheim, A., Babonneau, N., Crassous, P., Dennielou, B., Savoye, B., 2003. Direct observation of intense turbidity current activity in the Zaire submarine valley at 4000 m water depth. Marine Geology, 194: 151−158.

Kirschbaum, D. B., Adle, R., Hong, Y., Hill, S., Lerner-Lam, A. L., 2010. A global landslide catalog for hazard applications−Method, results, and limitations. Natural Hazards, 52: 561−575. http://dx.doi.org/10.1007/s11069−009−9401−4 (accessed December 27, 2014).

Klinger, Y., Rivera, L., Haessler, H., Maurin, J-C., 1999. Active faulting in the Gulf of Aqaba: New knowledge from the Mw 7.3 Earthquake of 22 November 1995. Bulletin of the Seismological Society of America, 89(4): 1025−1036.

Koning, H. L., 1982. On an explanation of marine flow slides in sand. In: Saxov, S., Nieuwenhuis, J. K., (eds). Marine Slides and Other Mass Movements. New York and London: Plenum Press, 83−94.

Koppejan, A. W., van Wamelan, B. M., Weinberg, L. J. H., 1948. Coastal flow slides in the Dutch province of Zeeland. In: Proceedings of the 2nd International Conference on Soil Mechanics and Foundation, Rotterdam, 5: 89−96.

Krastel, S., Behrmann, J-H., Völker, D., Stipp, M., Berndt, C., Urgeles, R., Chaytor, J., Huhn, K., Strasser, M., Harbitz, C. B., (eds). 2014. Submarine Mass Movements and Their Consequences. 6th International Symposium. Switzerland: Springer, Advances in Natural and Technological Hazards Research, 37. ISBN: 978−3−319−00971−1 (Print) 978−3−319−00972−8 (Online).

Krynine, P. D., 1948. The megascopic study and field classification of sedimentary rocks. The Journal of Geology, 56: 130−165.

Kudrass, H. R., Michels, K. H., Wiedicke, M., 1998. Cyclones and tides as feeders of a submarine canyon off Bangladesh. Geology, 26: 715−718.

Kuehl, S. A., Hariu, T. M., Moore, W. S., 1989. Shelf sedimentation off the Ganges-Brahmaputra river system: Evidence for sediment bypassing to the Bengal fan. Geology, 17: 1132−1135.

Kuenen, Ph. H., 1951. Properties of turbidity currents of high density. In: Hough, J. L., (ed). Turbidity Currents and the Transportation of Coarse Sediments to Deep Water, A Symposium. Tulsa, OK: SEPM Special Publication, 2: 14−33.

Labaume, P., Mutti, E., Seguret, M., 1987. Megaturbidites: A depositional model from the Eocene of the SW-Pyrenean foreland basin, Spain. Geo-Marine Letters, 7: 91−101.

Laberg, J. S., Kawamura, K., Amundsen, H., Baeten, N., Forwick, M., Rydningen, T. A., Vorren, T. O., 2014. A submarine landslide

complex affecting the Jan Mayen Ridge, Norwegian−Greenland Sea: Slide-scar morphology and processes of sediment evacuation. Geo-Marine Letters, 34: 51−58; DOI: 10.1007/s00367−013−0345−z.

Ladd, G. E., 1935. Landslides, subsidences and rockfalls. Bull. Am. Railway Eng. Ass., 37: 1091−1162.

Lawton, T. F., Shipley, K. W., Aschoff, J. L., Giles, K. A., Vega, F. J., 2005. Basinward transport of Chicxulub ejecta by tsunami-induced backflow, La Popa basin, northeastern Mexico, and its implications for distribution of impact-related deposits flanking the Gulf of Mexico. Geology, 33: 81−84.

Lee, H. J., 2005. Undersea landslides: Extent and significance in the Pacific Ocean, an update. Natural Hazards and Earth System Sciences, 5: 877−892.

Lee, H. J., 2009. Timing of occurrence of large submarine landslides on the Atlantic Ocean margin. Marine Geology, 264: 53−64.

Legros, F., 2002. The long-runout landslides. Engineering Geology, 63: 301−331.

Lewis, K. B., 1971, Slumping on a continental slope inclined at 1°−4°. Sedimentology, 16: 97−110.

Lewis, K., Collot, J.−Y., 2001. Giant submarine avalanche: Was this "Deep Impact" New Zealand style? Water and Atmosphere, 9: 26−27.

Li, T., 1989. Landslides—extent and economic significance in China. In: Brabb, E. E. Harrod, B. L. (eds). Landslides—Extent and Economic Significance. Rotterdam, The Netherlands: A. A. Balkema Publishers, 271−287.

Locat, J., Lee, H. J., 2000. Submarine Landslides: Advances and Challenges. In: Proceedings of the 8th International Symposium on Landslides, Cardiff, U.K., June 2000. http://www.landslides.ggl.ulaval.ca/saguenay/publi/locatleeul.pdf (accessed December 27, 2014).

Locat, J., Lee, H. J., 2002. Submarine landslides: Advances and challenges. Canadian Geotechnical Journal, 39(1): 193−212.

Locat, J., Lee, H. J., 2005. Subaqueous debris flows. In: Jakob, M., Hungr, O., (eds). Debris-flow hazards and related phenomena. Berlin, Heidelberg: Praxis-Springer, 203−245. Chapter 9.

Locat, J., Lee, H. J., ten Brink, U. S., Twichell, D., Geist, E., Sandansoucy, M., 2009. Geomorphology, stability and mobility of the Currituck slide. Marine Geology, 264: 28−40.

Lowe, D. R., 1976. Grain flow and grain flow deposits. Journal of Sedimentary Petrology, 46: 188−199.

Lowe, D. R., 1982. Sediment gravity flows: II. Depositional models with special reference to the deposits of high-density turbidity currents. Journal of Sedimentary Petrology, 52: 279−297.

Lowe, D. R., Guy, M., 2000. Slurry-flow deposits in the Britannia Formation (Lower Cretaceous), North Sea: A new perspective on the turbidity current and debris flow problem. Sedimentology, 47: 31−70.

Lucchitta, B. K., 1979. Landslides in Valles Marineris, Mars. Journal of Geophysical Research, 84: 8097−8113.

Lucchitta, B. K., 1987. Valles Marineris, Mars —— Wet debris flows and ground ice. Icarus, 72: 411−429.

Luczyński, P., 2012. The tsunamites problem. Why are fossil tsunamites so rare? Prz. Geol., 60: 598−604.

Macdonald, D. I. M., Moncrieff, A. C. M., Butterworth, P. J., 1993. Giant slide deposits from a Mesozoic fore-arc basin, Alexander Island, Antarctica. Geology, 21: 1047−1050.

Major, J. J., 1998. Pebble orientation on large, experimental debris-flow deposits. Sedimentary Geology, 117: 151−164.

Major, J. J., Iverson, R. M., 1999. Debris-flow deposition: Effects of pore-fluid pressure and friction concentrated at flow margins. GSA Bulletin, 111(10): 1424−1434.

Malahoff, A., Embley, R., Perry, R., 1978. Submarine Landslides—East Coast Continental Slope and Upper Rise: OCEANS '78: Washington DC, IEEE Explore Conference Publication, September 6−8, 1978, 503−509; DOI: 10.1109/OCEANS. 1978.1151087.

Malin, M. C., 1992. Mass movements on Venus: Preliminary results from Magellan Cycle I observations. Journal of Geophysical Research, 97(E10): 16,337−16,352.

Maltman, A. J., 1987. Microstructures in deformed sediments, Denbigh Moors, North Wales. Geological Journal, 22: 87−94.

Maltman, A., (ed), 1994. The Geological Deformation of Sediments. London: Chapman & Hall, 382.

Marr, J. G., Harff, P. A., Shanmugam, G., Parker, G., 2001. Experiments on subaqueous sandy gravity flows: The role of clay and water content in flow dynamics and depositional structures. GSA Bulletin, 113: 1377−1386.

Martinsen, O., 1994. Mass movements. In: Maltman, A., (ed). The Geological Deformation of Sediments. London: Chapman & Hall, 127−165.

Mascarenhas, A., 2004. Oceanographic validity of buffer zones for the east coast of India: A hydrometeorological perspective. Current Science, 86 (3): 399−406.

Maslin, M., Owen, M., Day, S., Long, D., 2004. Linking continental-slope failures and climate change: Testing the gun hypothesis. Geology, 32: 53−56.

Masson, D. G., van Niel, B., Weaver, P. P. E., 1997. Flow processes and sediment deformation in the Canary Debris Flow on the NW African Continental Rise. Sedimentary Geology, 110: 163−179.

Masson, D. G., Watts, A. B., Gee, M. J. R., Urgeles, R., Mitchell, N. C., Le Bas, T. P., Canals, M., 2002. Slope failures on the flanks of the western Canary Islands. Earth-Science Reviews, 57: 1−35.

Masson, D. G., Harbitz, C. B., Wynn, R. B., Pedersen, G., Løvholt, F., 2006. Submarine landslides: Processes, triggers, and hazard prevention. Royal Society of London Transactions, Series A 364 (1845): 2009−2039.

McAdoo, B. G., Pratson, L. F., Orange, D. L., 2000. Submarine landslide geomorphology, US continental slope. Marine Geology, 169: 103−136.

McEwen, A. S., 1989. Mobility of rock avalanches: Evidence from Valles Marineris, Mars. Geology, 17: 1111−1114.

McGregor, B. A., Rothwell, R. G., Kenyon, N. H., Twichell, D. C., 1993. Salt tectonics and slope failure in an area of salt domes in the northwestern Gulf of Mexico. In: Schwab, W. C., Lee, H. J., d Twichell, D. C., (eds). Submarine Landslides: Selected Studies

in the U.S. Exclusive Economic Zone. U.S. Geological Survey Bulletin, 2002: 92−96.

McPherson, J. G., Shanmugam, G., Moiola, R. J., 1987. Fan-deltas and braid deltas: Varieties of coarse-grained deltas. GSA Bulletin, 99: 331−340.

Meckel, T., 2010. Classifying and characterizing sand-prone submarine mass-transport deposits. AAPG Annual Convention and Exhibition, New Orleans, LA, April 11_14, 2010 (Search and Discovery Article #50270 (2010), Posted July 16, 2010). http://www.searchanddiscovery.com/documents/2010/50270meckel/ndx_meckel.pdf (accessed December 27, 2014).

Meckel, III, L. D., 2011. Reservoir characteristics and classification of sand-prone submarine mass-transport deposits. In: Shipp, R. C., Weimer, P., Posamentier H. W., (eds). Mass-Transport Deposits in Deepwater Settings. Tulsa, OK: SEPM Special Publication, 96: 423−454.

Melosh, H. J., 1979. Acoustic fluidization: A new geologic process? Journal of Geophysical Research, 84: 7513−7520.

Meyer, D., Zarra, L., Yun, J., 2007. From BAHA to Jack, Evolution of the Lower Tertiary Wilcox Trend In the Deepwater Gulf of Mexico. The Sedimentary Record, 5: 4−9.

Michalik, J., 1997. Tsunamites in a storm-dominated Anisian carbonate ramp (Vysoká Formation, Malé Karpaty Mts., western Carpathians). Geologica Carpathica, 48: 221−229.

Middleton, G. V., Hampton, M. A., 1973. Sediment gravity flows: Mechanics of flow and deposition. In: Middleton, G. V., Bouma, A. H., (eds). Turbidites and Deep-Water Sedimentation. Los Angeles, California: Pacific Section SEPM, 1−38.

Mienert, J., Berndt, C., Laberg, J. S., Vorren, T. O., 2002. Slope instability of continental margins. In: Wefer, G., Billet, D., Hebbeln, D., Jorgensen, B., Van Weering, T. C. E., Schlüter, M., (eds). Ocean Margin Systems. New York: Springer, 179−193.

Milia, A., Torrente, M. M. Giordano, F., 2006. Chapter 4 Gravitational instability of submarine volcanoes offshore Campi Flegrei (Naples Bay, Italy). Developments in Volcanology, 9: 69−83.

Mitchell, J. K., Holdgate, G. R., Wallace, M. W., Gallagher, S. J., 2007. Marine geology of the Quaternary Bass Canyon system, southeast Australia: A cool-water carbonate system. Marine Geology, 237: 71−96.

Miyamoto, H., Dohm, J. M., Baker, V. R., Beyer, R. A., Bourke, M., 2004. Dynamics of unusual debris flows on Martian sand dunes. Geophysical Research Letters, 31: L13701; DOI: 10.1029/2004GL020313, 2004.

Moernaut, J., De Batist, M., 2011. Frontal emplacement and mobility of sublacustrine landslides: Results from morphometric and seismostratigraphic analysis. Marine Geology, 285: 29−45.

Mohrig, D., Whipple, K. X., Hondzo, M., Ellis, C., Parker, G., 1998. Hydroplaning of subaqueous debris flows. GSA Bulletin, 110: 387−394.

Montgomery, D. R., Som, S. M., Jackson, M. P. A., Schreiber, B. C., Gillepsie, A. R., 2009. Continental-scale salt tectonics on Mars and the origin of Valles Marineris and associated outflow channels. GSA Bulletin, 121: 117−133.

Moore, D. G, Curray, J. R., Emmel, F. J., 1976. Large submarine slide (olistostrome) associated with Sunda arc subduction zone, northeast Indian Ocean. Marine Geology, 21: 211−226.

Moore, J. G., Clague, D. A., Holcomb, R. T., Lipman, P. W., Normark, W. R., Torresan, M. T., 1989. Prodigious submarine landslides on the Hawaiian Ridge. Journal of Geophysical Research, 94(B122): 17,465−17,484.

Moore, J. G., Normark, W. R., Holcomb, R. T., 1994. Giant Hawaiian landslides. Annual Reviews in Earth and Planetary Sciences, 22: 119−144.

Morgenstern, N. R., 1967. Submarine slumping and the initiation of turbidity currents. In: Richards., A. F., (ed). Marine Geotechnique. Urbana: University of Illinois Press, 189−220.

Moscardelli, L., Wood, L., 2008. New classification system for mass transport complexes in offshore Trinidad. Basin Research, 20: 73−98.

Moscardelli, L., Wood, L., Mann, P., 2006. Mass-transport complexes and associated processes in the offshore area of Trinidad and Venezuela. AAPG Bulletin, 90: 1059−1088.

Mosher, D. C., Moscardelli, L., Shipp, R. C., Chaytor, J. D., C. D. P. Baxter, C. D. P., Lee, H. J., Urgeles, R., 2010. Submarine Mass Movements and Their Consequences. In: Mosher, D. C., *et al.*, (eds). Submarine Mass Movements and Their Consequences: Advances in Natural and Technological Hazards Research, 28: 1−8.

Mulder, T., 2011. Gravity processes and deposits on continental slope, rise and abyssal plains. In: Hüneke, H., Mulder, T., (eds). Deep-Sea Sediments. Amsterdam: Elsevier, Developments in Sedimentology, 63: 25−148. Chapter 2.

Mulder, T., Cochonat, P., 1996. Classification of offshore mass movements. Journal of Sedimentary Research, 66: 43−57.

Mulder, T., Migeon, S., Savoye, B., Faugeres, J-C., 2001. Inversely graded turbidite sequences in the deep Mediterranean: A record of deposits from flood-generated turbidity currents? Geo-Marine Letters, 21; 86−93.

Mulder, T., Syvitski, J. P. M., Migeon, S., Faugeres, J.−C., Savoye, B., 2003. Marine hyperpycnal flows: Initiation, behavior and related deposits: A review. Marine and Petroleum Geology, 20: 861−882.

Mulder, T., Philippe, R., Faugères, J.-C., Gérard, J., 2011. Reply to the Discussion by Roger Higgs on 'Hummocky cross stratification-like structures in deep-sea turbidites: Upper Cretaceous Basque basins (Western Pyrenees, France)' by Mulder *et al.*, Sedimentology, 56: 997−1015, Sedimentology, 58: 671−577.

Murray, J., Renard, A. F., 1891. Report on deep-sea deposits based on specimens collected during the voyage of H. M. S. Challenger in the years 1872−1876. London: Government Printer, Challenger Reports.

Mutti, E., 1992. Turbidite Sandstones. Milan, Italy: Agip Special Publication, 275.

Mutti, E., Ricci Lucchi, F., 1972. Turbidites of the northern Apennines: Introduction to facies analysis (English translation by T. H. Nilsen, 1978). International Geology Review, 20: 125−166.

Mutti, E., Ricci Lucchi, F., Segure, T, M., Zanzucchi, G., 1984. Seismoturbidites: A new group of resedimented deposits. In: Cita, M. B., Ricci Lucchi, F., (eds). Seismicity and Sedimentation. Amsterdam: Elsevier Scientific Publication, 103−116.

Mutti. E., Tinterri, R., Remacha, E., Mavilla, N., Angella, S., Fava, L., 1999. An introduction to the analysis of ancient turbidite basins from an outcrop perspective. Tulsa, OK: AAPG Continuing Education Course Note Series, 39, 61.

Nardin, T. R., Hein, F. J., Gorsline, D. S., Edwards, B. D., 1979. A review of mass movement processes, sediment and acoustic characteristics, and contrasts in slope and base-of-slope systems versus canyon-fan-basin floor systems. In: Doyle, L. J., Pilkey, O. H., (eds). Geology of Continental Slopes. Tulsa, OK: SEPM Special Publication, 27: 61−73.

Natland, M. L., 1967. New classification of water-laid clastic sediments. AAPG Bulletin, 51: 476.

Nelson, C. H., Escutia, C., Damuth, J. E., Twichell, D. C., 2011. Interplay of mass-transport and turbidite-system deposits in different active tectonic and passive continental margin settings: External and local controlling factors. In: Shipp, R. C., Weimer, P., Posamentier, H. W., (eds). Mass-Transport Deposits in Deepwater Settings. SEPM Special Publication, 96: 39−66.

Nemec, W., 1990. Aspects of sediment movement on steep delta slopes. In: Colella, A., Prior, D. B., (eds). Coarse-Grained Deltas. International Association of Sedimentologists Special Publication, 10: 29−73.

Newton, C. S., Shipp, R. C., Mosher, D. C., Wach, G. D., 2004. Importance of mass transport complexes in the Quaternary development of the Nile Fan, Egypt. Offshore Technology Conference, 3−6 May, 2004, Houston, Texas. https://www.onepetro.org/conference-paper/OTC−16742−MS (accessed October 22, 2014).

Norem, H., Locat, J., Schieldrop, B., 1990. An approach to the physics and the modeling of submarine flowslides. Marine Geotechnology, 9: 93−111.

Normark, W. R., 1989. Observed parameters for turbidity-current flow in channels, Reserve Fan, Lake Superior. Journal of Sedimentary Petrology, 59: 423−431.

Normark, W. R., Moore, J. G., Torresan, M. E., 1993. Giant volcano-related landslides and the development of the Hawaiian Islands. In: Schwab, W. C., Lee, H. J., Twichell, D. C., (eds). Submarine Landslides: Selected Studies in the U.S. Exclusive Economic Zone. U.S. Geological Survey Bulletin, 2002: 184−196.

O'Leary, D. W., 1993. Submarine mass movement, a formative process of passive continental margins: The Munson-Nygren landslide complex and the Southeast New England complex. In: Schwab, W. C., Lee, H. J., Twichell, D. C., (eds). Submarine Landslides: Selected Studies in the U.S. Exclusive Economic Zone. U.S. Geological Survey Bulletin, 2002: 23−39.

Palanques, A., Durieu de Madron, X., Puig, P., Fabres, J., Guillén, J., Calafat, A. M., Canals, M. Bonnin, J., 2006. Suspended sediment fluxes and transport processes in the Gulf of Lions submarine canyons: The role of storms and dense water cascading. Marine Geology, 234: 43−61.

Parchure, T. M., 1980. Effect of Bed Shear Stress on the Erosional Characteristics of Kaolinite. Gainesville, FL: University of Florida. M.S. Thesis.

Parsons, J. D., Schweller, W. J., Stelting, C. W., Southard, J. B., Lyons, W. J., Grotzinger, J. P., 2003. A preliminary experimental study of turbidite fan deposits—reply. Journal of Sedimentary Research, 73: 839−841.

Paull, C. K., Mitts, P., Ussler III, W., Keaten, R., Greene, H. G., 2005. Trail of sand in upper Monterey Canyon: Offshore California. GSA Bulletin, 117: 1134−1145.

PBS (Public Broadcasting Service), 2014. Nova "Killer landslides", a TV documentary, broadcast on November 19, 2014 in the U.S. http://www.pbs.org/wgbh/nova/earth/killer-landslide.html (accessed December 27, 2014).

Petley, D., 2012. Global patterns of loss of life from landslides. Geology, 40(10): 927−930; DOI: 10.1130/G33217.1

Pickering, K. T., Hilton, V., 1998. Turbidite Systems of Southeast France. London: Vallis Press, p. 229.

Pickering, K. T., Hiscott, R. N., Hein, F. J., 1989. Deep-Marine Environments. London: Unwin Hyman, 416.

Pierson, T., 1981. Dominant particle support mechanisms in debris flows at Mt Thomas, New Zealand, and implications for flow mobility. Sedimentology, 28(1): 49−60.

Pierson, T., 1985. Initiation and flow behavior of the 1980 Pine Creek and Muddy River lahars, Mount St. Helens, Washington. GSA Bulletin, 96: 1056−1069.

Pierson, T., 1990. Perturbation and melting of snow and ice by the 13 November 1985 eruption of Nevado del Ruiz, Colombia, and consequent mobilization, flow and deposition of lahars. Journal of Volcanology and Geothermal Research, 41(1−4): 17−66.

Pierson, T. C., Costa, J. E., 1987. A rheologic classification of subaerial sediment-water flows. In: Costa, J. E., Wieczorek, G. F., (eds). Debris Flows/Avalanches: Process, Recognition, and Mitigation. GSA Reviews in Engineering Geology, 7: 1−12.

Piper, D. J. W., Aksu, A. E., 1987. The source and origin of the 1929 Grand Banks turbidity current inferred from sediment budgets. Geo-Marine Letters, 7: 177−182.

Piper, D. J. W., Shor, A. N., Hughes Clarke, J. E., 1988. The 1929 "Grand Banks" earthquake, slump, and turbidity current. In: Clifton, H. E., (ed). Sedimentologic Consequences of Convulsive Geologic Events. Boulder, CO. GSA Special Paper, 229: 77−92.

Piper, D. J. W., Cochonat, P., Morrison, M. L., 1999. The sequence of events around the epicenter of the 1929 Grand Banks earthquake: Initiation of debris flows and turbidity current inferred from sidescan sonar. Sedimentology, 46: 79−97.

Piper, D. J. W., Pirmez, C., Manley, P. L., Long, D., Flood, R. D., Normark, W. R., Showers, W., 1997. Mass-transport deposits of the Amazon Fan. In: Flood, R. D., Piper, D. J. W., Klaus, A., Peterson, L. C., (eds). Proceedings of the Ocean Drilling Program, Scientific Results, 155: 109−143.

Piper, D. J. W., Mosher, D. C., Campbell, D. C., 2012a. Controls on the distribution of major types of submarine landslides. In: Clague, J. J., Stead, D., (eds). Landslides: Types, Mechanisms,

and Modeling. Cambridge, UK: Cambridge University Press, 95−107.

Piper, D. J. W., Deptuck, M. E., Mosher, D. C., Hughes-Clarke, J. E., Migeon, S., 2012b. Erosional and depositional features of glacial meltwater discharges on the eastern Canadian continental margin. In: Prather, B. E., Deptuck, M. E., Mohrig, D. C., van Hoorn, B., Wynn, R. B., (eds). Application of Seismic Geomorphology Principles to Continental Slope and Base-of-Slope Systems: Case Studies from Seafloor and Near-Seafloor Analogues. Tulsa, OK: SEPM Special Publication, 99: 61−80.

Popenoe, P., Schmuck, E. A., Dillon, W. P., 1993. The cape fear landslide; slope failure associated with salt diapirism and gas hydrate decomposition. In: Schwab, W. C., Lee, H. J., Twichell, D. C., (eds). Submarine Landslides: Selected Studies in the U.S. Exclusive Economic Zone. U.S. Geological Survey Bulletin, 2002: 40−53.

Popov, I. V., 1946. A scheme for the natural classification of landslides. Doklady USSR Academy of Science, 54: 157−159.

Postma, G., Nemec, W., Kleinspehn, K. L., 1988. Large floating clasts in turbidites: A mechanism for their emplacement. Sedimentary Geology, 58: 47−61.

Postma, G., Kleverlaan, K., Cartigny, M. J. B., 2014. Recognition of cyclic steps in sandy and gravelly turbidite sequences, and consequences for the Bouma facies model. Sedimentology, 61(7): 2268−2290. DOI: 10.1111/sed.12135.

Prior, D. B., Coleman, J. M., 1979. Submarine landslides−Geometry and nomenclature. Zeitschrift für Geomorphologie N. F., 23: 415−426.

Prior, D. B., Coleman, J. M., 1984. Submarine slope instability. In: Brunsden, D., Prior, D. B. (eds). Slope Instability. Chichester: John Wiley & Sons Ltd, 419−455.

Prior, D. B., Suhayda, J. N., Lu, N.−Z., Bornhold, B. D., Keller, G. H., Wiseman, W. J., Wright, L. D., Yang, Z.−S., 1989. Storm wave reactivation of a submarine landslide. Nature, 341: 47−50.

Prior, D. B., Bornhold, B. D., 1990. The underwater development of Holocene fan deltas. In: Colella, A., Prior, D. B. (eds). Coarse-grained Deltas. Oxford, Blackwell Scientific, International Association of Sedimentologists Special Publication, 10: 7590.

Prior, D. B., Hooper, J. R., 1999. Sea floor engineering geomorphology: Recent achievements and future directions. Geomorphology, 31: 411−439.

Puig, P., Ogston, A. S., Mullenbach, B. L., Nittrouer, C. A., Sternberg, R. W., 2003. Shelf-to-canyon sediment-transport processes on the Eel continental margin (northern California). Marine Geology, 193: 129−149.

Purvis, K., Kao, J., Flanagan, K., Henderson, J., Duranti, D., 2002. Complex reservoir geometries in a deep water clastic sequence, Gryphon Field, UKCS: Injection structures, geological modeling and reservoir simulation. Marine and Petroleum Geology, 19: 161−179.

Reiche, P., 1937. The Toreva-Block —— A distinctive landslide type. The Journal of Geology, 45: 538−548.

Reynolds, S. H., 1932. Landslips. Proceedings of Bristol Naturalists′ Society, 7: 352−357.

Ritter, D. F., Kochel, R. C., Miller, J. R., 1995. Process Geomorphology, 3rd edition. Dubuque, Iowa, William C. Brown, 546.

Roberts, N. J., Evans, S.G., 2009. Controls on size and occurrence of the largest sub-aerial landslide on Earth: Seymareh (Saidmarreh) landslide, Zagros fold-thrust belt, Iran. American Geophysical Union, Fall Meeting 2009, abstract #NH41C−1260.

Rodriguez, M., Chamot-Rooke, N., Hébert, H., Fournier, M., Huchon, P., 2013. Owen Ridge deep-water submarine landslides: Implications for tsunami hazard along the Oman coast. Nat. Hazards Earth Syst. Sci., 13: 417−424. http://www.nat-hazards-earth-syst-sci.net/13/417/2013/doi:10.5194/nhess−13−417−2013.

Rouse, C., 1984. Flowslides. In: Brunsden, D., Prior, D. B., (eds). Slope Insatbility. Chichester: John Wiley & Sons, 491−522.

Saller, A. H., Lin, R., Dunham, J., 2006. Leaves in turbidite sands: The main source of oil and gas in the deep-water Kutei Basin, Indonesia. AAPG Bulletin, 90: 1585−1608.

Sanders, J. E., 1963. Concepts of fluid mechanics provided by primary sedimentary structures. Journal of Sedimentary Petrology, 33: 173−179.

Sanders, J. E., 1965. Primary sedimentary structures formed by turbidity currents and related resedimentation mechanisms. In: Middleton, G. V., (ed). Primary Sedimentary Structures and Their Hydrodynamic Interpretation. Tulsa, OK: SEPM, Special Publication, 12: 192−219.

Sanders, J. E., Friedman, G. M., 1997. History of petroleum exploration in turbidites and related deep-water deposits. Northeastern Geology and Environmental Sciences, 19 (1/2): 67−102.

Saxov, S., 1982. Marine slides —— Some introductory remarks. In: Saxov, S., Nieuwenhuis, J. K., (eds). Marine Slides and Other Mass Movements. New York and London: Plenum Press, 1−10.

Schaller, P. J., 1991. Analysis and implications of large Martian and terrestrial landslide: Pasadena, California. California Institute of Technology. Ph.D. dissertation, 596.

Scheidegger, A. E., 1973. On the prediction of the reach and velocity of catastrophic landslides. Rock Mechanics and Rock Engineering, 5: 231−236.

Scheidegger, A. E., 1975. Physical Aspects of Natural Catastrophes. New York: Elsevier Science, 289 p.

Schuster, R. L., 1983, Engineering aspects of the 1980 Mount St. Helens eruptions. Bulletin of the Association of Engineering Geologists, 20: 125−143.

Schuster, R. L., Highland, L. M., 2001. Socioeconomic and environmental impacts of landslides in the Western Hemisphere. U.S. Geological Survey Open-File Report 01−0276. http://pubs.usgs.gov/of/2001/ofr−01−0276/ (accessed December 27, 2014).

Schuster, R. L., Wieczorek, G. F., 2002. Landslide triggers and types. In: Rybar, J., Stemberk, J., d Wagner, P., (eds). Proceedings, 1st European Conference on Landslides, 24−26 June 2002. Prague: A. A. Balkema, 59−78.

Schwab, W. C., Lee, H. J., Twichell, D. C., (eds). 1993. Submarine Landslides: Selected Studies in the U.S. Exclusive Economic Zone: U.S. Geological Survey Bulletin 2002, 204.

Schwalbach, J. R., Edwards, B. D., Gorsline, D. S., 1996. Contemporary channel-levee systems in active borderland basin plains, California Continental Borderland. Sedimentary Geology, 104: 53−72.

Sepúlveda, S. A., Rebolledo, S., Lara, M., Padilla, C., 2006. Landslide hazards in Santiago, Chile: An overview. IAEG2006 Paper number 105. The Geological Society of London 2006 1. http://www2.cose.isu.edu/~crosby/teach/udec/reading/sepulveda_etal_ls_hazards_in_santiago_iaeg_2006.PDF (accessed December 27, 2014).

Shanmugam, G., 1978. The stratigraphy, sedimentology, and tectonics of the Middle Ordovician Sevier Shale Basin in East Tennessee. Knoxville, Tennessee: The University of Tennessee. Ph.D. dissertation, 222.

Shanmugam, G., 1996. High-density turbidity currents: Are they sandy debris flows? Journal of Sedimentary Research, 66: 2−10.

Shanmugam, G., 1997. Deep-water exploration: Conceptual models and their uncertainties. NAPE (Nigerian Association of Petroleum Explorationists) Bulletin, 12/01: 11−28.

Shanmugam, G., 2000. 50 years of the turbidite paradigm (1950s−1990s): Deep-water processes and facies models—A critical perspective. Marine and Petroleum Geology, 17: 285−342.

Shanmugam, G., 2002. Ten turbidite myths. Earth-Science Reviews, 58: 311−341.

Shanmugam, G., 2003. Deep-marine tidal bottom currents and their reworked sands in modern and ancient submarine canyons. Marine and Petroleum Geology, 20: 471−491; DOI: 10.1016/S0264−8172(03)00063−1.

Shanmugam, G., 2006a. Deep-water processes and facies models: Implications for sandstone petroleum reservoirs. Amsterdam, Elsevier, Handbook of Petroleum Exploration and Production, 5: 476.

Shanmugam, G., 2006b. The tsunamite problem. Journal of Sedimentary Research, 76: 718−730.

Shanmugam, G., 2007. The obsolescence of deep-water sequence stratigraphy in petroleum geology. Indian Journal of Petroleum Geology, 16 (1): 1−45.

Shanmugam, G., 2008a. Leaves in turbidite sand: The main source of oil and gas in the deep-water Kutei Basin, Indonesia: Discussion. AAPG Bulletin, 92: 127−137.

Shanmugam, G., 2008b. The constructive functions of tropical cyclones and tsunamis on deep-water sand deposition during sea level highstand: Implications for petroleum exploration. AAPG Bulletin, 92: 443−471.

Shanmugam, G., 2009. Slides, slumps, debris flows, and turbidity currents. In: Steele, J. H., Thorpe, S. A., Turekian, K. K., (eds). Encyclopedia of Ocean Sciences, 2nd ed. Waltham, Massachusetts: Academic Press (Elsevier), 447−467.

Shanmugam, G., 2012a. New perspectives on deep-water sandstones: Origin, recognition, initiation, and reservoir quality. Amsterdam: Elsevier, Handbook of Petroleum Exploration and Production, 9: 524.

Shanmugam, G., 2012b. Process-sedimentological challenges in distinguishing paleo-tsunami deposits. In: Kumar, A., Nister, I., (eds). Paleo-tsunamis. Natural Hazards, 63: 5−30.

Shanmugam, G., 2013a. Slides, Slumps, Debris Flows, and Turbidity Currents. In: Elias, S. A. (ed). Reference Module in Earth Systems and Environmental Science. Elsevier Online. http://dx.doi.org/10.1016/B978−0−12−409548−9.04380−3.

Shanmugam, G., 2013b. Modern internal waves and internal tides along oceanic pycnoclines: Challenges and implications for ancient deep-marine baroclinic sand. AAPG Bulletin, 97(5): 767−811.

Shanmugam, G., 2013c. Comment on “Internal waves, an underexplored source of turbulence events in the sedimentary record” by L. Pomar, M. Morsilli, P. Hallock, and B. Bádenas [Earth-Science Reviews, 111 (2012): 56−81]. Earth-Science Reviews, 116: 195−205.

Shanmugam, G., 2013d, Deep-water processes. Blog. http://g-shanmugam.blogspot.com/ (accessed December 27, 2014).

Shanmugam, G., 2014a. Modern internal waves and internal tides along oceanic pycnoclines: Challenges and implications for ancient deep-marine baroclinic sands: Reply. AAPG Bulletin, 98: 858−879.

Shanmugam, G., 2014b. Review of research in internal-wave and internal-tide deposits of China: Discussion. Journal of Palaeogeography, 3 (4): 332−350.

Shanmugam, G., Benedict, G. L., 1978. Fine-grained carbonate debris flow, Ordovician basin margin, Southern Appalachians. Journal of Sedimentary Petrology, 48: 1233−1240.

Shanmugam, G., Walker, K. R., 1978. Tectonic significance of distal turbidites in the Middle Ordovician Blockhouse and lower Sevier formations in east Tennessee. American Journal of Science, 278: 551- 578.

Shanmugam, G., Walker, K. R., 1980. Sedimentation, subsidence, and evolution of a foredeep basin in the Middle Ordovician, Southern Appalachians. American Journal of Science, 280: 479-496.

Shanmugam, G., Moiola, R. J., 1982. Eustatic control of turbidites and winnowed turbidites. Geology, 10: 231−235.

Shanmugam, G., Moiola, R. J., 1988. Submarine fans: Characteristics, models, classification, and reservoir potential. Earth-Science Reviews, 24: 383−428.

Shanmugam, G., Clayton, C. A., 1989. Reservoir description of a sand rich submarine fan complex for a steamflood project: Upper Miocene Potter Sandstone, North Midway Sunset Field, California. AAPG Bulletin, 73: 411.

Shanmugam, G., Moiola, R. J., 1995. Reinterpretation of depositional processes in a classic flysch sequence in the Pennsylvanian Jackfork Group, Ouachita Mountains. AAPG Bulletin, 79: 672−695.

Shanmugam, G., Zimbrick, G., 1996. Sandy slump and sandy debris flow facies in the Pliocene and Pleistocene of the Gulf of Mexico: Implications for submarine fan models. In: AAPG International Congress and Exhibition, Caracas, Venezuela, Official Program, A45.

Shanmugam, G., Moiola, R. J., Sales, J. K., 1988a. Duplex-like structures in submarine fan channels, Ouachita Mountains, Arkansas. Geology, 16: 229−232.

Shanmugam, G., Moiola, R. J., McPherson, J. G., O'Connell, S., 1988b. Comparison of turbidite facies associations in modern passive-margin Mississippi Fan with ancient active-margin fans. Sedimentary Geology, 58: 63−77.

Shanmugam, G., Lehtonen, L. R., Straume, T., Syversten, S. E., Hodgkinson, R. J., Skibeli, M., 1994. Slump and debris flow dominated upper slope facies in the Cretaceous of the Norwegian and Northern North Seas (61°−67° N): Implications for sand distribution. AAPG Bulletin, 78: 910−937.

Shanmugam, G., Bloch, R. B., Mitchell, S. M., Beamish, G. W. J., Hodgkinson, R. J., Damuth, J. E., Straume, T., Syvertsen, S. E., Shields, K. E., 1995. Basin-floor fans in the North Sea: Sequence-stratigraphic models vs. sedimentary facies. AAPG Bulletin, 79: 477−512.

Shanmugam, G., Spalding, T. D., Rofheart, D. H., 1993a. Process sedimentology and reservoir quality of deep-marine bottom-current reworked sands (sandy contourites): An example from the Gulf of Mexico. AAPG Bulletin, 77: 1241−1259.

Shanmugam, G., Spalding, T. D., Rofheart, D. H., 1993b. Traction structures in deep-marine bottom current-reworked sands in the Pliocene and Pleistocene, Gulf of Mexico. Geology, 21: 929−932.

Shanmugam, G., Shrivastava, S. K., Das, B., 2009. Sandy debrites and tidalites of Pliocene reservoir sands in upper-slope canyon environments, offshore Krishna-Godavari Basin (India): Implications. Journal of Sedimentary Research, 79: 736−756.

Sharpe, C. F. S., 1938. Landslides and Related Phenomena. New York: Columbia University Press, 137.

Shepard, F. P., Dill, R. F., 1966. Submarine Canyons and Other Sea Valleys. Chicago: Rand McNally & Co., 381.

Shepard, F. P., Emery, K. O., 1973. Congo submarine canyon and fan valley. AAPG Bulletin, 57: 1679−1691.

Shepard, F. P., Marshall, N. F., 1978. Currents in submarine canyons and other sea valleys. In: Stanley, D. J., Kelling, G., (eds). Sedimentation in Submarine Fans, Canyons, and Trenches. Stroudsburg, Pennsylvania: Hutchinson and Ross, 3−14.

Shipp, R. C., Weimer, P., Posamentier, H. W., (eds). 2011. Mass-Transport Deposits in Deepwater Settings. Tulsa, OK: SEPM Special Publication, 96.

Shoaei, Z., Ghayoumian, J., 1998. Seimareh landslide, the largest complex slide in the world. In: Moore, D., Hungr, O., (eds). Proceedings of 8th International Congress of the International Association for Engineering Geology and the Environment. Rotterdam: Balkema, 1−5: 1337−1342.

Shreve, R. L., 1968. The Blackhawk Landslide. GSA Special Paper, 108: 47.

Singer, K. N., McKinnon, W. B., Schenk, P. M., Moore, J. M., 2012. Massive ice avalanches on Iapetus mobilized by friction reduction during flash heating. Nature Geoscience, 5: 574−578.

Skempton, A. W., 1960. Terzaghi's discovery of effective stress. In: Bjerrum, L., Casagrande, A., Peck, R. B., Skempton, A. W., (eds). From Theory to Practice in Soil Mechanics. Hoboken, New Jersey: John Wiley, 42−53.

Smit, J., Roep, T. B., Alvarez, W., Montanari, A., Claeys, P., Grajales-Nishimura, J. M., *et al.*, 1996. Coarse-grained, clastic sandstone complex at the K-T boundary around the Gulf of Mexico: Deposition by tsunami waves induced by the Chicxulub impact? In: Ryder, G., *et al.*, (eds). The Cretaceous-Tertiary Event and Other Catastrophes in Earth History. Boulder, CO: GSA Special Paper, 307: 151−182.

Snedden, J. W., Nummedal, D., Amos, A. F., 1988. Storm-and fair-weather combined flow on the Central Texas continental shelf. Journal of Sedimentary Petrology, 58: 580−595.

Solheim, A., Bryn, P., Sejrup, H. P., Mienert, J., Berg, K., 2005a. Ormen Lange—An integrated study for the safe development of a deep-water gas field within the Storegga Slide Complex, NE Atlantic continental margin; executive summary. Marine and Petroleum Geology, 22: 1−9.

Solheim, A., Berg, K., Forsberg, C. F., Bryn, P., 2005b. The Storegga slide complex: Repetitive large scale sliding with similar cause and development. Marine and Petroleum Geology, 22: 97−107.

Sowers, G., 1979. Introductory Soil Mechanics and Foundations. Geotechnical Engineering, 4th ed. New Jersey: Prentice Hall, 640.

Stanley, D. J., Palmer, H. D., Dill, R. F., 1978. Coarse sediment transport by mass flow and turbidity current processes and downslope transformations in Annot Sandstone canyon-fan valley systems. In: Stanley, D. J., Kelling, G., (eds). Sedimentation in Submarine Canyons, Fans, and Trenches. Stroudsburg, Pennsylvania: Hutchinson and Ross, 85−115.

Stow, D. A. V., 1985. Deep-sea clastics: Where are we and where are we going? In: Brenchly, P. J., Williams, P. J., (eds). Sedimentology: Recent Developments and Applied Aspects. Oxford: Blackwell Scientific Publications, Published for the Geological Society, 67−94.

Suhayda, J. N., Prior, D. B., 1978. Explanation of submarine landslide morphology by stability analysis and rheological models. Houston, Texas: Offshore Technology Conference, May 8−11, 1978. http://oai.dtic.mil/oai/oai?verb=getRecord&metadataPrefix=html&identifier=ADA054927 (accessed December 27, 2014).

Sultan, N., P., Cochonat, M., Canals, A., Cattaneo, B., Dennielou, H., Haflidason, J. S., Laberg, D., Long, J. J., Mienert, F., Trincardi, R., Urgeles, T. O., Vorren, C., Wilson, 2004. Triggering mechanisms of slope instability processes and sediment failures on continental margins: A geotechnical approach. Marine Geology, 213(1−4): 291−321.

Sundborg, A., 1956. The River Klarälven: A study of fluvial processes. Geografiska Annaler, Seies A, 38: 197.

Takayama, H., Tada, R., Matsui, T., Iturralde-Vinent, M. A., Oji, T., Tajika, E., *et al.*, 2000. Origin of the Penalver Formation in northwestern Cuba and its relation to K/T boundary impact event. Sedimentary Geology, 135: 295−320.

Talling, P. J., 2014. On the triggers, resulting flow types and frequen-

cies of subaqueous sediment density flows in different settings. Marine Geology, 352: 155−182.

Talling, P. J., Wynn, R. B., Masson, D. G., Frenz, M., Cronin, B. T., Schiebel, R., Akhmetzhanov, A. M., Dallmeier-Tiessen, S., Benetti, S., Weaver, P. P. E., Georgiopoulou, A., Zühlsdorff, C., Amy, L. A., 2007. Onset of submarine debris flow deposition far from original giant landslide. Nature, 450: 541−544.

Talling, P. J., Masson, D. G., Sumner, F. J., Malgesini, G., 2012. Subaqueous sediment density flows: Depositional processes and deposit types. Sedimentology, 59: 1937−2003.

Tappin, D. R., 2010. Submarine mass failures as tsunami sources: Their climate control. Philosophical Transactions of the Royal Society A, 368: 2417−2434; DOI:10.1098/rsta.2010.0079.

Teale, T., Young, J. R., 1987. Isolated olistoliths from the Longobucco Basin Calabria, S. Italy. In: Leggett, J. K., Zuffa, G. G., (eds). Advances in Marine Clastic Sedimentology. London, U.K.: Graham & Trotman, 75−88.

Terzaghi, K., 1936. The Shear Resistance of Saturated Soils. Cambridge, MA: Proceedings of the First International Conference on Soil Mechanics and Foundation Engineering, 1: 54−56.

Terzaghi, K., 1950. Mechanism of landslides. In: Paige, S., (ed). Application of Geology to Engineering Practice (Berkey Volume). New York: Geological Society of America, 83−123.

Terzaghi, K., Peck, R. B., Mesri, G., 1996. Soil Mechanics in Engineering Practice, 3rd Edition. Hoboken: Wiley, 592.

The Learning Channel, 1997. Landslides (videotape), produced for the Learning Channel (a cable television channel in the U.S.) by the BBC Television, London, England.

Tilling, R. I., Topinka, L., Swanson, D. A., 1990. Eruptions of Mount St. Helens: Past, Present, and Future. U.S. Geological Survey Special Interest Publication, 56.

Trincardi, F., Cattaneo, A., Correggiari, A., Mongardi, S., Breda, A., Asioli, A., 2003. Submarine slides during relative sea level rise: Two examples from the eastern Tyrrhenian margin. In: Locat, J., Mienert, J., (eds). Submarine Mass Movements and their Consequences. Dordrecht: Kluwer Academic Publishers, 469−478.

Tripsanas, E. K., Piper, D. J. W., Jenner, K. A., Bryant, W. R., 2008. Submarine mass-transport facies: New perspectives on flow processes from cores on the eastern North Atlantic margin. Sedimentology, 55: 97−136.

Tyszkowski, S., Kaczmarek, H., Słowiński, M., Kozyreva, E., Brykała, D., Rybchenko, A., Babicheva, V. A., 2014. Geology, permafrost, and lake level changes as factors initiating landslides on Olkhon Island (Lake Baikal, Siberia). Landslides. http://link.springer.com/article/10.1007%2Fs10346−014−0488−7 (accessed December 27, 2014).

Twichell, D. C., Chaytor, J. D., ten Brink, U. S., Buczkowski, B., 2009. Morphology of late Quaternary submarine landslides along the U.S. Atlantic continental margin. Marine Geology, 264: 4−15.

Urgeles, R., Canals, M., Baraza, J., Alonso, B., Masson, D., 1997. The most recent megalandslides of the Canary Islands: El Golfo debris avalanche and Canary debris flow, west El Hierro Island. Journal of Geophysical Research, 102(B9): 20305−20323.

Urgeles, R., Camerlenghi, A., Ercilla, G., Anselmetti, F., Brückmann, W., Canals, M., Grácia, E., Locat, J., Krastel, S., Solheim, A., 2007. Scientific ocean drilling behind the assessment of geohazards from submarine slides: Barcelona, Spain, 25−27 October 2006. Eos Trans. AGU 88(17): 192. http://dx.doi.org/10.1029/2007EO170009 (accessed December 27, 2014).

USACE (U.S. Army Core of Engineers), 2003. Slope Stability: Washington, D. C., Department of the Army, Engineers Manual, EM 1110−2−1902, 31 October 2003, 205.

USGS (U.S. Geological Survey), 1994. Geologic features of the sea bottom around a municipal sludge dumpsite near 39_N, 73_W, Offshore New Jersey and New York: U.S. Geological Survey Open-file Report 94−152. http://pubs.usgs.gov/of/1994/of94−152/description.html (accessed December 27, 2014).

USGS (U.S. Geological Survey), 2004. Landslide Types and Processes: USGS Fact Sheet 2004−3072. http://pubs.usgs.gov/fs/2004/3072/fs−2004−3072.html (accessed December 27, 2014).

USGS (U.S. Geological Survey), 2010. Worldwide Overview of Large Landslides of the 20th and 21st Centuries. http://landslides.usgs.gov/learning/majorls.php (accessed January 2, 2013).

Vail, P. R., Audemard, F., Bowman, S. A., Eisner, P. N., Perez-Cruz, C., 1991. The stratigraphic signatures of tectonics, eustacy and sedimentology —— An overview. In: Einsele, G., Ricken, W., Seilacher, A., (eds). Cycles and Events in Stratigraphy. Berlin: Springer-Verlag, 618−659.

Vallance, J. W., Scott, K. M. 1997. The Oseola mudflow from Mount Rainier: Sedimentology and hazard implications of a huge clay-rich debris flow. GSA Bulletin, 109: 143−163.

Van der Lingen, G. J., 1969. The turbidite problem. New Zealand Journal of Geology and Geophysics, 12: 7−50.

van Loon, A. J., 1972. A prograding deltaic complex in the Upper Carboniferous of the Cantabrian Mountains (Spain): the Prioro-Tejerina Basin. Leidse Geologische Mededelingen, 48: 1−81.

Varnes, D. J., 1958. Landslide types and processes. In: Eckel, E. B. (ed). Landslide and Engineering Practice. Highway Research Board Special Report, 29: 20−47.

Varnes, D. J., 1978. Slope movement types and processes. In: Schuster, R. L. Krizek, R. J., (eds). Landslides: Analysis and Control. Washington, D. C. National Academy of Science, Special Report, 176: 11−33.

Varnes, D. J., 1984. Landslide hazard zonation: A review of principles and practice. Paris: UNESCO, International Association of Engineering Geology, Commission on Landslides and Other Mass Movements on Slopes, 60.

Voight, B., Faust, C., 1982. Frictional heat and strength loss in some rapid landslides. Geotechnique, 32(1): 43−54.

Voight, B., Janda, R. J., Glicken, H., Douglass, P. M., 1983. Nature and mechanics of the Mount St. Helens rockslide-avalanche of May 1980. Geotechnique, 33: 243−273.

Vrolijk, P. J., Southard, J. B., 1997. Experiments on rapid deposition of sand from high-velocity flow. Geoscience Canada, 24: 45−54.

Ward, W. H., 1945. The stability of natural slopes. Geographical Journal, 105: 170−197.

Ward, S. N., 2001. Landslide tsunami. Journal of Geophysical Research, 106: No. B6, 11,201−11,215.

Warme, J. E., Slater, R. A., Cooper, R. A., 1978. Bioerosion in submarine canyons. In: Stanley, D. J., Kelling, G. K., (eds). Sedimentation in Submarine Canyons, Fans, and Trenches. Stroudsburg, Pennsylvania: Dowden, Hutchinson & Ross, Inc., 65−70.

Weber, M. E., Wiedicke, M. H., Kudrass, H. R., Huebscher, C., Erlenkeuser, H., 1997. Active growth of the Bengal Fan during sea-level rise and highstand. Geology, 25: 315−318.

Weidinger, J. T., Korup, O., 2009. Frictionite as evidence for a large Late Quaternary rockslide near Kanchenjunga, Sikkim Himalayas, India-Implications for extreme events in mountain relief destruction. Geomorphology, 103: 57−65.

Weimer, P., 1989. Sequence stratigraphy of the Mississippi Fan (Plio-Pleistocene), Gulf of Mexico. Geo-Marine Letters, 9: 185−272

Weimer, P., 1990. Sequence stratigraphy, facies geometries, and depositional history of the Mississippi Fan, Gulf of Mexico. AAPG Bulletin, 74: 425−453.

Welbon , A. I. F., Brockbank, P. J., Brunsden, D., Olsen, T. S., 2007. Characterizing and producing from reservoirs in landslides: Challenges and opportunities. In: Jolley, S. J., Barr, D., Walsh, J. J., Knipe, R. J., (eds). Structurally complex reservoirs. London: Geological Society Special Publication, 292: 49−74.

Wieczorek, G. F., Snyder, J. B., 2009. Monitoring slope movements. In: Young, R., Norby, L., (eds). Geological Monitoring. Boulder, Colorado: GSA, 245−271.

Wikipedia (the free Encyclopedia), 2014. 2014 Oso mudslide. http://en.wikipedia.org/wiki/2014_Oso_mudslide (accessesed November 20, 2014).

Woodcock, N. H., 1976. Structural style in slump sheets: Ludlow Series, Powys, Wales. Journal of Geological Society of London, 132: 399−415.

Woodcock, N. H., 1979. Sizes of submarine slides and their significance. Journal of Structural Geology, 1: 137−142.

Wynn, R. B., Masson, D. G., Stow, D. A. V, Weaver, P. P. E, 2000. The Northwest African slope apron: A modern analogue for deep-water systems with complex seafloor topography. Marine and Petroleum Geology, 17: 253−265.

Xu, J. P., Noble, M. A., Rosenfeld, L. K., 2004. In-situ measurements of velocity structure within turbidity currents. Geophysical Research Letters, 31, L09311. 10.1029/2004GL019718, 2004.

Yatsu, E., 1967. Some problems on mass movements. Geografiska Annaler Series A, 49a(2−4): 396−401.

Zaruba, Q., Mencl. V., 1969. Landslides and Their Control. Prague: Academia & Elsevier, 205.

Zou, C., Wang, L., Li, Y., Tao, S., Hou, L., 2012. Deep-lacustrine transformation of sandy debrites into turbidites, Upper Triassic, Central China. Sedimentary Geology, 265−266: 143−155.

(Edited by Yuan Wang)